

THE APPLICATION OF FACILITATED ION TRANSFER ACROSS MEMBRANE
STABILIZED INTERFACE BETWEEN TWO IMMISCIBLE ELECTROLYTE
SOLUTIONS IN CLINICAL ANALYSIS.

A Thesis Presented to the
School of Graduate Studies
Addis Ababa University

In Partial Fulfilment of
the Requirements for the Degree
of Master of Science in Chemistry

By
Tarekegn Berhanu

June, 1994

Acknowledgement

I would like to express my deepest gratitude to my advisors Dr. B. Hundhammer and Dr. Theodros Solomon who have shouldered the onerous task of advising me to bring this study into effect. I appreciate all the efforts they made, valuable criticisms they gave and precious time they expended towards the completion of this paper. A grateful acknowledgements are hereby made to the National Research Institute of Health(NRIH) for providing me with the blood serum samples. My sincere thanks are due to Ato Gonfa Ayana, Ato Mengistu and Ato Kimdar Sherefa, members of this institute, who have facilitated, arranged and prepared the blood serum samples. My heartfelt thanks should specially go to Ato Mengistu who has done the flame photometric measurements.

Special thanks are due to Dr.K. Rowberg who have introduced me to the basic know how of computer in chemistry and for allowing me to use her own computer for writing my thesis. Also, I would like to express my indebtedness to w/o Manyahlisal Mekoya who has facilitated conditions to use the computer.

Further, I'm beholden to my friends Ahmed Mustefa, Azeb Yigezu, Estifanos Kebede, Osman Ali, Samuel Mekonnen, and my brother Kebede Berhanu for their generosity, moral support and encouragement.

Moreover, many thanks are attributed to all my colleagues in

JIHS who have taken care of my family pending the completion of my graduate study.

My sincere appreciations also go to Jimma Institute of Health Sciences for giving me the opportunity to participate in the graduate programme and for various support.

I'm pretty much obliged to the Department of Chemistry for providing me with all assistance, facilities, and otherwise throughout the research work.

TABLE OF CONTENTS

	page
Acknowledgement	iv
Table of Contents	vi
List of Figures	viii
List of Tables	xii
Abstract	xiii
1. INTRODUCTION	1
2. THEORY	11
2.1. Charge Transfer Equilibria	11
2.2. Simple ion transfer	14
2.3. Facilitated ion transfer	15
2.4 Electrochemical Methods	19
2.5. Diffusion at membrane stabilized interface	20
3. Experimental	23
3.1 Chemicals and Reagents	23
3.2. Electronic set ups and apparatus	24
3.3. Potassium selective electrode	28
4. RESULT and DISCUSSION	29
4.1. Evaluation of thermodynamic quantities from flow injection and cyclic voltammetries	29
4.2. Flow Injection Amperometric Investigation	46
4.3. Flow Injection Amperometry Vs Flame Photometry	63

4.4. Potentiometric Measurements	69
5. CONCLUSION	74
6. Appendix	76
7. REFERENCES	92

LIST OF Figures

Figures	page
1. Diffusion layer	21
2. The four electrode potentiostat	24
3. Block diagram of flow injection system	24
4. Block diagram of electronic set up for ac and dc cyclic voltammetric experiments	25
5. Wall-jet electrochemical cell	27
6. Flow injection peaks for the transfer of ClO_4^- in ac responses	30
7. Flow injection peaks for the transfer of ClO_4^- in dc responses	31
8. The dependence of the flow injection peak current on the applied potential difference for the transfer of ClO_4^- across water/nitrobenzene interface	32
9. Ac cyclic voltammograms of the transfer of ClO_4^- and NO_3^- ions across water/nitrobenzene interface .	33
10. Dc cyclic voltammograms of the transfer of K^+ and Na^+ ions across membrane stabilized water/nitrobenzene interface in the presence of B15C5	35
11. Dc cyclic voltammogram of the transfer of K^+ and Na^+ ions across membrane stabilized	

water/nitrobenzene interface in the presence of DB24C8 in the organic phase	36
12. Dc cyclic voltammogram of the transfer of K^+ and Na^+ across membrane stabilized water/nitrobenzene interface in the presence of 18C6	37
13. Ac cyclic voltammograms of the transfer of K^+ and Na^+ across membrane stabilized water/nitrobenzene interface in the presence of DB24C8	40
14. Ac cyclic voltammograms of the transfer of K^+ and Na^+ ion across membrane stabilized water/nitrobenzene interface in the presence of B15C5	41
15. Ac cyclic voltammograms of the transfer of K^+ and Na^+ ions in the presence of DB18C6 in the organic phase	42
16. Typical flow injection peak current- time response of the transfer of K^+ ion across membrane stabilized water/nitrobenzene interface	48
17. Flow injection peak current-potential relationship for the transfer of 7mM K^+ for the ac mode	49
18. Flow injection peak current-potential relationship for the transfer of 7mM Na^+ for the ac mode	50
19. Dependence of the flow injection peak current on the applied potential difference for transfer of 7 mM K^+ ion in the presence of 18C6	51
20. Dependence of the flow injection peak current on	

	the applied potential difference for transfer of 7 mM Na ⁺ ion in the presence of 18C6	52
21.	Dependence of the flow injection peak current on the applied potential difference for the transfer of K ⁺ and Na ⁺ in the presence of DB24C8	54
22.	Dependence of the flow injection peak current on the applied potential difference for the transfer of K ⁺ and Na ⁺ in the presence of B15C5	55
23.	Typical flow injection analysis peaks for the transfer of different concentrations of Na ⁺	56
24.	Typical flow injection analysis peaks for the transfer of Na ⁺ after elongation of the distance between the sample loop and the sensor	58
25.	Comparison of flow injection amperometric results with flame photometric data for K ⁺ ion measurements (dilution, after the sample)	64
26.	Comparison of flow injection amperometric results with flame photometric data for Na ⁺ ion (dilution, after the sample)	64
27.	Comparison of flow injection amperometric results with flame photometric data for K ⁺ ion measurements(direct, before the sample)	65
28.	Comparison of flow injection amperometric results with flame photometric data for Na ⁺ measurements (direct, before the sample)	65
29.	The relationship between the relative partial	

sensitivities of Na ⁺ and K ⁺ ions (i_{Na^+}/i_{K^+}) and the change in potential difference (scale was $\Delta E - \Delta E_{1/2, K^+}$)	66
30. Calibration curve for potentiometric measurement of K ⁺ ion in the presence of varying concentration of the interfering Na ⁺	71
31. Calibration curve for potentiometric measurement of K ⁺ ion in the absence of Na ⁺	72

LIST OF TABLES

Table	Page
1. Values of peak potentials	38
2. Stability constants and half-wave potentials for the transfer of K^+ and Na^+ ions	43
3. Hole-size and cation diameter of some ionophores and cations	45
4. Equivalent conductivity and specific conductance of Na^+ , Mg^{2+} , NO_3^- and SO_4^{2-}	59
5. Partial sensitivities obtained from the calibration curves of the determination of K^+ and Na^+	62
6. The ratios of the partial sensitivities of K^+ and Na^+ ions at the two chosen potentials	67
7. The results obtained from potentiometric measurements	73

ABSTRACT

AC and DC voltammetry and flow injection amperometry methods were employed in this work. The influence of ionophores on the facilitated transfer of K^+ and Na^+ ions across membrane stabilized water/nitrobenzene interface was investigated. According to this investigation benzo 15 crown 5 (B15C5) was found best for K^+ ion and dibenzo 24 crown 8 (DB24C8) for Na^+ . B15C5 was an appropriate ionophore in simultaneous determination of K^+ and Na^+ ions. DB24C8 was found to be poor in this regard. Stability constants of metal-ionophore complex were estimated. The values for K^+ -ionophore (K-DB24C8, K-DB18C6) were in good agreement with literature values, while those of Na^+ -ionophores (Na-DB24C8, Na-DB18C6) are higher than the literature values. Concentrations of Na^+ and K^+ in blood serum were determined simultaneously using flow injection amperometry and flame photometry. The results obtained from voltammetric and flow injection amperometric investigations indicate that the membrane stabilized interface is a promising as a voltammetric sensor in clinical analysis of blood electrolytes.

1. INTRODUCTION

Hospital clinical chemistry laboratories are responsible for carrying out the majority of analyses of naturally occurring analytes in blood serum plasma, urine, and other biological fluids and materials of patients. Of these, sodium and potassium are usually the most frequently requested tests. Eventhough no studies have been carried out as to how much sodium and potassium analyses are performed each day in each hospital in Ethiopia, one recent review [1] has indicated that an average sized district general hospital in UK, serving population of 250,000, would carry out 150 -200 analyses of sodium and potassium on each working day.

Sodium and potassium are the two most abundant cations present in the extracellular and intracellular fluids respectively. The clinical conditions and possible consequences of hypernatraemia (elevated plasma sodium concentration), hyponatraemia (lowered plasma sodium concentration), hyperkalaemia (elevated potassium plasma concentration), and hypokalaemia (lowered plasma potassium concentration) are summarized in reference [1].

The potassium ion plays an important role in body fluids. Normal functioning of body cells hinges on maintenance of the cell membrane potential, which is largely controlled by a concentration gradient of potassium ions across the cell membrane. In open heart surgery with extracorporeal blood circulation, potassium measurement is of special importance [2].

The constancy of the extracellular ionic environment may be essential for proper functioning of the extracellular compartment. For instance, sodium, the major extracellular monovalent cation, is a key element in the control of extracellular volume and tonicity [3]. So the analyses of these cations is carried out for diagnosis of disease, the monitoring of its progress and/or treatment, or for a screening of healthy population.

Historically most analyses required in large numbers have employed spectrophotometric methods as these are relatively easy to carry out and automate. Kinetic methods often making absorption measurements in the ultraviolet spectrum, have been developed with the increasing use of automatic analyzers [1]. This, however, has not been the way in which the measurement of sodium and potassium has developed. Eventhough several spectrophotometric methods based on the use of ionophores such as crown ethers and a chromolyte have been reported in recent years[4], at early times neither element lent itself to the formation of a coloured complex and subsequent measurement by spectrophotometry. Their properties are such that they are not easily assayed satisfactorily by chemical methods and consequently clinical chemists turned to physical methods for analyses.

The introduction of flame photometry as an analytical tool led rapidly to its application to the measurements of sodium and potassium in biological fluids [5]. This may be regarded as the advent of modern analytical clinical chemistry as it

enabled analysis to be carried out for the first time, on relatively large number of specimens, using small volumes of sample, but at the same time producing an acceptable analytical precision. Until the advent of the use of ion-selective electrodes (ISE) and their application to clinical chemistry [6], the analyses of sodium and potassium were carried out solely by flame photometry. Ion-selective electrodes are being used increasingly for the determination of these cations in body fluids.

The introduction of ISEs has resulted in two different types of instrumentation: the high-capacity analyzer, which normally uses diluted patient samples and is referred to as an indirect reading ISE or indirect potentiometry and the lower capacity instrument used for "on-off" measurements where a patient's sample is introduced directly into the electrode with no pre-dilution step, referred to as the direct reading ISE or direct potentiometry [1].

The measurements of serum sodium and potassium ions with ion-selective electrodes has been the centre of an increased controversy arising from the discrepancies which exist in interpretation of results when correlating direct potentiometry with flame photometry [7,8,9,10]. This will have an impact on the clinicians acceptance of all direct electrode measurements in biological fluids. The origins of these discrepancies are different, for example, Levy compared direct and indirect potentiometric measurements by illustrating the effects of lipids and proteins on the measured sodium ion concentration

[11]. Baron discussed how the sodium ion is measured in whole plasma or plasma water [12], and Coleman et al discussed the effect of the degree of sodium binding to bicarbonate in the sample [13].

At present ISEs are widely used for direct potentiometric measurements of these important electrolytes in body fluids by minimizing the discrepancies. In doing so considerable effort has been given to the synthesis and characterization of new macrocyclic structures with improved selectivity and detection limits [14,15].

Great efforts are being made to develop new analytical methods that are increasingly selective, sensitive, easy to build, and amenable to applications in clinical analyses. The application of ion transfer across membrane stabilized interface between two immiscible electrolyte solutions in clinical analyses is one of these efforts.

The study of ITIES was started in 1902 [16]. The work of Ross [17] on liquid state ion-selective electrode and the work of Gavach and his coworkers [18] on the relationship between the interfaces of ITIES and that of metal-electrolyte solutions from polarization point of view has stirred up the interest of electrochemist. Since then a wide range of charge transfer reactions at ITIES have been studied. The focuses of interest were in the study of simple ion transfer, facilitated ion transfer, electron transfer and double layer studies across ITIES.

A general deal of deserved interest has centred on the nature of ionophore facilitated transfer of ions, such as K^+ and other alkali ions, across the aqueous-immiscible organic liquid interface, a reaction attracting attentions from groups as diverse as neurophysiologists and electroanalytical chemists [19]. An ionophore is a molecule which, mainly due to complex formation enables ions to be transferred across the hydrophillic medium of biological membrane [20]. The transfer of K^+ facilitated by valinomycin [21,22], nonactin [21, 23], and crown ethers [21, 23] has been extensively studied by Koryta [24], and his groups [25-30], Wang and Pang [31], and Yoshida and Freiser [32] using various electrochemical techniques [33]. The ion transfer reactions of alkali metal ions in the presence of these ionophores are fast and the half-wave potential of the facilitated ion-transfer gives information on the stoichiometry and the stability constant of the complex formation reaction.

Facilitated transfer of hydrogen ion by carboxylic ionophore like nigericin [34] and synthetic carboxylic acid ionophores [45] has also been studied. The transfer of alkaline earth metal ions facilitated by crown ethers at water/nitrobenzene interface [45]) has been also investigated. Besides divalent or tervalent ion complexes like $Cd(II)$, $Zn(II)$, $Co(II)$, $Ni(II)$, $Fe(II)$ and $Fe(III)$ with 1,10-phenanthroline and 2,2'-bipyridine [34] the facilitated transfer of tervalent lanthanides with methylene bis(diphenylphosphine oxide) [45] and 4-acyl-5-pyrazolone [35]

at the water/DCE interface have been studied. The transfer of Ni(II), Cd(II) and Fe(II) facilitated by 2,2'-bipyridine [36] has also been investigated.

These studies show that the transfer of ions across the interfaces can be influenced by the presence of suitable ionophores such as those mentioned above. These ionophores are either macrocyclic or acyclic but form cyclic structures when entering into complexes with the metal ions [37].

Pedersen led the way for the development of macrocyclic ethers [38]. He showed that alkali and alkaline earth metal ions bind crown ethers to form highly structured complexes. When they form these stable complexes the cations are placed in the ligand cavities. The ratio between the size of the cavity of the crown ligand to the ionic radius of the central cation is the decisive or at least the important factor for the stability of the formed complex compound [39].

It is this complex forming properties of the crown ethers which is of great analytical interest. From the view point of analytical application the complex formation of alkali metal ions with macrocyclic ionophores in the organic phase has been shown by Homolka and his coworkers [21]. This can be used for quantitative determination of alkali and alkaline earth metal ions.

Homolka et al [21] also indicated that without these ion carriers the standard potential of these cations would be so positive that the supporting electrolyte of narrow potential window is transferred before these cations. In the mechanism

of ionophore-mediated ion transfer, the central question about the site of the complex formation, i.e. whether it is in the organic phase, in the aqueous phase, or at the interface is not yet settled [23, 62, 63]. Koryta et al [21, 24, 25, 64] believe that the complex formation takes place via two mechanisms in parallel. That is, the simple K^+ ion underwent electrochemical transfer followed by K^+ -ionophore complex formation in the organic phase. This was resisted by Yoshida and Freiser [32] and by Sinru et al [62] who demonstrated the transfer of K^+ -valinomycin complex from aqueous to the organic phase. This shows that first the transport of the ionophore from organic to the aqueous takes place and then formation of the complex in the aqueous phase. The carrier mechanism involves selective complex formation at one side, or at the interface and diffusion of the complex to the other side. This mechanism was effectively demonstrated with valinomycin, nonactin and dibenzo-18-crown-6 which facilitate the transfer of alkali metal ions across the water/nitrobenzene interface [21, 40].

The determination of stability constant of the ionophore-metal ion complex is very important, since they are the measure of the stability of the complex and the selectivity of the ionophore. The stability constants can be determined either in excess of the metal ion [21], or in excess of the ionophore [22]. Since the stability constant varies with the solvents used, an appropriate choice of solvent is also important for the stability of the complexes [22].

Several electroanalytical techniques have been employed in the study of ion transfer across ITIES, such as chronopotentiometry [21, 41, 42], ac and dc cyclic voltammetry, and polarography [19, 43, 44-46], potential-step chronopotentiometry, chronopotentiometry with cyclic linear current-scanning [30], square wave voltammetry, etc.

Electrochemical information on the charge (ion or electron) transfer at the liquid-liquid interface is important for a better understanding of the solvent extraction of ions, of liquid membrane ISEs, and of the biological membrane and its model systems [47]. These electrochemical studies on ion transfer across the polarized oil/water interface have also shown that the interface can be employed for voltammetric and amperometric determination of ions as an alternative to the common potentiometric methods at zero current [48,49]. Amperometric methods have the principal advantage that the electrical current signal is directly proportional to the concentrations and that the selectivity of the detector can be varied by means of change in the electrode potential [50]. Another advantage of amperometric method over potentiometric one is that two or more ions can be determined simultaneously with a single electrode if the half-wave potentials of the ions are reasonably separated [45].

The problem connected with the analytical application of the oil/water interface as a voltammetric sensor are the mechanical instability of the oil/water interface and keeping the thickness of the diffusion layer constant. Polymer-

electrolyte gel electrodes such as the polyvinyl chloride - nitrobenzene (PVC-NB) gel electrode [47] appear promising to overcome this problem. Another important development in this regard is a membrane -stabilized interface [51]. For example, the nitrobenzene/water interface is stabilized by placing a thin hydrophillic dialysis membrane. The interface is then formed by interfacial tension at the pores of the membrane. The thickness of the diffusion layer can be kept at constant value by using a wall-jet arrangement of the sensor in a flow system. So a wall-jet detector with a hydrophobic or hydrophillic membrane filter has proved significant for the determination of common inorganic ions by flow injection analysis [51]. Accordingly, ammonia has been determined by the use of hydrophillic dialysis membrane[50] , sodium and potassium ions and volatile amines have been determined in food stuff [52] and blood serum [53]. Nitrate and chloride ions have been determined simultaneously by flow-injection amperometry in river water [50].

The concept of flow-injection analysis(FIA) is a well established analytical technique [54]. Since its conception in the early 1970s [55], FIA has grown enormously. In FIA the sample is introduced as a plug via a valve or syringe. Mixing is mainly by diffusion-controlled processes, and the response curve do not reach the steady state plateau, but have the form of sharp peaks [55]. The requisite apparatus can be easily assembled from existing standard laboratory equipments, easily manufactured or purchased as a complete unit [56]. Several

novel detectors have been developed for the use with FIA [56, [57]. FIA assay systems have been described for many different compounds in wide variety of areas, such as clinical chemistry, agricultural chemistry, environmental chemistry, biochemistry and immunological chemistry ([57] and references cited there in). The large number of electrolyte determinations carried out in the clinical laboratory necessitated an efficient procedure which would reduce the time taken for these determinations. To supply needed data effectively and quickly it would be an advantage to have a rapid, accurate, precise and reliable method available for the simultaneous determination of sodium and potassium in blood serum and other biological fluids [55]. In this regard the main objective of this work is to investigate the analytical application of facilitated cation transfer across the membrane stabilized interface between two immiscible electrolyte solutions in clinical analyses and comparing the method with other analytical methods statistically and to investigate the influence of the employed ionophore on the selectivity of the method.

2. THEORY

2.1. Charge Transfer Equilibria

The influence of the distribution of electrolytes between water and oils on the electrical potential change at the interface has been investigated by Karpfen and Randles [59]. According to this investigation the thermodynamic basis of ionic equilibria in oil/water systems can be summarized as follows [59]: The electrochemical potential of a univalent positive ion M^+ ($z = 1$) in a phase whose inner potential is ϕ may be expressed as

$$\mu_{M^+} = \mu_{M^+}^o + RT \ln a_{M^+} + z\phi F \quad (1)$$

and for a univalent negative ion X^- ($z = -1$)

$$\mu_{X^-} = \mu_{X^-}^o + RT \ln a_{X^-} - z\phi F \quad (2)$$

where μ is the electrochemical potential, μ^o is the standard chemical potential which is not accessible to direct measurement, a is the activity of the ion, the superscripts w and o indicates the water and oil phases respectively, and R , T , and F have their usual meanings.

According to Karpfen and Randles [59], when a salt MX is distributed between oil and water, the condition of equilibrium is that the electrochemical potential of each ion must be the same in both phases and also each phase must be electrically neutral. i.e.,

$$\mu_{M^+}^{(w)} = \mu_{M^+}^{(o)} \quad \text{and} \quad \mu_{X^-}^{(w)} = \mu_{X^-}^{(o)} \quad (3)$$

Substituting equations (1) or (2) into (3), we have

$$\begin{aligned} \mu_{M^+}^{o,(w)} + RT \ln a_{M^+}^{(w)} + z\phi^w F &= \mu_{M^+}^{o,(o)} + RT \ln a_{M^+}^o + z\phi^o F \quad \text{or} \\ \mu_{X^-}^{o,(w)} + RT \ln a_{X^-}^{(w)} + z\phi^w F &= \mu_{X^-}^{o,(o)} + RT \ln a_{X^-}^o + z\phi^o F. \end{aligned} \quad (4)$$

At the interface a Galvani potential difference $\Delta_o^w \phi$ is formed

$$\begin{aligned} \Delta_o^w \phi &= \phi^w - \phi^o = [\mu_{M^+}^{o,(o)} - \mu_{M^+}^{o,(w)}] / zF + RT/zF \ln \{a_{M^+}^o / a_{M^+}^{(w)}\} \\ \text{or } \Delta_o^w \phi &= -\{\mu_{X^-}^{o,(o)} - \mu_{X^-}^{o,(w)}\} / zF - RT/zF \ln \{a_{X^-}^o / a_{X^-}^{(w)}\} \end{aligned} \quad (5)$$

The quantity $\mu_i^{o,(o)} - \mu_i^{o,(w)} = \Delta G_{tr,i}^{o,w-o}$ is the standard Gibbs energies of transfer of ion i (where $i = M^+$) from water into the oil phase. This quantity is the difference of the standard Gibbs energies of solvation of ion i in oil and water phases respectively [24]. When the quantity $\Delta G_{tr,i}^{o,w-o}$ is divided by the Faraday's constant, F , it gives the standard Galvani potential difference $\Delta_o^w \phi^o$,

$$\Delta_o^w \phi^o = \Delta G_{tr,i}^{o,w-o} / zF \quad (6)$$

Substituting equation (6) in (5), we have

$$\Delta_o^w \phi = \Delta G_{tr,i}^{o,w-o} / zF + RT/zF \ln a_i^{(o)} / a_i^{(w)} \quad (7)$$

$$\Delta_o^w \phi = \Delta_o^w \phi_i^o + (RT/zF) \ln a_i^{(o)} / a_i^{(w)} \quad (8)$$

Thermodynamic quantities such as standard Gibbs energies of transfer, Galvani potential difference and standard chemical potential for an individual ion, in contrast to an electrolyte as a whole cannot be measured directly [60]. The quantitative determination of these thermodynamic quantities is possible only after certain extrathermodynamic assumptions are made. The most widely used assumption is the "Tetraphenylarsonium tetraphenylborate" (TPAsTPB) assumption [61]. This assumption

is stated as the standard energies of transfer of tetraphenylarsonium cation and tetraphenylborate anion between any pair solvents are equal,

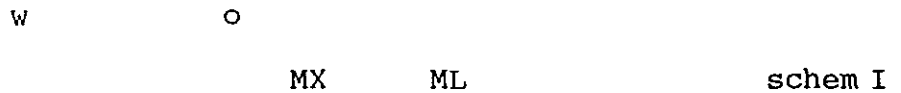
$$\Delta G_{tr,TPAs^+}^{\circ} = \Delta G_{tr,TPB^-}^{\circ} = 1/2 \{ \Delta G_{otr,TPAsTPB}^{\circ} \}$$

In the case of one electrolyte distributed between the water and oil phases, we obtain from (1) and (2) the following relationship [59],

$$\Delta_o^w \phi^{\circ} = 1/2 \{ \Delta G_{tr,M^+,o,w}^{\circ} - \Delta G_{tr,X^-,o,w}^{\circ} \} / zF. \quad (9)$$

The potential difference depends on the ability of the anion and the cation to be transferred from water to oil phases expressed by standard Gibbs transfer energies.

If we consider two electrolytes one in each phase with common cation, say, M^+ and different anions, say X^- and L^-

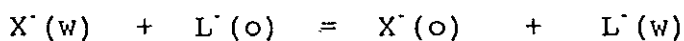


The transfer of the anions to the respective phases is difficult in this case. Therefore, the Galvani potential difference between oil and water will be determined only by the activities of M^+ in both phases if the concentration of the salts in water and oil have comparable values.

Another case is when one electrolyte is practically confined only to one phase while the other to the other phase.



The equilibria of the exchange reactions



and

$$M^+(w) + N^+(o) = M^+(o) + N^+(w) \quad (10)$$

are strongly shifted to the left-hand side in this case.

According to Koryta et al [28], under these conditions there exists a range of the $\Delta_0^w\phi$ where the determination of the potential difference by the activities of the ions present in the system is not possible. As they pointed out, the $\Delta_0^w\phi$ in this case is determined by the charge in the double layer. This charge can be changed by charging the phases from an external source. This is the condition which is called ideally polarized interface of two immiscible electrolyte solutions.

2.2. Simple ion transfer

Ion transfer at ITIES is classified into two, simple and facilitated ion transfer [24].

Consider the case given in schem (II) but assuming a third salt in the water phase, such as AY; in this situation MX and NL serve as base electrolytes as used in polarography. The cation A^+ has a similar characteristics as M^+ in schem I. If current is not flowing through the system, an equilibrium is established in the system. The equilibrium potential difference is determined by equation (8). If a larger potential difference than the equilibrium potential difference is applied from an external source, charge would be introduced into the system. The charge introduced partly used for the transfer of A^+ across

the interface and partly used for the charging of the double layer. If one neglects the charging current, the remaining current will be due to a simple charge transfer across the interface.

$$A^+(w) = A^+(o) \quad (11)$$

The Galvani potential difference formed at the interface, under this condition assuming reversible diffusion controlled ion transfer, can be given by equation (8). Since $a = \gamma c$, equation (8) can be rewritten as

$$\begin{aligned} \Delta_o^w \phi_i &= \Delta_o^w \phi_i^o + (RT/zF) \ln\{\gamma_i(o)/\gamma_i(w)\} \\ &+ (RT/zF) \ln\{C_i(o)/C_i(w)\} \end{aligned} \quad (12)$$

where γ_i is the activity coefficient of the ion i ($i = A^+$ in this case). The flux balance at the half-wave potential is given by

$$D_i^{1/2}(w)C_i(w) = D_i^{1/2}(o)C_i(o) \quad (13)$$

Where D_i is the diffusion coefficient of the ion i and C_i is the concentration of the ion i .

The half-wave potential is given by

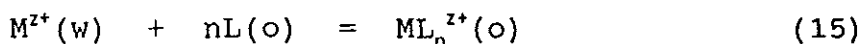
$$\begin{aligned} \Delta_o^w \phi_{1/2,i} &= \Delta_o^w \phi_i^o + (RT/2zF) \ln\{D_i(w)/D_i(o)\} \\ &+ (RT/zF) \ln\{\gamma_i(o)/\gamma_i(w)\} \end{aligned} \quad (14)$$

2.3. Facilitated ion transfer

The number of ionic species which can be transferred across ITIES depends on the range of accessible potential difference between the two phases. If this range of accessible potential difference across the two phases is wide the number

of ionic species which can be transferred also increases. If the range is narrow only limited number of ionic species can be transferred. But, it is fortunate that the ionic species that cannot be studied by transfer across ITIES due to the narrow range of accessible potential difference across the phases, can be made possible in the presence of ionophores in the nonaqueous phase [24]. Alkali and alkaline earth metal ions are the prominent examples of these groups.

As described else where, the presence of ionophore shifts the potential at which the cations are transferred to a more negative values, within the polarizable potential range. The magnitude of this shift in the potential at which the cation is transferred depends on the stability constant of the complex formed. The facilitated transfer of alkali metal ions at the organic/water interface is fast and diffusion controlled process when studied using electrochemical methods. The general complexation reaction in facilitated ion transfer is given by



where M^{z+} is a metal cation with charge z and L is the ionophore. For the reversible charge transfer across ITIES, the potential difference between the aqueous and the organic phases is given by

$$\begin{aligned} \Delta_o^w \phi &= \Delta_o^w \phi_{M^{z+}}^o + (RT/zF) \ln \{ a_{M^{z+}}(o) / a_{M^{z+}} \} \\ &= \Delta_o^w \phi_{ML_n^{z+}}^o + (RT/zF) \ln \{ a_{ML_n^{z+}}(o) / a_{ML_n^{z+}} \} \end{aligned} \quad (16)$$

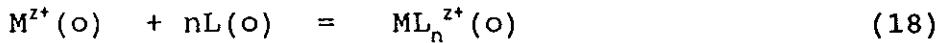
As described else where, when the concentration of the ionophore in the organic phase is considerably lower than the

concentration of the cation in the aqueous phase, the current generating process is entirely controlled by diffusion of the ionophore to the ITIES and the diffusion of the complex formed from ITIES into the bulk of the organic phase [24, 65].

The partition of the cation M^+ between the organic and the aqueous phases

$$M^{z+}(w) = M^{z+}(o) \quad (17)$$

is followed by a chemical equilibrium



The Galvani potential difference for this system is given by

$$\Delta_o^w \phi = \Delta_o^w \phi_{M^+} + (RT/zF) \ln C_{ML_n^{z+}}(o) / K_{ML_n^{z+}} C_L^n(o) C_{M^{z+}}(w) + (RT/zF) \ln \gamma_{M^+}(o) / \gamma_{M^+}(w) \quad (19)$$

$$\text{where } K_{ML_n^{z+}}(o) = C_{ML_n^{z+}}(o) / C_{M^{z+}}(o) C_L^n(o) \quad (20)$$

where $K_{ML_n^{z+}}$ is the stability constant of the cation-ionophore complex.

Since $M^+(w)$ is in excess its diffusion needn't be considered. The only diffusing species are ML^+ and L . Then, for the polarographic half-wave potential, the flux balance is given by

$$D_{ML_n^{z+}}^{1/2, o} C_{ML_n^{z+}}(o) = D_L^{1/2, o} C_L^n(o) \quad (21)$$

where D_{ML} and D_L are the diffusion coefficients of the complex and the ionophore, respectively. The half-wave potential is then given by the relationship

$$\Delta_o^w \phi_{1/2, ML_n^{z+}} = \Delta_o^w \phi_{M^+}^o + (RT/2zF) \ln \{D_L/D_{ML_n^{z+}}\} - (RT/zF) \ln K_{ML_n^{z+}} C_{M^{z+}}^w \quad (22)$$

where $\Delta_o^w \phi_{M^+}^o$ is the formal potential for ion transfer which includes the activity coefficient terms.

In view of this equation, stronger complexation and higher concentration of the metal ion cause larger shift of the half-wave potential (and, in the same way of the peak potential) to more negative potential.

Assuming $\gamma = 1$ and $D_{ML^+} = D_L$ it is possible to calculate the stability constant using equation (22) [21]. An alternative way for the determination of the stability constant is to consider the polarographic half-wave potential of a simple reversible transfer of the univalent cation through the interface [28], which is given by equation (14) and that of facilitated transfer of the cation given by equation (22). From this shift of the half-wave potential of ion-transfer across ITIES in the absence and the presence of the ionophore in the organic phase, it is possible to calculate the stability constant of the complex formed by using the following equation by assuming $D_{ML^+} = D_L$.

$$\Delta_o^w \phi_{1/2, M^+} - \Delta_o^w \phi_{1/2, ML^+} = \Delta \Delta \phi_{1/2} = (RT/2F) \ln D_{M^+}(w)/D_{M^+}(o) + (RT/F) \ln K_{ML^{n+z}} C_{M^+} \quad (23)$$

It is also possible to study the transfer of ions across ITIES when the ionophore present in the organic phase is in excess to the cation in the aqueous phase. In this case the diffusion of the ionophore need not be considered and the diffusing species are $ML^+(o)$ and $M^+(w)$. Following similar procedure as in the case of excess metal cation, it is possible to have the following expression for the half-wave potential

$$\Delta_o^w \phi_{1/2, ML^+} = \Delta_o^w \phi_{M^+}^o + (RT/2zF) \ln \{D_{ML^+}/D_{M^+}\} - (RT/zF) \ln \{K_{ML^{n+z}} C_L^n(o)\} \quad (24)$$

Again it is possible to calculate the stability constant of the complex formed by using equation (24) provided that we know D_{MLn^+} and D_{M^+} or one can estimate the stability constant by assuming $D_{ML^+} = D_{M^+}$.

2.4 Electrochemical Methods

In dc cyclic voltammetry a triangular dc voltage is applied to the electrochemical cell and the current response is recorded as a function of the applied voltage [67]. According to Nicolson and Shain [68], the peak potential in cyclic voltammogram is related to the half-wave potential by

$$\Delta_o^H \phi_{p,i} = \Delta_o^H \phi_{1/2,i} \pm 1.09RT/zF \quad (25)$$

$$\text{or } \Delta_o^H \phi_{p,i} = \Delta_o^H \phi_{1/2,i} \pm 0.0285/z \quad (26)$$

where + and - stand for the negative and positive current respectively. Nicolson and Shain [68] have set a diagnostic criteria for diffusion controlled reversible processes, when studied by dc cyclic voltammetry. These are: linear dependence of the peak current on the square root of the sweep rate (I_p on $\nu^{1/2}$), the peak separation should be $60/z$ mV, the ratio of the anodic and cathodic peak current should be unity, i.e. $i_{p,a}/i_{p,c} = 1$, and the half-peak potential should precede the peak potential difference ΔE_p by 0.056 V. The dc cyclic voltammetry has been extended to the ac format by superimposing an ac voltage onto the dc triangular ramp and either the fundamental or second harmonic ac response is recorded as a function of the applied dc potential [69]. Ac cyclic

voltammetry has a considerable advantage over the dc one in read out format because of both improved wave shape (evaluation of half-wave potential is very easy) and discrimination against charging current [69] (better sensitivity).

2.5. Diffusion at membrane stabilized interface

In a wall-jet arrangement a jet of solution issued from a circular nozzle strikes a wall of the sensor (the electrode or the interface) perpendicularly and then spreads over the surface of the wall. The counter electrode is kept away from the wall-jet. In this case a very thin layer is formed adjacent to the surface in which the velocity gradient normal to the surface is very large. This thin layer according to Gunasingham and Fleet [70], is termed as the hydrodynamic boundary layer. For a solution flowing over the hydrophillic membrane there is a region in the immediate vicinity of the membrane where a rapidly changing concentration profile is found. This region is termed as diffusion layer [70].

The wall-jet arrangement of the ITIES in FIA, then, ensures the establishment of this hydrodynamic boundary layer within which a hypothetical stagnant diffusion layer, σ_{dl} , adjacent to the hydrophillic membrane exists. According to Gunasingham and Fleet [70], the empirical average thickness of this diffusion layer is given by

$$\sigma_{dl} = 2.28 D_w^{1/3} a^{1/2} \nu^{5/12} R^{5/4} V^{-3/4} \quad (27)$$

where a is the diameter of the nozzle; ν is the kinematic

viscosity; R is the radius of the sensor; V is the volume flow rate, and D_w is the diffusion coefficient in water of the ion under study.

This diffusion layer exists within the hydrodynamic boundary layer, formed by the flow of solution in the wall-jet arrangement over the hydrophillic membrane. The thickness of this boundary layer again according to Gunasingham and Fleet [70] is given by

$$\sigma_{bl} = 5.8\pi^{3/4} a^{1/2} \nu^{3/4} x^{5/4} V^{-3/4} \quad (28)$$

where x is the dimension along the interface, all others have the same significance as in equation (27).

Hundhammer et al [53] developed a theory for diffusion at membrane stabilized interface for the flow injection analysis. Accordingly, when a concentration step (changing the flow of the carrier to carrier solution containing the ion under investigation) or a concentration pulse (injection of a small amount of the ion under study into the carrier solution) is applied to ITIES, a concentration -distance profile as shown in Fig.1 will exist at $t = 0$

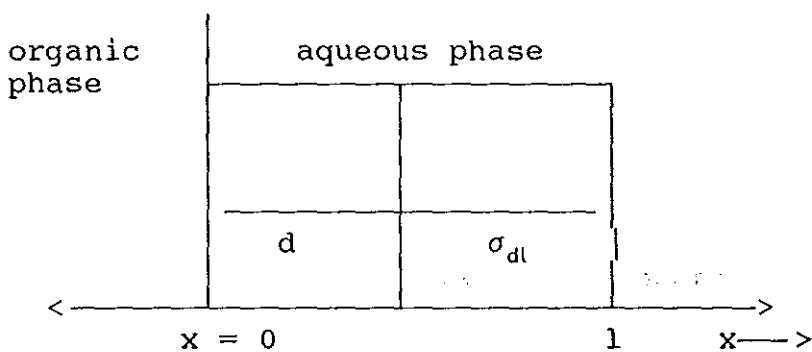


Fig.1. The diffusion layer

The water/oil interface is supposed to be at $x = 0$, the

membrane extends to $x = d$ and the empirical stagnant diffusion layer, σ , extends from $x = d$ to $x = 1$. With this precondition the diffusion problem can be solved by Laplace-transformation [53]). The initial and boundary conditions are

$$t = 0$$

$$c = 0 ; \quad -\infty < x < 1 \quad (29)$$

$$c = c_b ; \quad x \geq 1 \quad (30)$$

$$t > 0$$

$$c(t) = c_b - S_{tp}(t)C_b ; \quad x \geq 1 \quad (31)$$

$$c = 0 \quad x \rightarrow -\infty$$

$$C_o\gamma_o/C_w\gamma_w = \exp [zF(\Delta_o^H\phi - \Delta_o^H\phi^0)]/RT ; \quad x = 0 \quad (32)$$

$$C_w = C_m ; \quad x = d$$

(33) the flux balance under this condition is given by

$$D_o(dC_o/dx) = D_m(dC_m/dx) ; \quad x = 0 \quad (34)$$

$$D_m(dC_m/dx) = D_w(dC_w/dx) ; \quad x = d \quad (35)$$

where $S_{tp}(t)$ is unit step function defined as

$$S_{tp}(t) = 0 \quad \text{for } 0 \leq t \leq t_p \quad (36)$$

$$\text{and } S_{tp}(t) = 1 \quad \text{for } t > t_p \quad (37)$$

t_p is the length of the concentration pulse acting on the sensor. Finally an effective diffusion coefficient, D , was introduced to simplify the solution. This diffusion coefficient acts from $x = 0$ to $x = 1$ and is given by

$$D = 1/(\sigma/D_w + d/D_m) \quad (38)$$

By solving the flux $j(t)$ for unit concentration and unit area at $x = 0$ and taking the measurable current instead of the flux, the following expression is obtained

$$\ln(t^{1/2}i) = \ln\{2zFAC_b [D/\pi]^{1/2}\} - l^2/4Dt \quad (39)$$

3. Experimental

3.1. Chemical and Reagents

Dibenzo-24-crown-8 (Aldrich), benzo-15-crown-5 (Aldrich) 18-crown-6 (Aldrich), sodium chloride (BDH, analar), sodium nitrate (Riedel-de-Haen), potassium chloride (BDH, analar), potassium nitrate (Fluka), magnesium sulfate (BDH, analar), crystal violet chloride (Fluka), sodium tetraphenyl borate (NaTPB) (Fluka), lithium perchlorate (Fluka), and silver nitrate (Fluka) were used as such without further purification. The nitrobenzene used in the experiment (Fluka) was shaken three times with 10% sulfuric acid and three times with 10% sodium hydroxide and was washed several times with twice distilled water to the point of neutral reaction before use. Crystal violet tetraphenyl borate (CVTPB) and ethyl violet tetraphenyl borate (EtVTPB) were prepared by dissolving equimolar amount of crystal violet chloride or ethyl violet chloride and sodium tetraphenyl borate in methanol and precipitated by adding twice distilled water and washed several times by twice distilled water until negative chloride test by AgNO_3 was observed.

3.2. Electronic set ups and apparatus

Fig.2 and 3 show the block diagram of the experimental set ups used in the experiments.

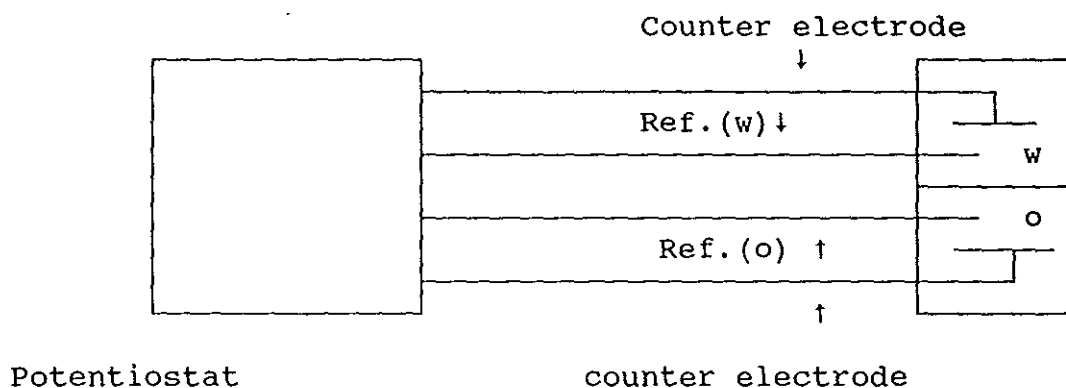


Fig.2. The four-electrode potentiostat

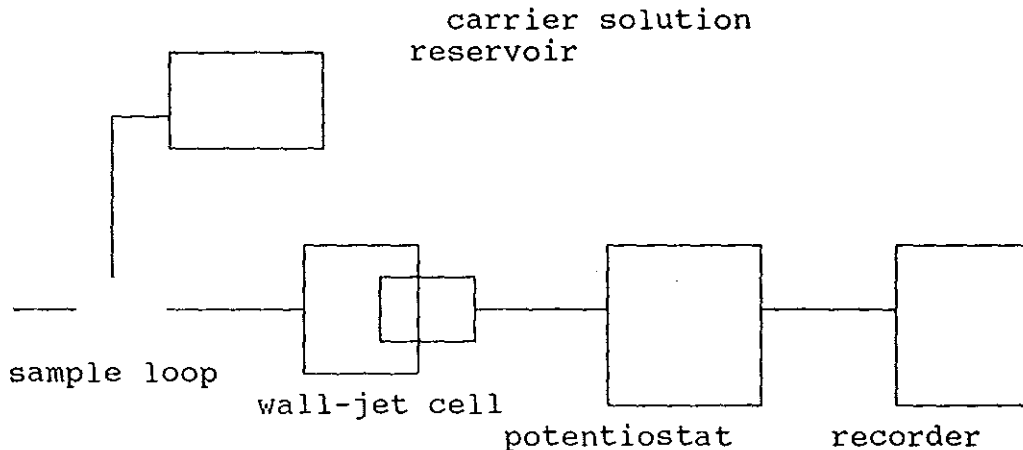


Fig. 3. Block diagram of the flow injection system

Ac and dc cyclic voltammetry and flow-injection amperometry was used in the experiments. The block diagram of the electronic set-up used for the ac and dc cyclic voltammetric experiments is as described in [43] which is shown in Fig.4

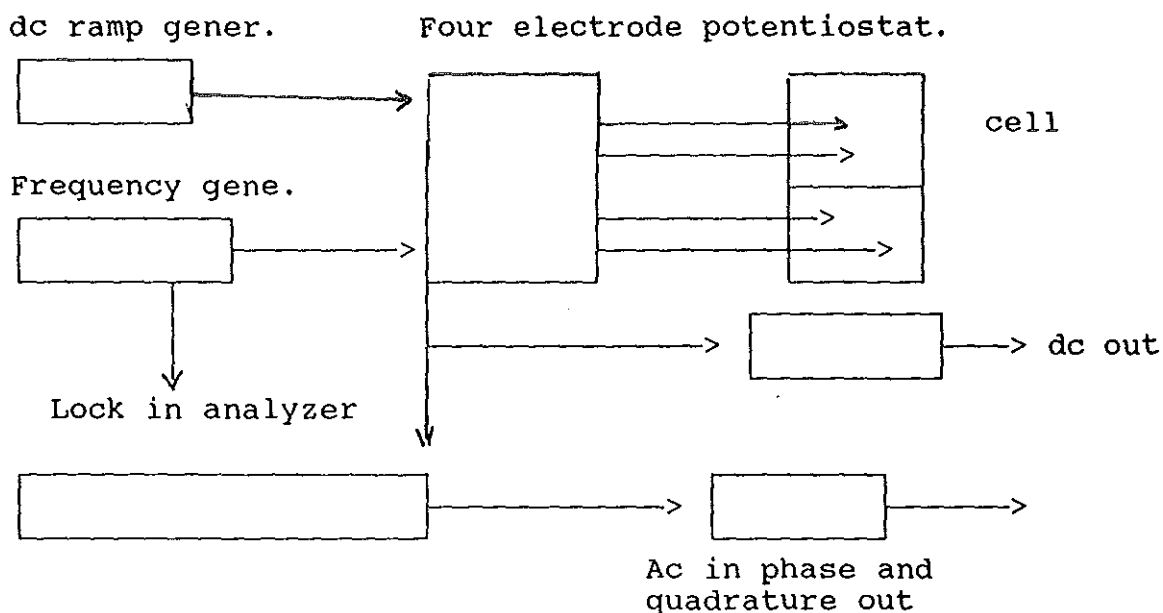


Fig.4. Block diagram of electronic set up for ac and dc cyclic voltammetry.

10 mM MgSO_4 and 10 mM CVTPB or EtVTPB were used as supporting electrolytes in the aqueous and nitrobenzene phases, respectively. 10 mM MgSO_4 was also used as a carrier solution. All the aqueous solutions were prepared with doubly distilled water. A wall-jet electrochemical cell which is shown in Figure 5 was employed in the experiment.

The membrane used to stabilize the interface between two immiscible electrolyte solutions were PT 325 and PT 600 dialysis membrane (Kjeomfeld & co-GmbH). A disc, 19 mm in diameter of the respective membrane was immersed in 10 ml of MgSO_4 solution for 12 hrs. After mounting the membrane on the membrane holder, the inner compartment was filled with about 1.5 ml of the organic phase (10 mM CVTPB or EtVTPB containing 10 mM crown ethers) in nitrobenzene. Then the membrane holder was dipped in the aqueous phase and allowed to equilibrate for about 30 minutes.

The potential difference across the membrane stabilized interface was controlled by means of a four-electrode potentiostat with IR compensation. The IR compensation of the potentiostat was set to the nearest point before oscillation.

Copper wire was used as counter electrode in the organic phase while the jet-inlet capillary (stainless steel) was used as counter electrode in the aqueous phase. Silver/silver chloride electrode was the reference both in the aqueous and organic phases. The electrolyte of the reference electrode in the aqueous phase was 10 mM $MgSO_4$ and that of organic phase was 10mM CVTPB or EtVTPB. The aqueous and organic phases were mutually saturated before use.

A 25 μ l volume of the standard and blood serum samples were injected into the carrier electrolyte solution. Direct and diluted samples of the blood serum was used in the measurements. The dilution was made 1:50 by doubly distilled water. Comparative determination of sodium and potassium were made using MD Dr. Lange flame photometer following standard procedures.

In all the amperometric, ac and dc measurements x-y recorder (Lloyd instruments PL3 x-y recorder) was used.

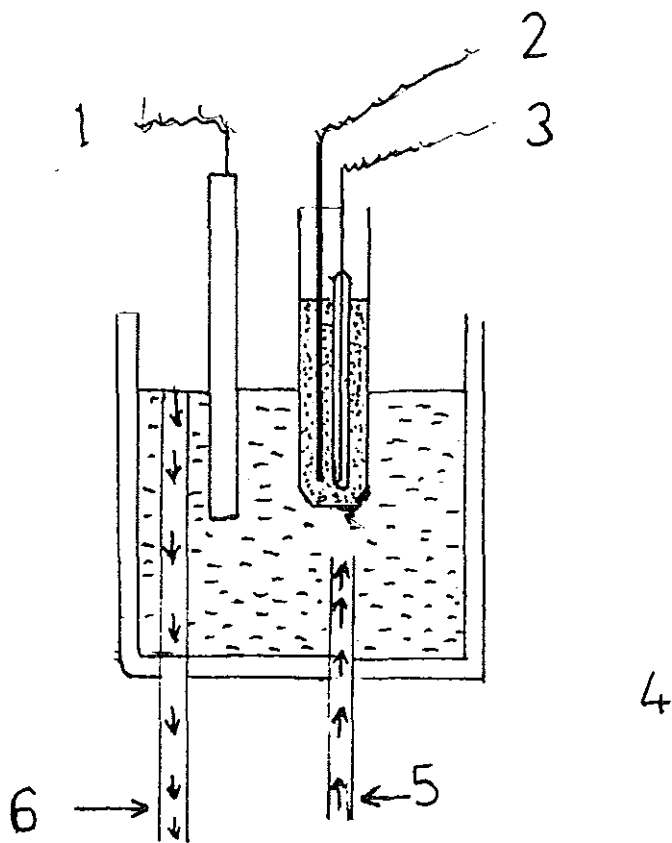


Fig. 5 Wall-jet electrochemical cell, (1), (3), Reference electrode, (2) Counter electrode in the organic phase, (4) Membrane, (5) Jet in let (stainless steel) serves as counter electrode, (6) out let

3.3. Potassium selective electrode

Potassium selective electrode was prepared by dissolving 50 mg of potassium tetrakis(4-chlorophenyl)borate and 4.5 mg DB 24 c 8 in 10 ml nitrobenzene as a stalk solution. 10^{-4} M of an internal filling solution was prepared out of the stalk solution for the K^+ -selective electrode.

The electrode body was made of a glass tube and a hydrophillic dialysis membrane which was swollen in 10 mM $MgSO_4$ for about 1 hr. used to close one end of the glass tube and filled with an ion selective solution and then the inner-reference solution (100 mM KCl) was transferred by the use of syringe on top of that. Silver/silver chloride electrode was the external reference electrode. All emf measurements were made at 20 ± 2 °c lab. temprature with pw 9409 Philips model digital pH/mV meter. The potential of the solution of a constant level of Na^+ (interfering ion) and varying concentration of the analyte(K^+) was plotted vs $-\log [K^+]$. The electrode has been preconditioned overnight in 1mM potassium chloride solution.

4. RESULT and DISCUSSION

4.1. Evaluation of thermodynamic quantities from flow injection and cyclic voltammeteries

For the test of the system, the transfer of perchlorate and nitrate ions was investigated by flow injection technique and ac cyclic voltammetry. Fig. 6 and 7 show the flow injection peaks for the transfer of ClO_4^- ion in both dc and ac responses. As it is evident from this figure, the peak height is maximum in the limiting region in the case of dc cyclic voltammetry and it is maximum at the half-wave potential in the case of ac cyclic voltammetry. The result obtained from the injection peaks is depicted in Fig. 8. As can be seen from this figure the half-wave potential of the ClO_4^- overlaps in the two cyclic voltammograms. This was in accordance with what was expected. Fig. 9 shows the ac cyclic voltammogram of the transfer of ClO_4^- and NO_3^- ions across water/nitrobenzene membrane stabilized interface. As it is observed from this figure, the difference in the half-wave potential of ClO_4^- and NO_3^- ions is larger than the difference in the standard Galvani potentials of the two ions, i.e.

$$\Delta_o^H E_{1/2, \text{NO}_3^-} - \Delta_o^H E_{1/2, \text{ClO}_4^-} = -0.190\text{v.} \quad (40)$$

$$\Delta_o^H \phi_{\text{NO}_3^-}^o - \Delta_o^H \phi_{\text{ClO}_4^-}^o = -0.170\text{v.} \quad (41)$$

But, this value is reasonably close to the value reported by Mai [71] which was -0.186v for hydrophillic dialysis membrane. The observed half-wave width of 90mV for the transfer of ClO_4^-

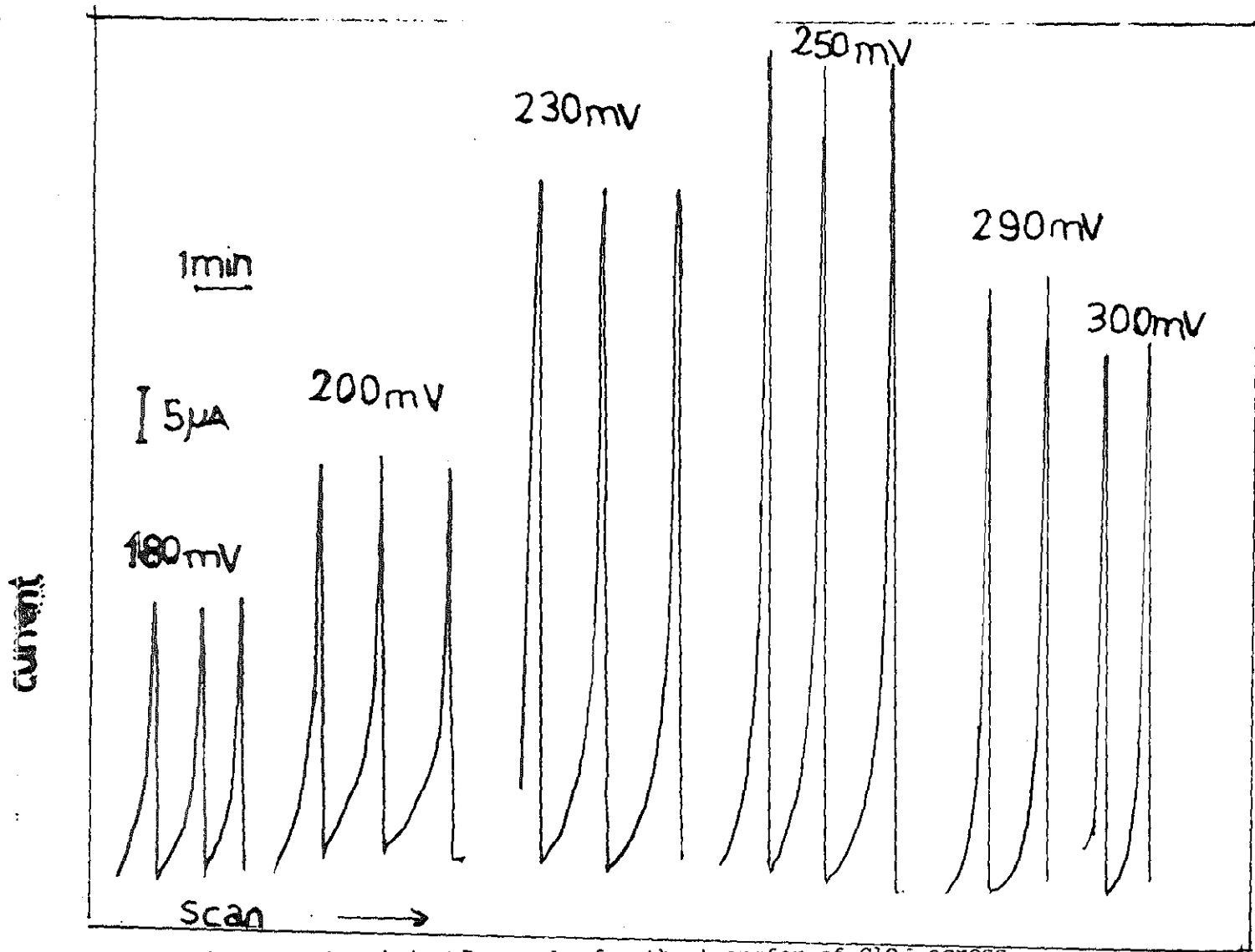


Fig. 6. Flow injection peaks for the transfer of ClO_4^- across membrane stabilized water/nitrobenzene interface in the ac responses.

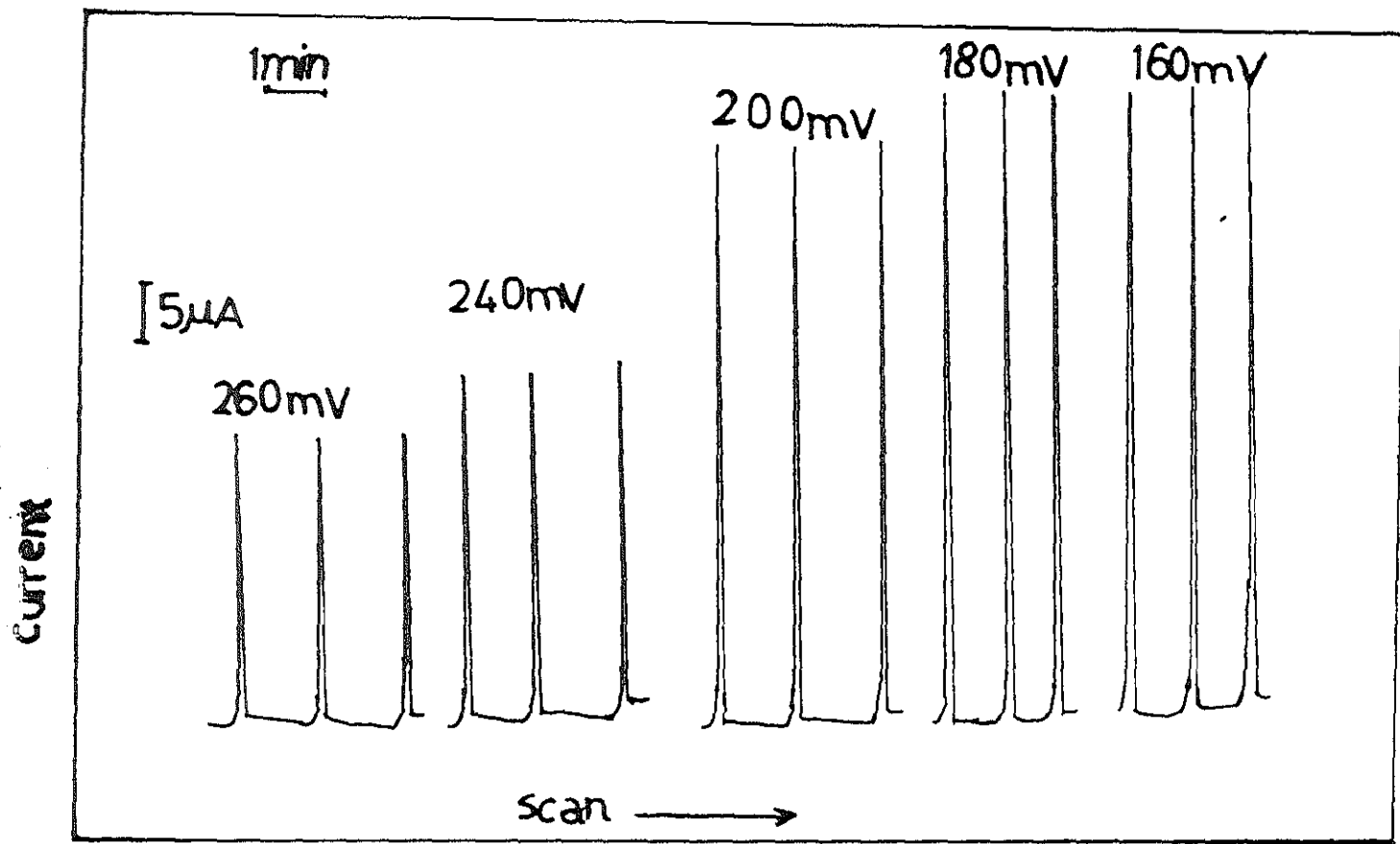


Fig. 7 Flow injection peaks for the transfer of ClO_4^- across membrane stabilized water/nitrobenzene interface in the dc responses.

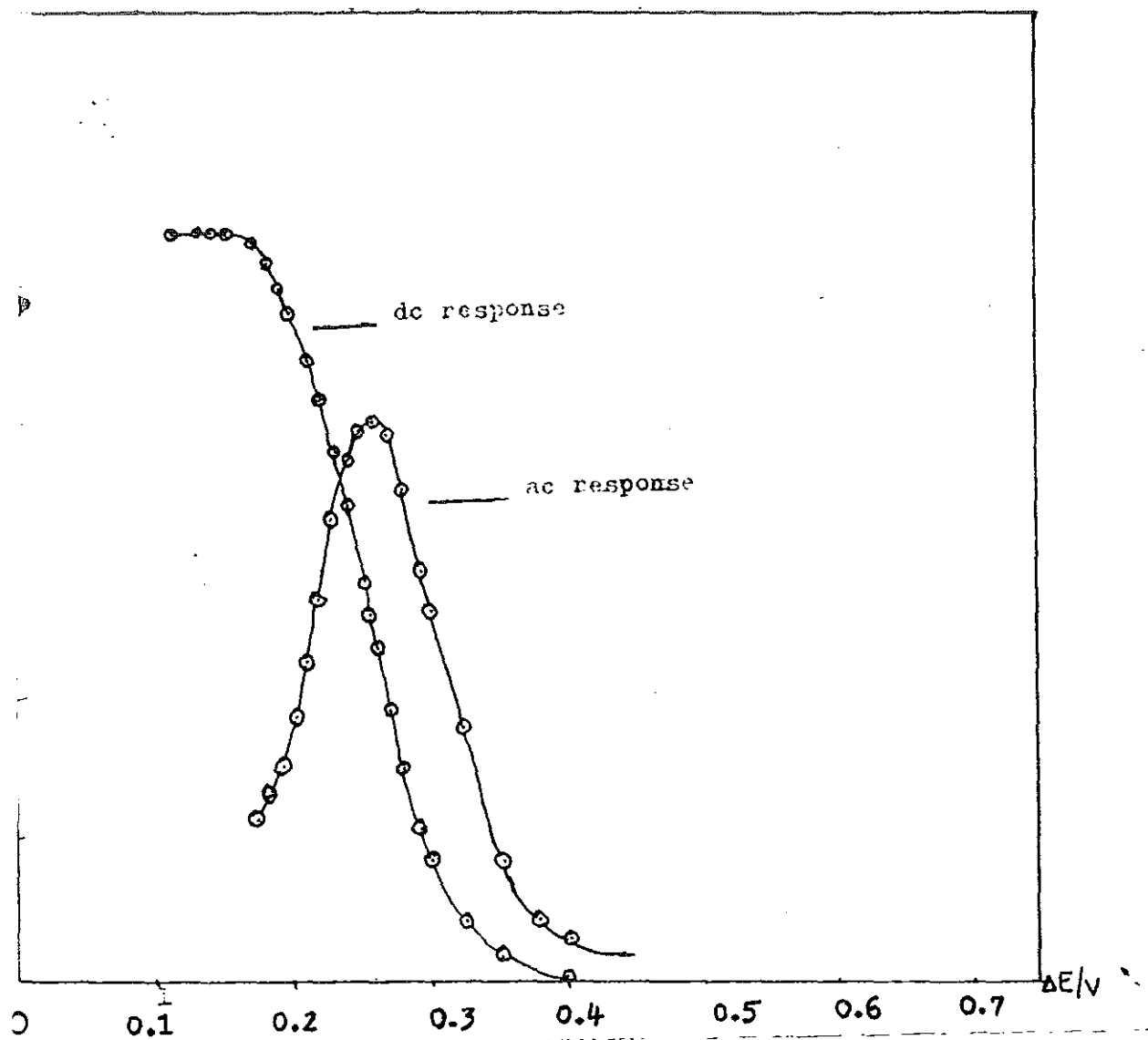
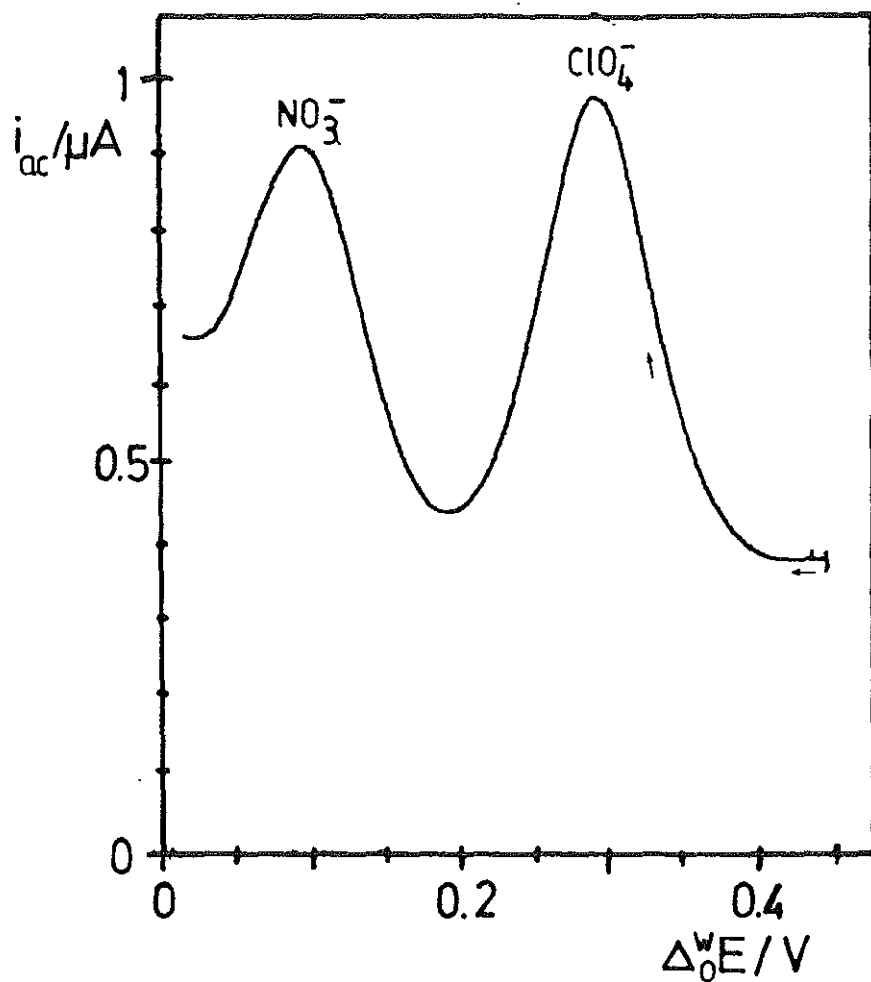


Fig. 8 The dependence of the flow injection peak current on the applied potential difference for the transfer of ClO_4^- ion across membrane stabilized water/nitrobenzene interface. 10 mM MgSO_4 and 10 mM CVTPB are the supporting electrolytes in aqueous and organic phases, respectively. Membrane: S & S regenerate cellulose of 20 μm pore size. Ac: $f = 70$ Hz, U_{in} (rms) = 1.9 mV. Flow rate was 0.166 mls^{-1}



g. 9. Ac cyclic voltammograms of the transfer of ClO_4^- and NO_3^- ions across membrane stabilized water/nitrobenzene interface. $f = 35$ Hz, membrane: PT 325 dialysis membrane. All other conditions are as in Fig 8.

under experimental conditions, proves its reversibility. Therefore, from these results it is possible to use NO_3^- ion as an internal standard instead of ClO_4^- ion.

The results also indicate that the system can be applied to the study of the transfer of ClO_4^- and NO_3^- ions across water/nitrobenzene interface and hence, can also be applied to the study of the transfer of Na^+ and K^+ ions across water/nitrobenzene membrane stabilized interface. The potential window was determined for the base electrolytes in the presence of different ionophores such as B15C5, DB24C8, and 18C6. The voltammograms obtained are shown by dash lines in Figs. 10, 11, and 12. As can be seen from these voltammograms the potential window is almost the same in all the cases. This indicates that the transfer of the ions of the base electrolytes is not affected by the presence of the ionophores.

The voltammograms of the transfer of Na^+ and K^+ ions across water/nitrobenzene membrane stabilized interface in the presence of 10 mM of B15C5, DB24C8, and 18C6 are given in Figs. 10, 11 and 12 in solid lines. The results obtained from these figures are summarized in Table I. The peak to peak separation (which is one of the diagnostic criteria of diffusion controlled reversible process) in all the cases it is in good agreement with the value set by Nicolson and Shain [68], 60 mV/z.

For diffusion controlled reversible process the half-peak potential should precede the peak potential by 0.056 v, in this regard, the values given in Table 1 are within reasonable range.

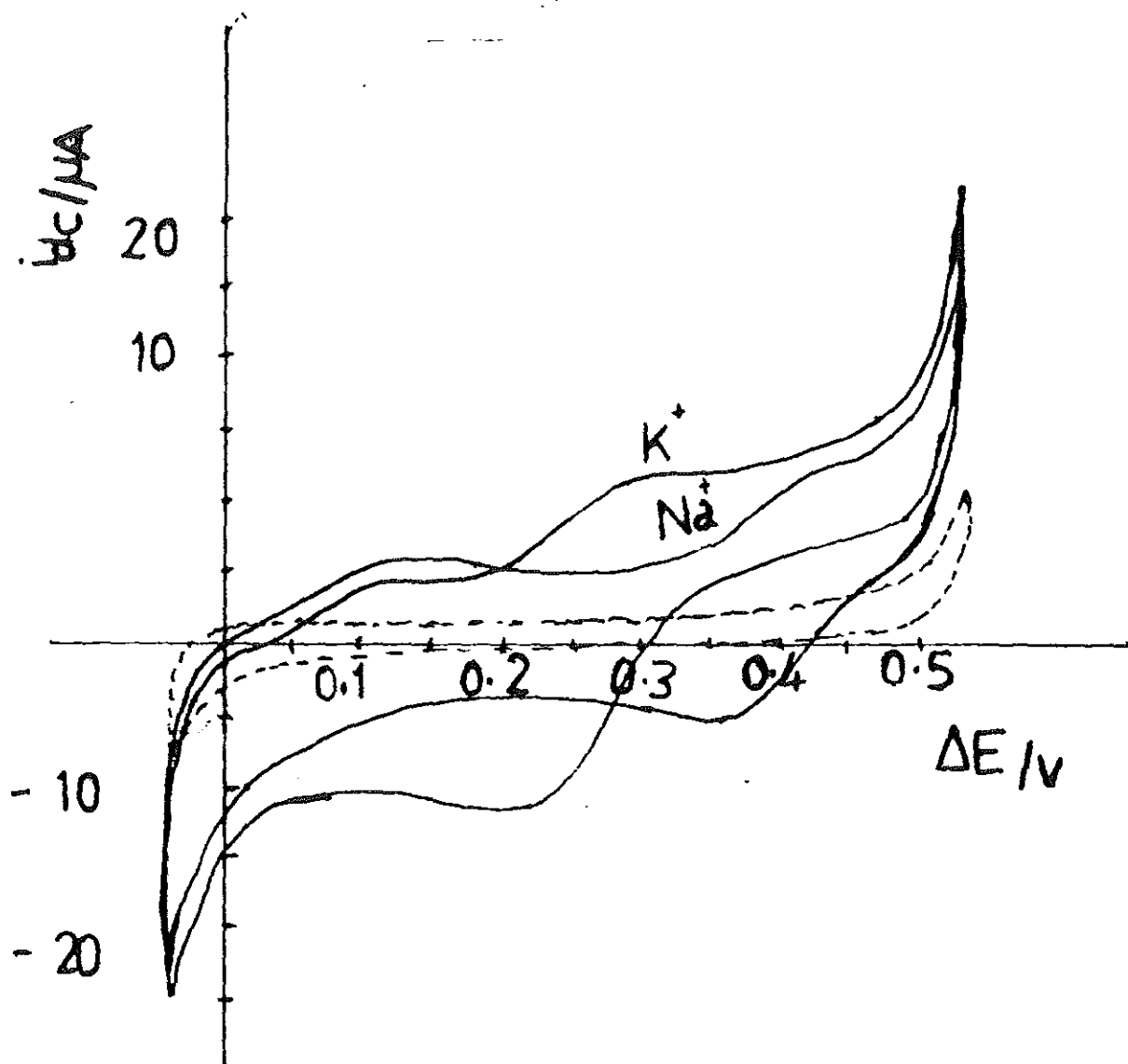
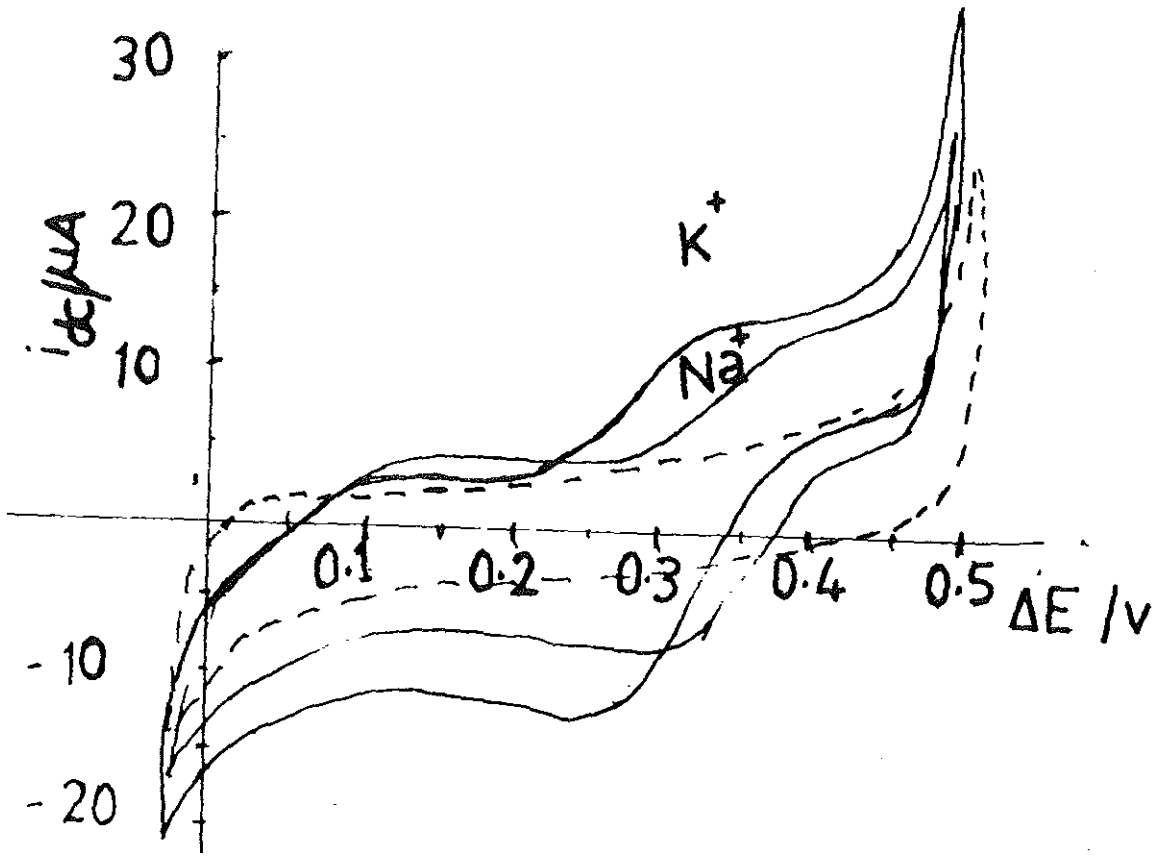


Fig. 10. Dc cyclic voltammograms of the transfer of K^+ and Na^+ ions across membrane stabilized water/nitrobenzene interface in the presence of B15C5. Electrolytes: 10 mM $MgSO_4$ and 10 mM CVTPB in aqueous and organic phases, respectively. Sweep rate : 25 mvs^{-1}



ig. 11. Dc cyclic voltammograms of the transfer of K^+ and Na^+ ions across membrane stabilized water/nitrobenzene interface in the presence of DB24C8 in the organic phase. All other conditions as in Fig. 10

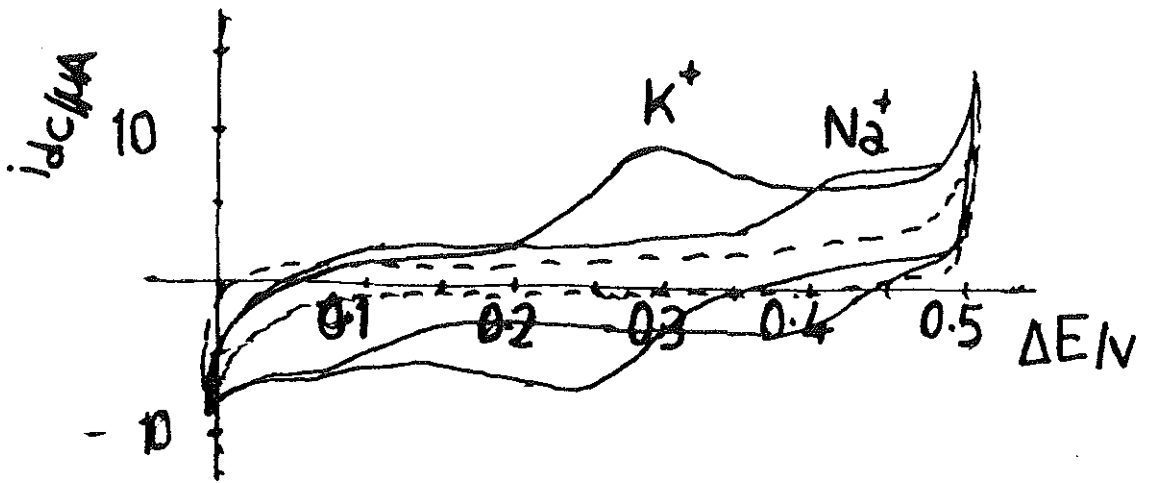


Fig. 12 Dc cyclic voltammograms of the transfer of K^+ and Na^+ across membrane stabilized water/nitrobenzene interface in the presence of 18C6 in the organic phase. All other conditions as in Fig. 10.

Table I. Results obtained from the evaluation of DC cyclic voltammograms. E_{p^+} is the peak potential in the positive direction, E_{p^-} is the peak potential in the reverse direction, $E_{p/2}$ is the half-peak potential and ΔE_p

	B15C5		DB24C8		18C6	
	Na ⁺	K ⁺	Na ⁺	K ⁺	Na ⁺	K ⁺
E_{p^+}/v	0.425	0.285	0.375	0.320	0.425	0.292
E_{p^-}/v	0.375	0.225	0.320	0.265	0.375	0.235
$\Delta E_p/v$	0.05	0.06	0.055	0.055	0.05	0.057
$E_{p/2}/v$	0.375	0.240	0.330	0.275	0.390	0.242
$E_p - E_{p/2}/v$	0.05	0.045	0.045	0.045	0.035	0.0495
mid pot./v	0.4	0.255	0.35	0.29	0.4	0.26

The value for the transfer of Na^+ in the presence of 18C6 is lower than the expected one.

The mid potentials are listed in Table I. These values are assumed to be similar to the quantity $\Delta E_{1/2}$, which is analogous to the reversible polarographic half-wave potential of the transfer of Na^+ and K^+ .

Figs. 13, 14, and 15 show the ac cyclic voltammograms of the transfer of Na^+ and K^+ , in the presence of 10 mM of DB24C8, and B15C5 and DB18C6. These figures along with Figs 10, 11 and 12 show the influence of different ionophores on the transfer of Na^+ and K^+ across water/nitrobenzene interface.

In the absence of neutral carrier, the transfer of a highly hydrophilic cation across the oil/water interface takes place at a positive potential beyond the polarizable potential range. The presence of ionophore in the organic phase generally shifts the transfer potential of the cation to a more negative potential within the polarizable range [48]. This shift in the transfer potential for Na^+ and K^+ was observed in all the voltammograms. This is attributed to the ability of the crown ethers to form complexes with alkali and alkaline earth metal cations [72]. The ac current peak potential lies exactly on the position of the half-wave potential of the dc cyclic voltammograms. Therefore, the half-wave potentials for the transfer of Na^+ and K^+ was determined directly from the peaks of the ac cyclic voltammograms given in Figs 13, 14 and 15. By considering NO_3^- as an internal standard and from the shift of the half-wave potential it is possible to estimate the

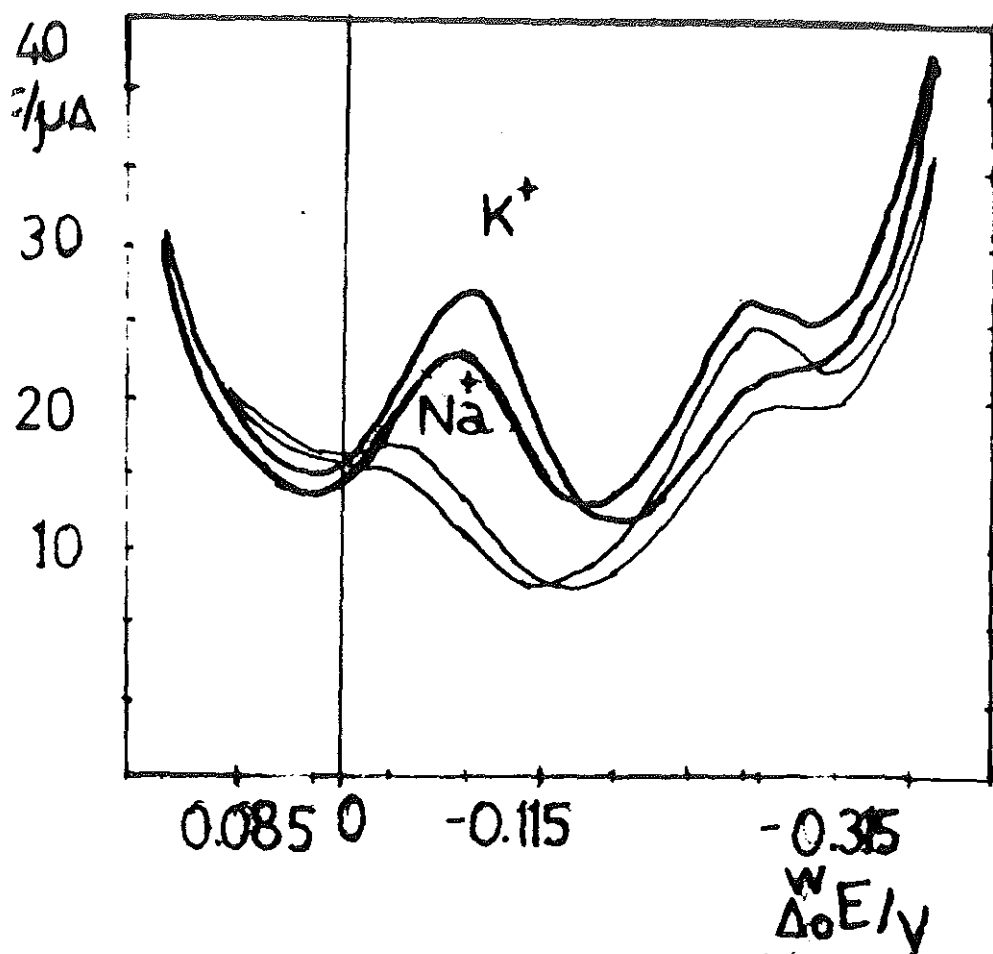


Fig. 13 Ac cyclic voltammograms of the transfer of K^+ and Na^+ across membrane stabilized water/nitrobenzene interface in the presence of DB24C8 in the organic phase. sweep rate: 25 mVs^{-1} , $f = 35 \text{ Hz}$.

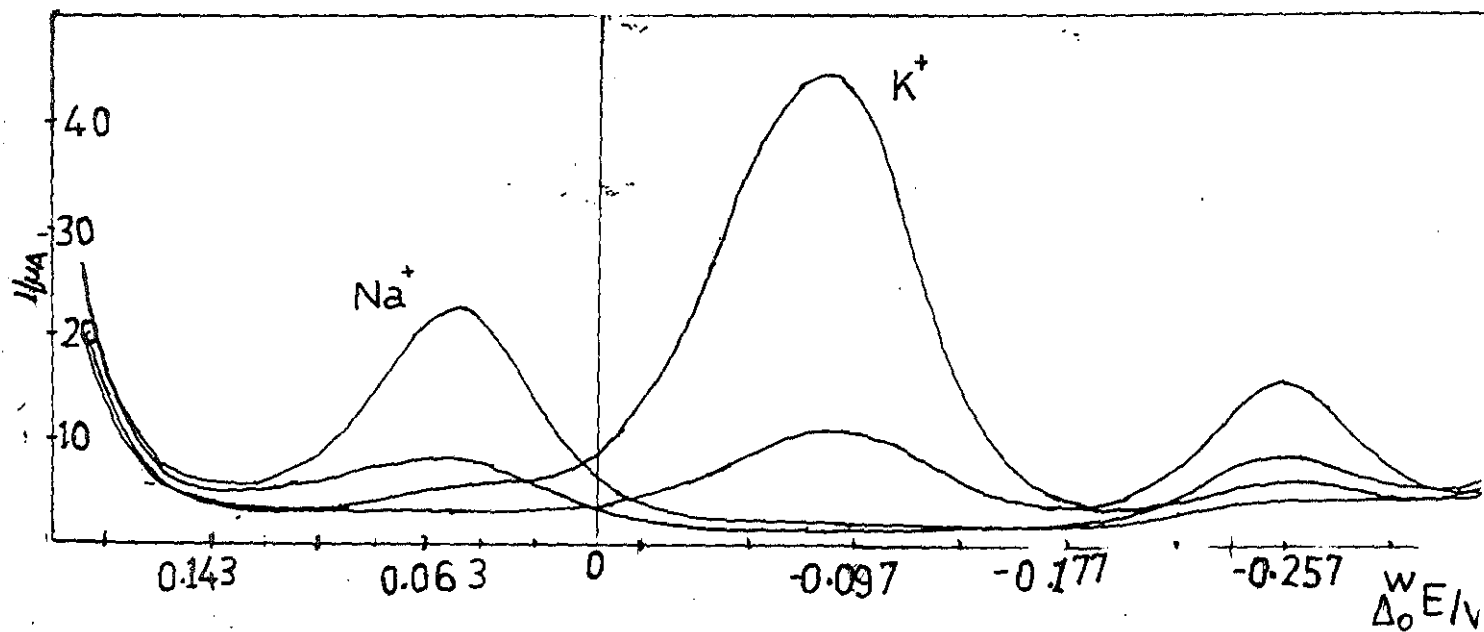


Fig. 14 Ac cyclic voltammograms of the transfer of K^+ and Na^+ ion across membrane stabilized water/nitrobenzene interface in the presence of B15C5 in the organic phase. All other conditions as in Fig. 13.

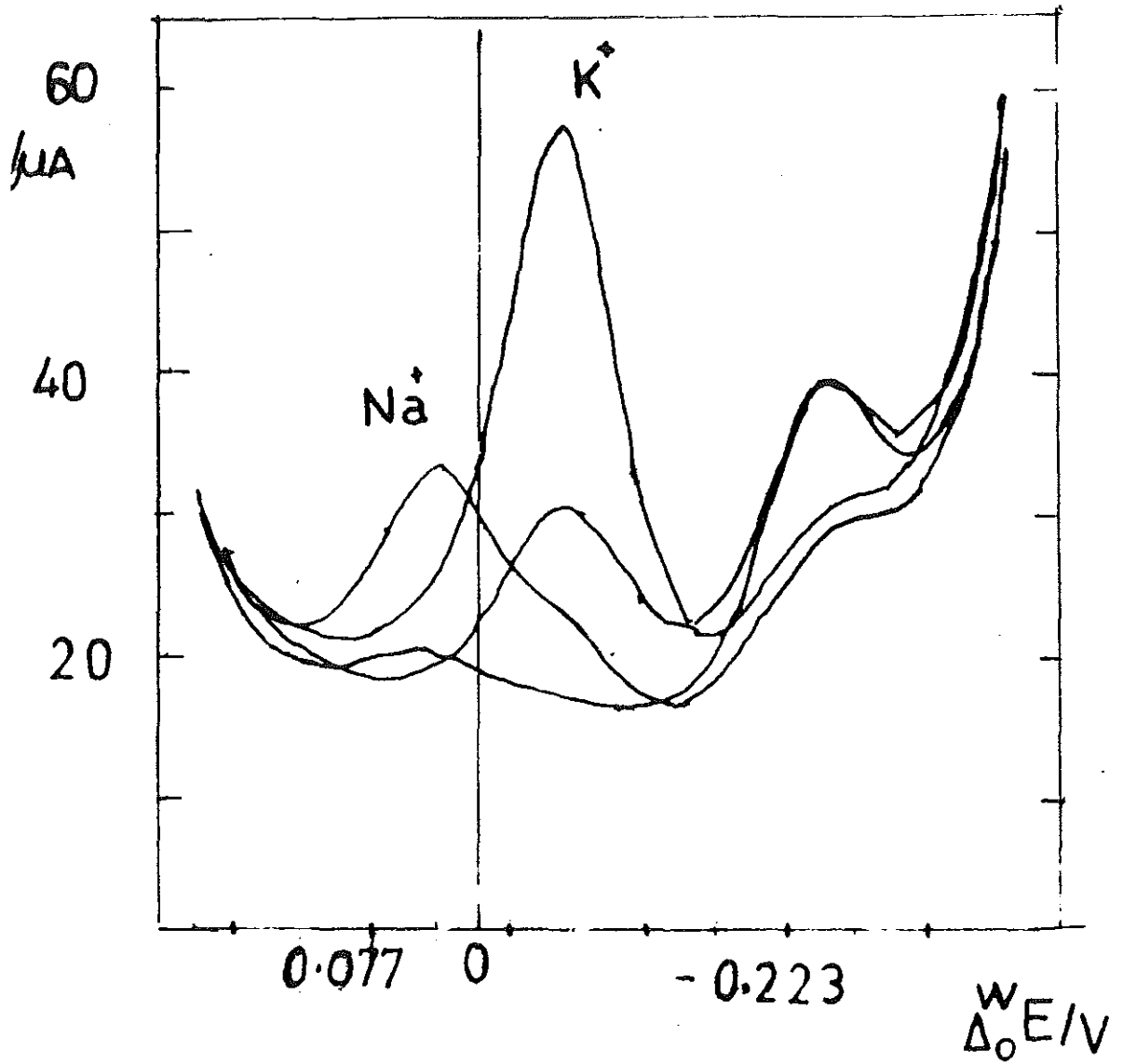


Fig. 15 AC cyclic voltammograms of the transfer of K^+ and Na^+ ions in the presence of DB18C8 in the organic phase. All other conditions as in Fig. 13.

Table II. The stability constants and half-wave potentials obtained by different methods in comparison with some literature values.

	B15C5		DB24C8		DB18C6		18C6	
	Na'	K'	Na'	K'	Na'	K'	Na'	K'
$\Delta_o^w \phi_{1/2}/v$ (ac)	.055	-0. 086	- .00 3	- 0.05 7	0.0 21	- 0.07 1	-	-
$\log K_{st}$	7.07	9.56	8.0 5	7.07	7.6 4	7.30	-	-
$\Delta_o^w \phi_{1/2}/v$ (FIA, ac)	-	-	- 0.0 28	- 0.04 8	-	-	-	-
$\log K_{st}$	-	-	8.4 7	6.92	-	-	-	-
$\Delta_o^w \phi_{1/2}/v$ (FIA, dc)	-	-	-	-	-	-	0.0 97	- 0.048
$\log K_{st}$	-	-	-	-	-	-	6.3 6	6.92
$\log K_{st, lit.}^1$	-	-	7.6 7	7.10	7.3 0	7.11	-	-

¹ All values are taken from ref.[80].

stability constant of the metal cation-ionophore complex using equation (24). The values obtained in this way are given in Table II, in comparison with some of the literature values. The values for K^+ ion are in good agreement with the literature values. But the stability constants estimated for Na^+ ion-ionophore complex are different from the literature values.

The relative shift of potential for K^+ ion transfer is highest when B15C5 was used and when DB24C8 was used for Na^+ (Table 1). The observation made by Mallinson and Truter [73] indicates that potassium ions form a 1:2 complex with B15C5. Since the ionophore exists in excess, we expect the formation of 1:2 complex between K^+ and B15C5. Therefore, the cooperative effect of the two crown ether rings may contribute to the formation of a stable complex and hence selective transfer of K^+ at more negative potential than Na^+ which forms 1:1 complex. The value of the stability constant estimated (Table II) based on a 1:2 complex formation for K^+ -B15C5 strengthens this idea.

The other factor which was believed to contribute to the formation of a stable complex between alkali metal cations and crown ethers is the hole-size cation-diameter principle [74]. When the size of the hole of the crown ether ring and the diameter of the cation are comparable, stable complex are assumed to be formed, because the cation fits into the cavity of the ring of the crown ethers and is held firmly. This hole-size cation-diameter relationship can be observed in two ways: ionophore selectivity for cations of a certain size, or cation

selectivity for ionophore of certain size. Table III gives the hole-size and the cation diameter of some crown ethers and cations, respectively.

Table III. Hole-size and cation diameter of some ionophores and cations respectively (taken from ref. [74])

ionophores	hole-size(Å)	cations	diameter(Å)
B15C5	1.7-2.2	Na ⁺	1.94
18C6	2.6-3.2	K ⁺	2.66
DB24C8	>3.2	NH ₄ ⁺	2.86

The data in this table suggest that, for example, B15C5 should be selective for Na⁺ over K⁺. Similarly, since DB24C8 is larger than any of the crown ethers listed in the table, one should assume that B15C5 would be selective for Na⁺ than DB24C8. But from the relative shift of the transfer potential (Table I) and the values of stability constants (Table II), it is possible to see that the hole-size cation diameter relationships do not hold. According to Reisse and Michaux's report based on the enthalpies of binding between Na⁺ and K⁺ and 12-18 membered crown ethers, the hole-size cation diameter relationships do not obeyed [75]. Gokel et al [76, 77] have investigated the hole-size cation diameter relationships for crown ether rings ranging from 12-crown-4 to 24-crown-8 based on the equilibrium stability constants of the complex between these crown ethers and Na⁺, K⁺, NH₄⁺ and Ca²⁺ ions in anhydrous methanol solution. They concluded that the widely recounted "hole-size cation-diameter principle" was not applicable to

the species of simple macrocycles they have studied. These studies, which were based on ion-selective electrodes and calorimetric methods show that K^+ cation was bound most strongly by all the macrocycles in the series and the strongest binding for all cations studied was that with 18C6. According to these studies, there are at least four factors that contribute significantly to the binding of cations by crown ethers; a) the cation-diameter hole-size relationship, b) the solvation enthalpies and entropies of cations and the ligand, c) the number of donor atoms participating in binding, d) the conformation of the bound and unbound macrorings.

The results from cyclic voltammeteries correlate well with the results obtained in the above methods in that a) the relative shift of potential for the transfer of K^+ ion was pronounced with all the ionophores studied (Table I), b) the estimated stability constants and the shift in the half-wave potential of the transfer of Na^+ and K^+ were contrary to the hole-size cation-diameter principle.

4.2. Flow Injection Amperometric Investigation

When a constant potential is applied across the membrane stabilized interface an equilibrium is established across the interface. This equilibrium can be perturbed by a concentration pulse. The concentration pulse is realized by an injection of a small amount of the ion under study into the carrier stream.

In flow injection analysis the axial concentration profile of the ion under investigation which is caused by a concentration pulse, is monitored by the current-time response. This current-time response can be of dc or ac mode (see chapter 2). Typical ac and dc current-time responses when a 25 μ l of the standard solution of KNO_3 was injected into the carrier solution at different applied potential difference are shown in Fig. 16. By evaluating the peak heights of these current-time responses at a given potential difference, it is possible to get the dependence of the flow-injection peak-current on the applied potential difference.

Figs 17 and 18 show the ac response for the dependence of flow injection peak-current on the applied potential difference when 7 mM metal nitrate was injected into 10 mM MgSO_4 carrier solution in the presence of 10 mM DB24C8 dissolved in the organic phase. From these results it is possible to determine the half-wave potential of the facilitated transfer of metal ions taking NO_3^- as an internal standard as indicated above. The half-wave potentials determined by using NO_3^- as an internal standard are summarized in Table II. By using these half-wave potentials the stability constants of the metal-ionophore complex was also estimated. These values are given in Table II. As can be seen from this table, again the values for Na-DB24C8 complex are higher by one magnitude order than the literature values. Those of K-DB24C8 complex are in a good agreement with the literature values. Figs 19 and 20 show the dc response of the dependence of the flow-injection

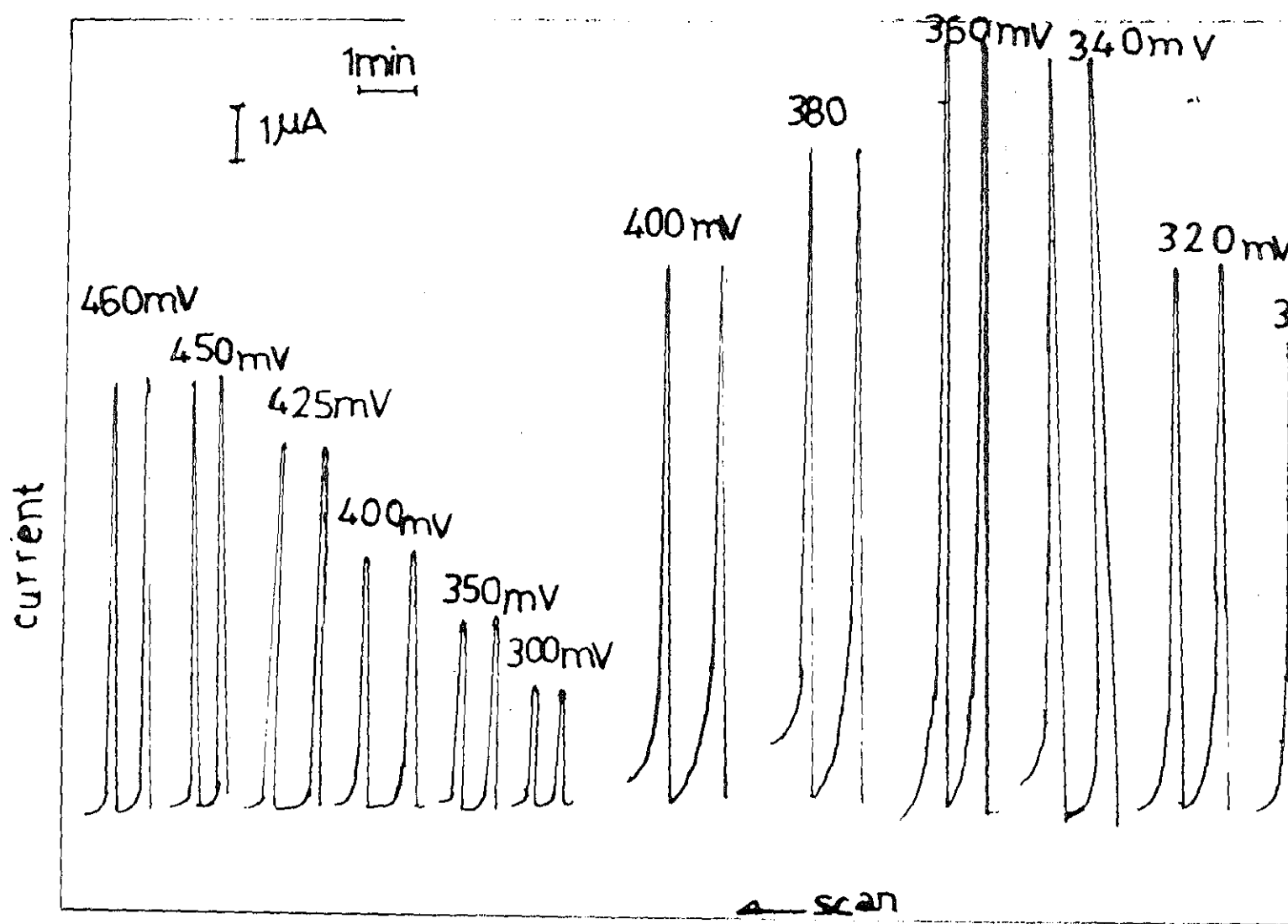


Fig. 16 Typical flow injection peak-current time responses for ac and dc modes in the transfer of K^+ ion across membrane stabilized water/nitrobenzene interface.

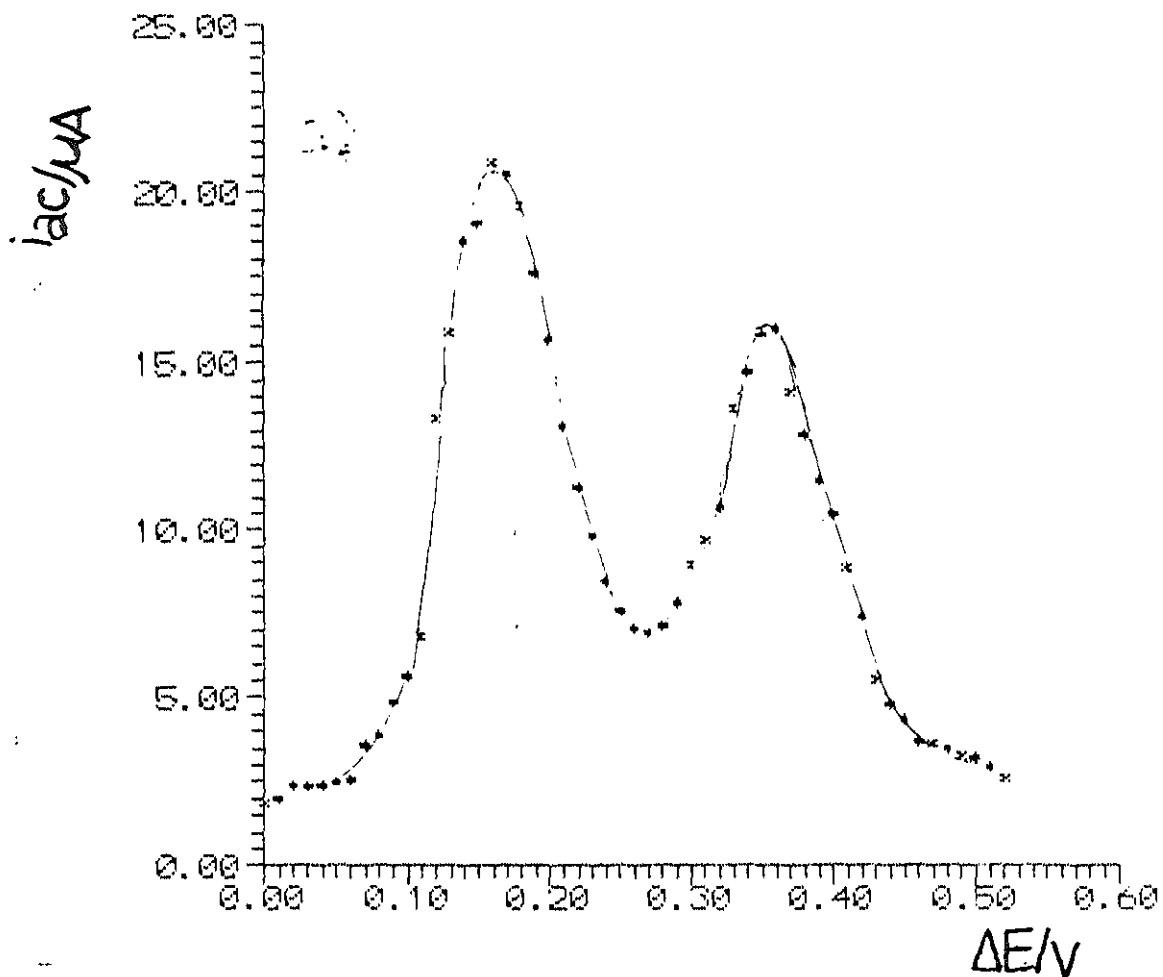


Fig. 17 The flow injection peak current - applied potential relationship for the transfer of 7 mM K^+ across membrane stabilized water/nitrobenzene interface for the ac mode in the presence of DB24C8 in the organic phase. $f = 35$ Hz.

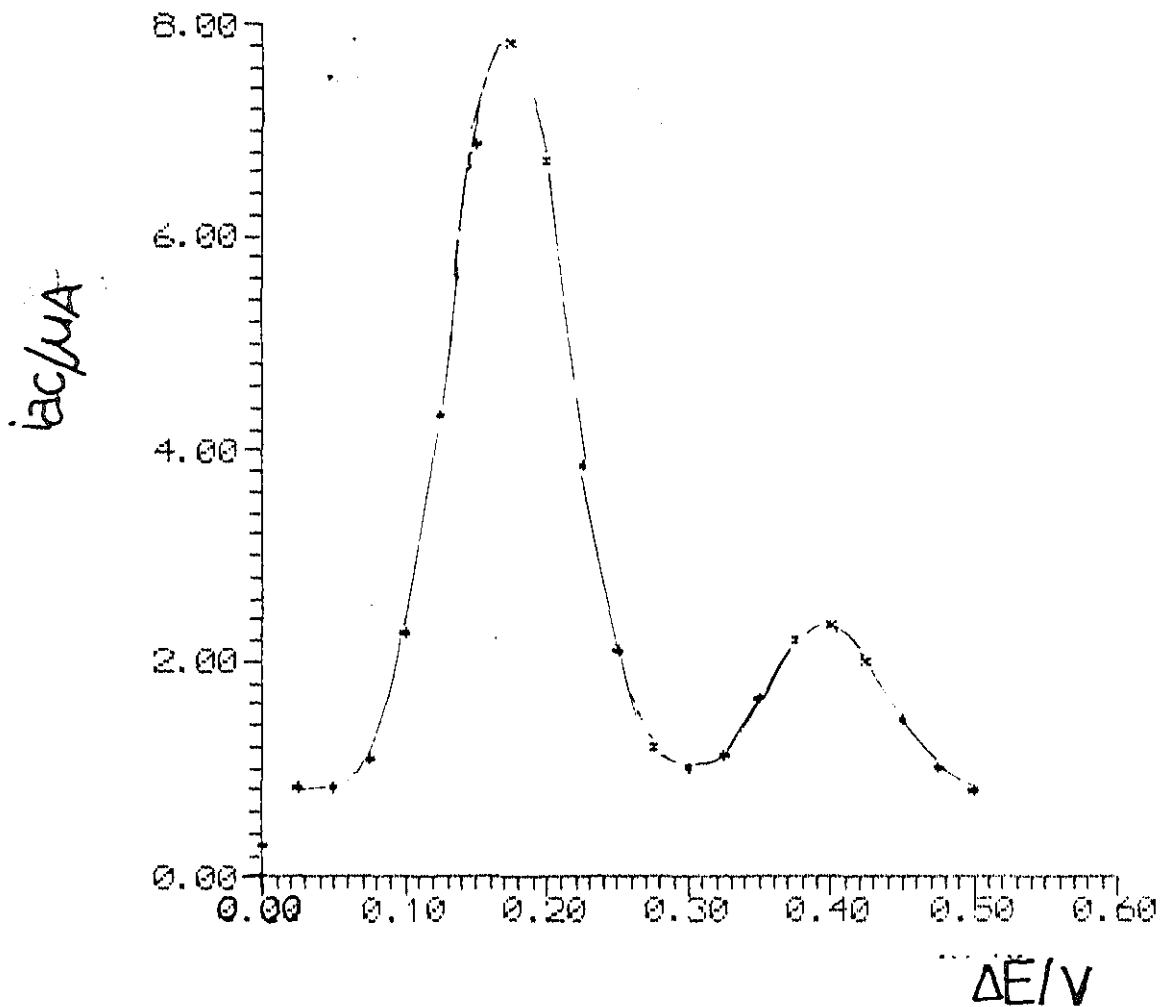


Fig. 18 The flow injection peak current - applied potential relationship for the transfer of 7 mM Na⁺ across membrane stabilized water/nitrobenzene interface in the presence of DB24C8 in the organic

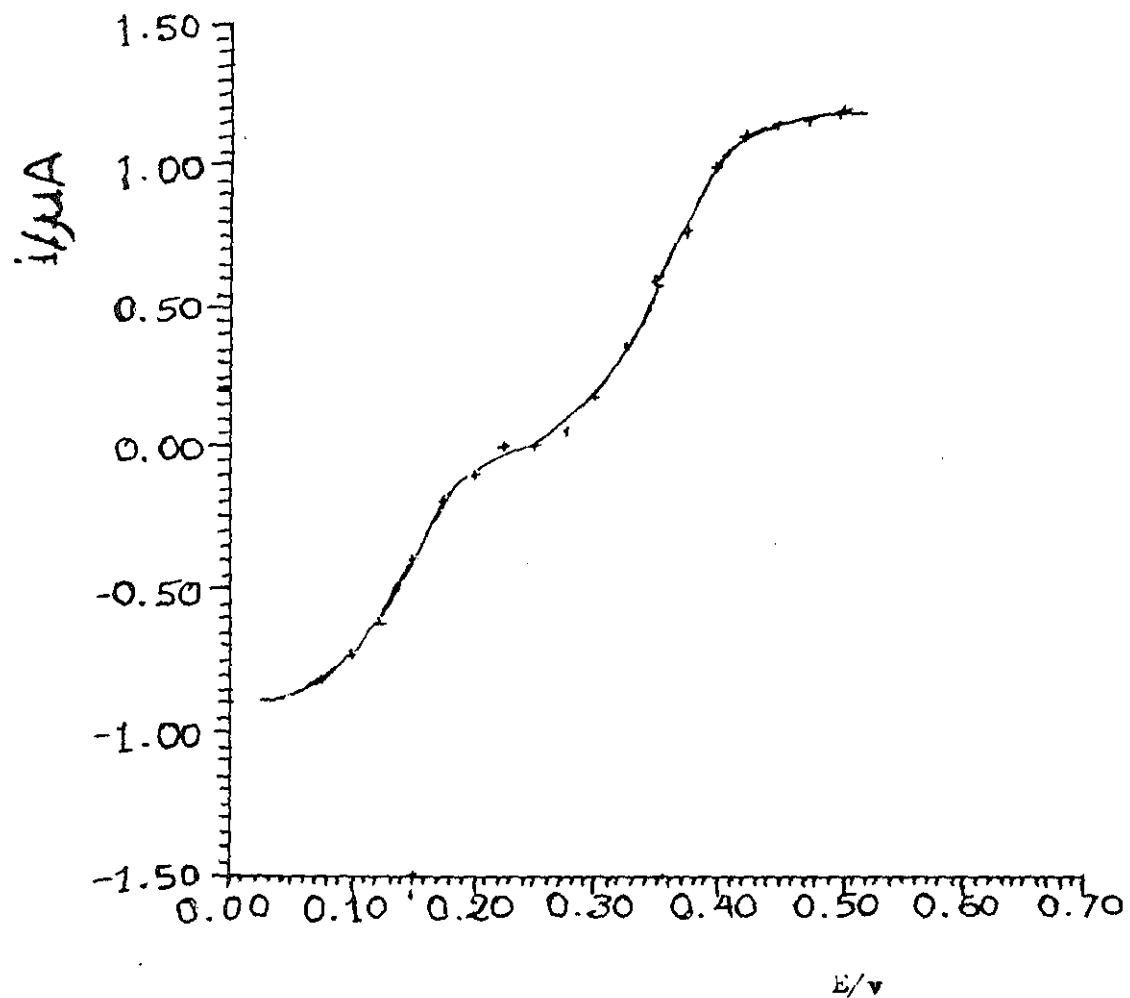


Fig. 19 The dependence of the flow injection peak current on the applied potential difference for the transfer of K^+ ions across membrane stabilized water/nitrobenzene emulsion in the organic phase.

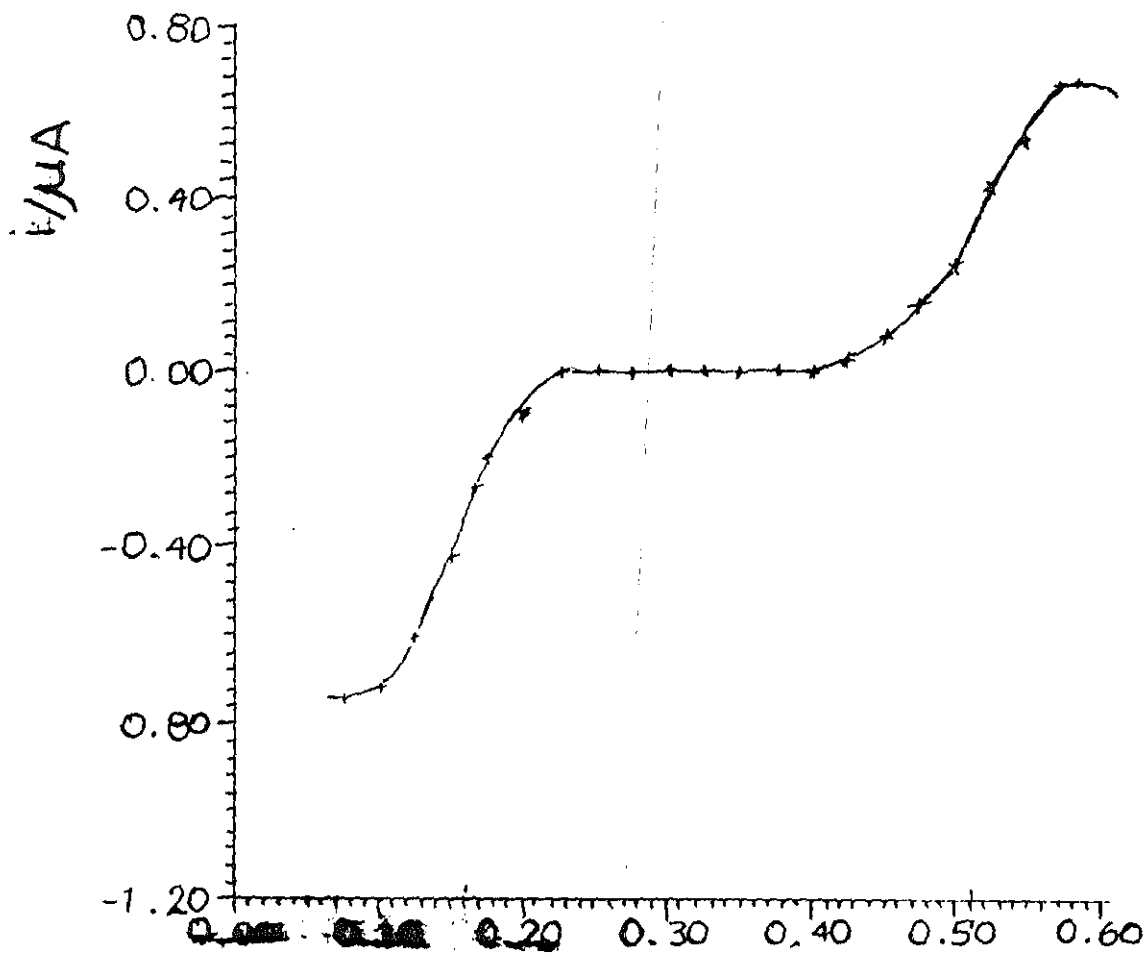


Fig. 20 The dependence of the flow injection peak current on the applied potential difference for the transfer of Na^+ ions across membrane stabilized water/nitrobenzene interface in the presence of 18C6 in the organic phase.

peak-current on the applied potential difference when 7 mM metal nitrate was injected into the carrier solution in the presence of 10 mM 18C6 dissolved in the organic phase. The half-wave potentials and stability constants obtained using these figures are given in Table II. This further substantiates the feasibility of the determination of the stability constants of the metal cation-ionophore complexes by using NO_3^- as an internal standard.

Fig 21 and 22 show the dc response for the dependence of flow-injection peak-current on the applied potential difference for the transfer of 11 mM metal ions across membrane stabilized water/nitrobenzene interface in the presence of DB24C8 and B15C5, respectively. As can be observed from the two figures the transfer of K^+ and Na^+ starts at low potential difference and increase passing through the half-wave potential difference and reaches a point where the current is independent of the applied potential difference. This gives a typical S-shaped i - E curve. It is also evident from figure 21 that the difference in the half-wave-potentials of K^+ and Na^+ ions is very small (0.06v) when DB24C8 was used and is large as can be seen from Fig. 22, when B15C5 was used (0.138v). Based on these values it is possible to conclude that B15C5 is an appropriate ionophore for simultaneous determination of K^+ and Na^+ ions while DB24C8 is poor to be used for this purpose.

Fig 23 shows the typical flow injection current-time responses obtained for the transfer of sodium standard solution of different concentrations across the membrane stabilized

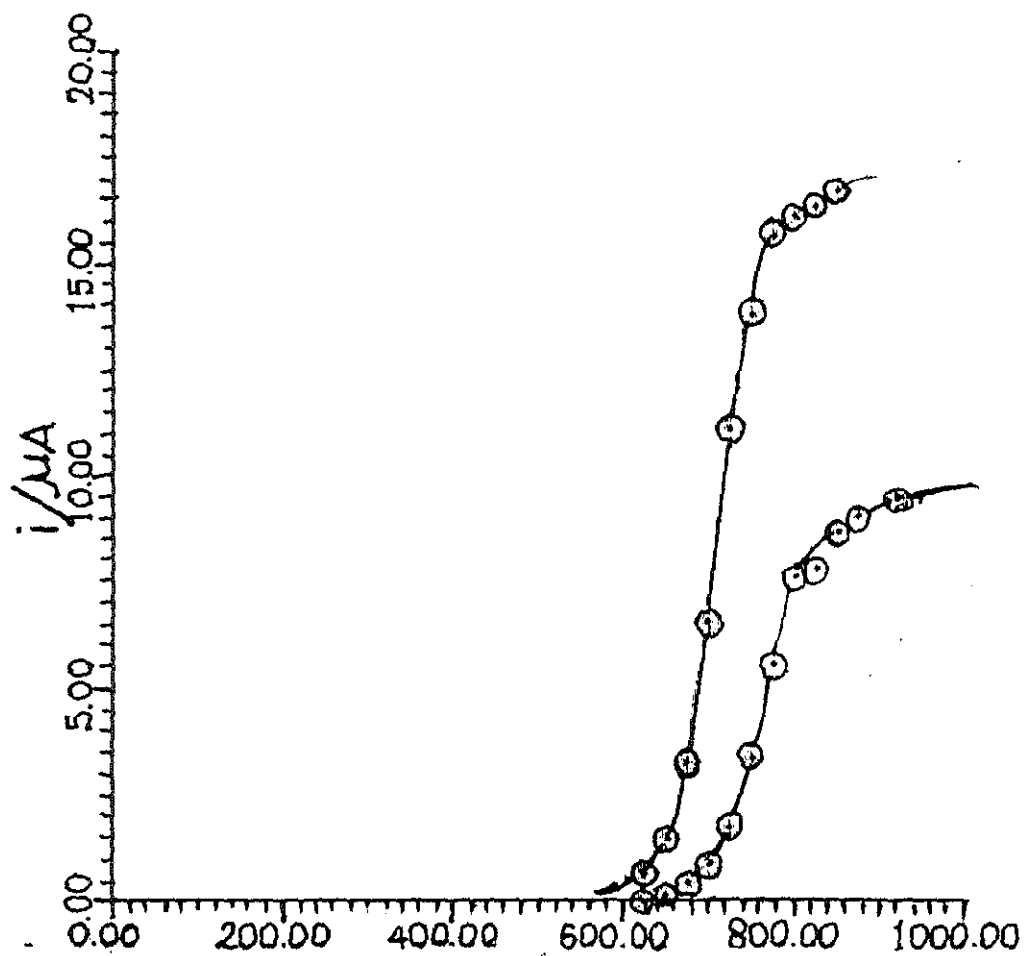


Fig. 21 The dependence of the flow injection peak current on the applied potential difference for the transfer of K^+ and Na^+ ions across membrane stabilized water/nitrobenzene interface in the presence of DB24C8 in the organic phase.

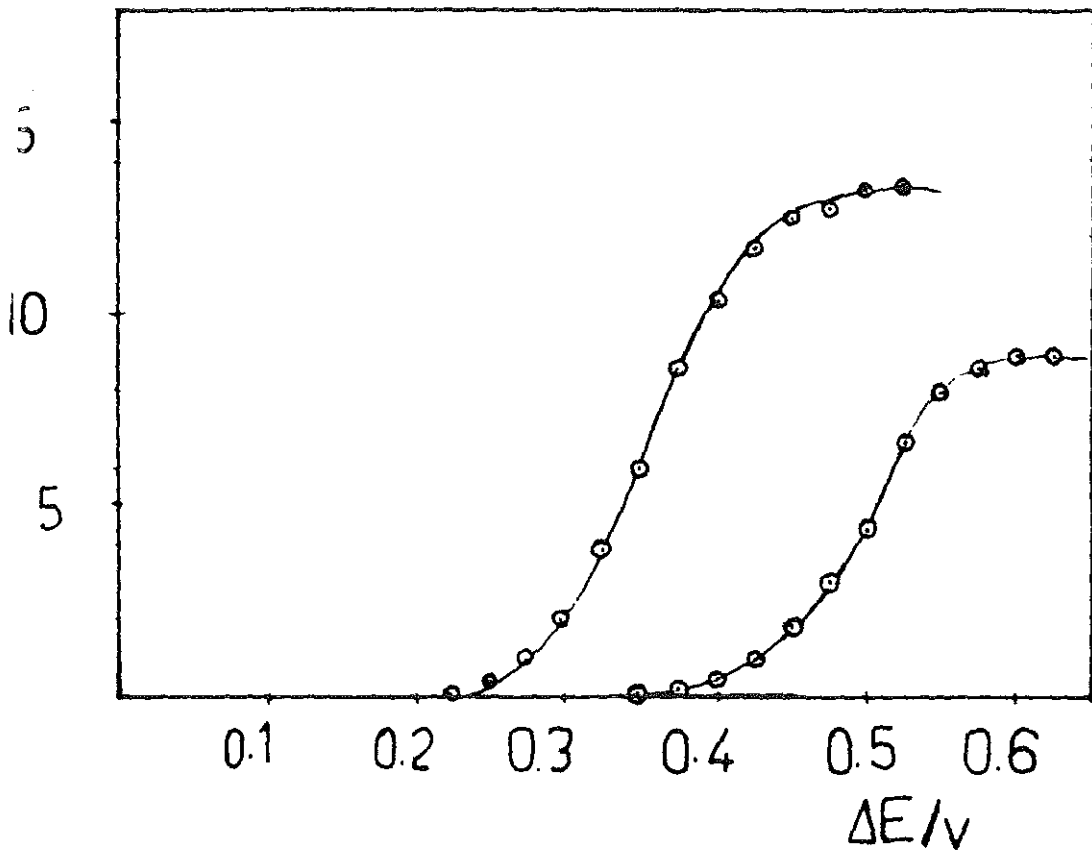


Fig. 22 Dependence of the flow injection peak current on the applied potential difference for the transfer of K^+ and Na^+ ions across membrane stabilized water/nitrobenzene interface in presence of B15C5 in the organic phase.

current

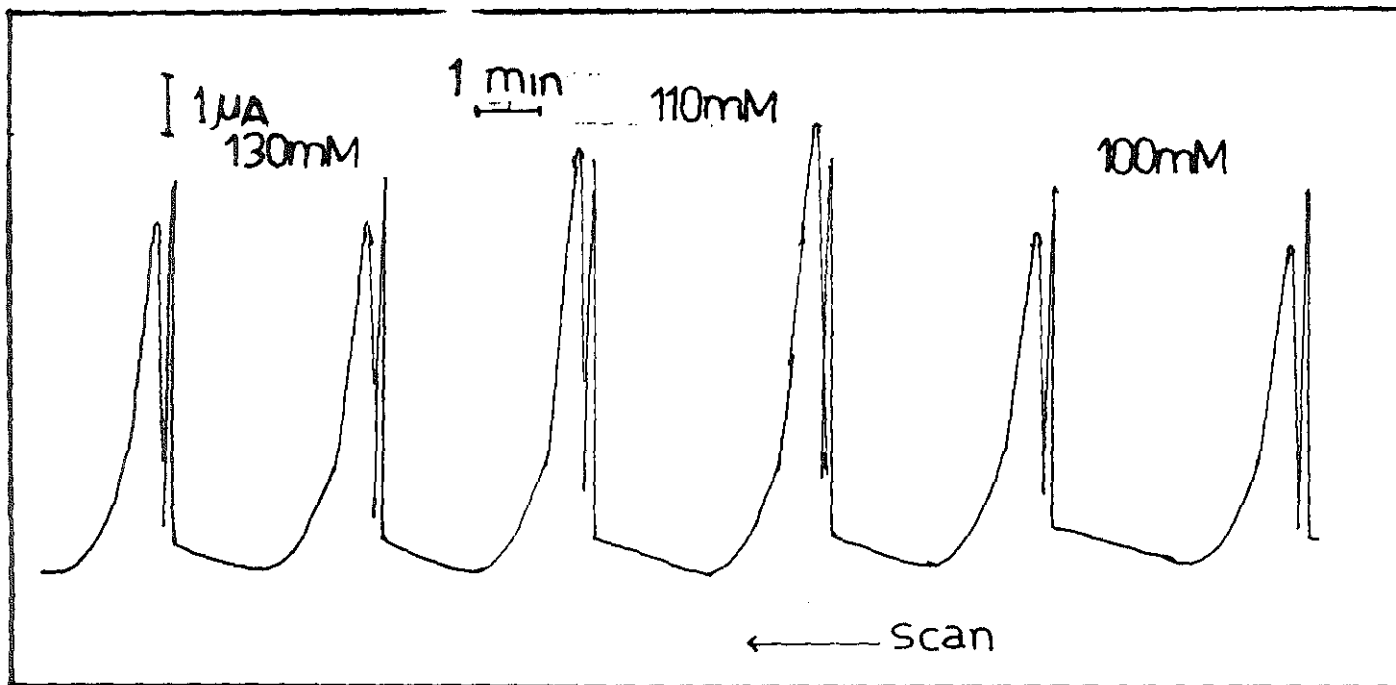


Fig. 23 Typical flow injection analysis peaks for the transfer of different concentrations of Na^+ ion across membrane stabilized water/nitrobenzene interface.

water/nitrobenzene interface. Unlike those shown in Fig 16, double peaks are observed in all the concentrations.

Under normal conditions the total applied potential (E_{ap}) to the cell consists of the working potential (E_w) of the cell and a potential drop through the solution owing to its resistance (iR).

$$E_{ap} = E_w + iR. \quad (42)$$

The iR voltage drop was compensated by a positive feed-back of the four electrode potentiostat. But when there is any perturbation in the solution by either dilution or any other phenomenon which increase or decrease the resistance of the solution a change in iR drop would be observed. This leads to a change in the applied potential difference (E_{ap} , eq.42) and thus a changing current due to the change in potential with time ($\partial E/\partial t$) is expected. As can be seen from Table 4 the injected NaNO_3 solution has a higher conductance than the carrier and thus we assume the double peak is caused by resistance of the electrolyte. The resistance of the solution can be kept at minimum by either increasing the concentration of the electrolyte or by increasing the distance between the sample loop and the sensor to allow the dispersion of the sample. Fig. 24 gives typical flow injection peaks after elongating the distance between the sample loop and the sensor.

B15C5, which was considered as an ionophore of choice in simultaneous determination of Na^+ and K^+ and DB24C8 which was considered as a poor one were employed for the determination of Na^+ and K^+ ions in blood serum. This was done in two ways:

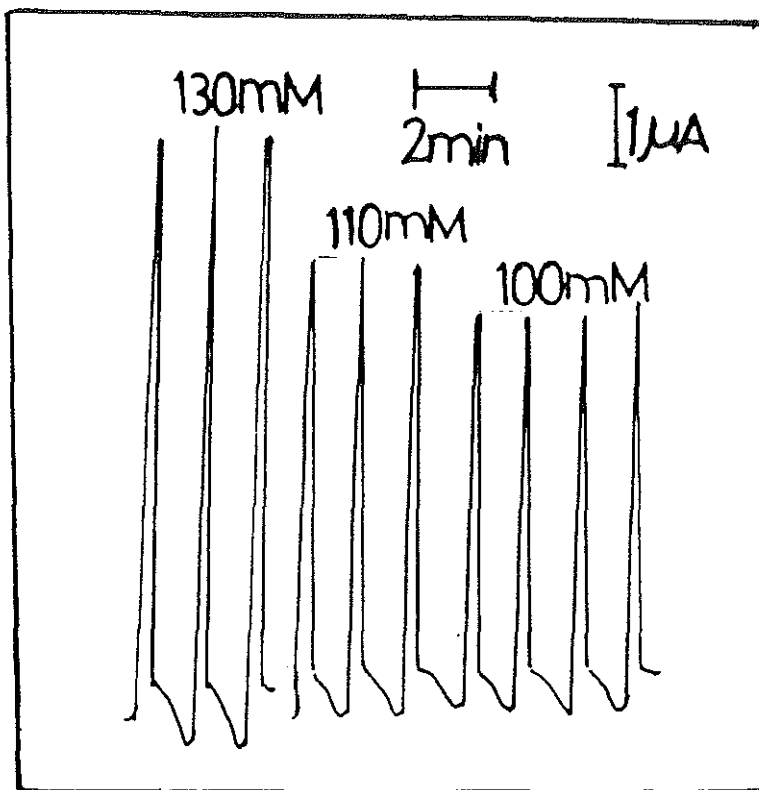


Fig. 24 Typical flow injection analysis peaks for the transfer of different concentrations of Na^+ ion after elongation of the distance between the sample loop and the sensor.

direct and indirect measurements. In the direct measurement the blood serum was directly injected into the carrier solution and the flow injection peak current determined. In the indirect measurement the blood serum was diluted in 1:50 ratio and the diluted solution was injected into the carrier solution and the corresponding peak current was recorded.

Table IV. The limiting equivalent ionic conductance of Na^+ , NO_3^- , Mg^{2+} , and SO_4^{2-} (taken from ref. [78]) and the calculated specific conductivities of NaNO_3 and MgSO_4 . $\Lambda = \times 10^{-4} \text{ m}^2 \text{ S mol}^{-1}$, $\kappa = \text{m}^2 \text{ S}$.

Λ_{Na^+}	$\Lambda_{\text{NO}_3^-}$	$\Lambda_{\text{Mg}^{2+}}$	$\Lambda_{\text{SO}_4^{2-}}$	K_{NaNO_3}	K_{MgSO_4}
50.08	71.42	53.00	80.00	1.22×10^{-3}	1.33×10^{-4}

The concentration of the metal cations in the original sample was calculated. Only direct measurement was done in the case of DB24C8. The standard solutions were injected into the carrier solution immediately before the sample and after the sample. Calibration curves were plotted for both injections of the standard solutions.

A high concentration of Na^+ ion in blood serum would interfere in the determination of K^+ amperometrically as the current measured in amperometry is the sum of the partial current of the particular ionic species in the sample.

This can be written as [50]

$$i = \sum K_j C_j \quad (42)$$

where K_j is the partial sensitivity of the ion j at concentration C_j . AS was observed from Figs 14 and 22 the

half-wave potentials of the two ions Na^+ and K^+ are reasonably well separated when their transfer across membrane stabilized water/nitrobenzene interface was facilitated by B15C5. Therefore, advantage can be taken of the potential-dependence response of the amperometric detector, and both ions can be determined simultaneously from two measurements at different electrode potentials, ΔE_1 and ΔE_2 . The corresponding peak current i_{p1} and i_{p2} are described by the following linear equation [53].

$$i_{p1} = S_{1,\text{K}^+} C_{\text{K}^+} + S_{1,\text{Na}^+} C_{\text{Na}^+} \quad (43)$$

$$i_{p2} = S_{2,\text{K}^+} C_{\text{K}^+} + S_{2,\text{Na}^+} C_{\text{Na}^+} \quad (44)$$

where S_{i,K^+} and S_{i,Na^+} are the partial sensitivities of K^+ and Na^+ ion ($i = 1, 2$). The partial sensitivities of the ions at two applied potentials ΔE_1 and ΔE_2 can be obtained either from the slope of the respective ion at ΔE_1 and ΔE_2 or by injecting standard solutions.

The calibration curves for the flow injection amperometric determination of Na^+ and K^+ in blood serum in the presence of 10 mM B15C5 and DB24C8 at two different applied potential differences ΔE_1 and ΔE_2 (0.350v and 0.500v) are given in the Appendix. The electrode potential differences ΔE_1 and ΔE_2 were chosen so that the ratio of the sensitivities for the two ions differs considerably on changing between ΔE_1 and ΔE_2 . The partial sensitivities obtained from slopes of the calibration graphs are given in Table V.

The intercepts of the calibration graphs were different from zero in each instance a circumstance that we can not

explain yet. Their effect on the calculated concentration was investigated by including and precluding the intercepts in the calculations. The results are summarized in the appendix.

As can be seen from Table V, when B15C5 was used the partial sensitivities obtained from the injection of the standard solution before the injection of the sample are different from those obtained after the sample. Therefore, the concentrations of the ions are also different in both cases. In the indirect measurement all values of the concentrations of K^+ ion are very low in the former case and within clinically acceptable concentration range (normal range 3.4 - 5.2 mM) [79] in the latter case. The values of the concentrations of Na^+ ion are close to the clinically acceptable concentration range (normal range 138 - 151 [79]) in the former case than the latter one which are very high. In the direct measurement the values of the concentrations of the K^+ ion are within clinically acceptable range in both cases. But the values of Na^+ ion concentration are very low in this case.

When DB24C8 was used instead of B15C5 all the values of concentrations of K^+ and Na^+ ions in both cases are out of the range of clinically acceptable concentration range. They are very high for K^+ ion and low for Na^+ ion. As the half-wave potentials of Na^+ and K^+ were very close to one another

(Fig. 21) when DB24C8 was used as an ionophore in the transfer of K^+ and Na^+ across membrane stabilized water/nitrobenzene interface, discrepancies in the results from simultaneous determination of Na^+ and K^+ was expected.

Table 5. Partial sensitivities obtained from the slopes of the calibration graphs (nA/mM).

Ionophore.	Time of measurement	S_{1,Na^+}	S_{1,K^+}	S_{2,Na^+}	S_{2,K^+}
B15C5	Before the sample.	2.5	614.13	368.55	2213.86
	After the sample	2.8	701.33	462.95	2214.76
B15C5	Before the sample.	19.18	975.22	479.02	1222.81
	After the sample	4.55	645.51	350.62	1022.36
DB24C8	Before the sample.	6.1	67.9	155.8	644.5
	After the sample.	4.74	59.25	95.60	588.5

4.3. Flow Injection Amperometry Vs Flame Photometry

As indicated above, due to the change in partial sensitivities as time changes (i.e before and after the sample injection) the concentrations obtained were different in both cases. As a result the comparison between flow injection amperometry and flame photometry was made on the individual cases in flow injection amperometry. Accordingly, the values of the concentrations of K^+ ion obtained using the partial sensitivities from the injection of the standard solutions before the injection of the sample, in the case of indirect measurement was totally different from those results obtained by flame photometry. The correlation between flow injection amperometry and flame photometry in the case of after the sample for indirect measurement is shown in Fig. 25 and 26 for K^+ and Na^+ , respectively.

The correlation of direct flow injection amperometry with flame photometry in the case of before the sample is given in Figs. 27 and 28 for K^+ and Na^+ ions, respectively. As it can be seen from the figures there is poor correlation between flow injection amperometry and flame photometry.

To investigate the source of the discrepancies the relative partial sensitivities of Na^+ and K^+ ions (i_{Na^+}/i_{K^+}) obtained from Fig. 22 were plotted as shown in Fig. 29 against the change in potential difference ΔE (scale was $\Delta E - \Delta E_{1/2}$ v).

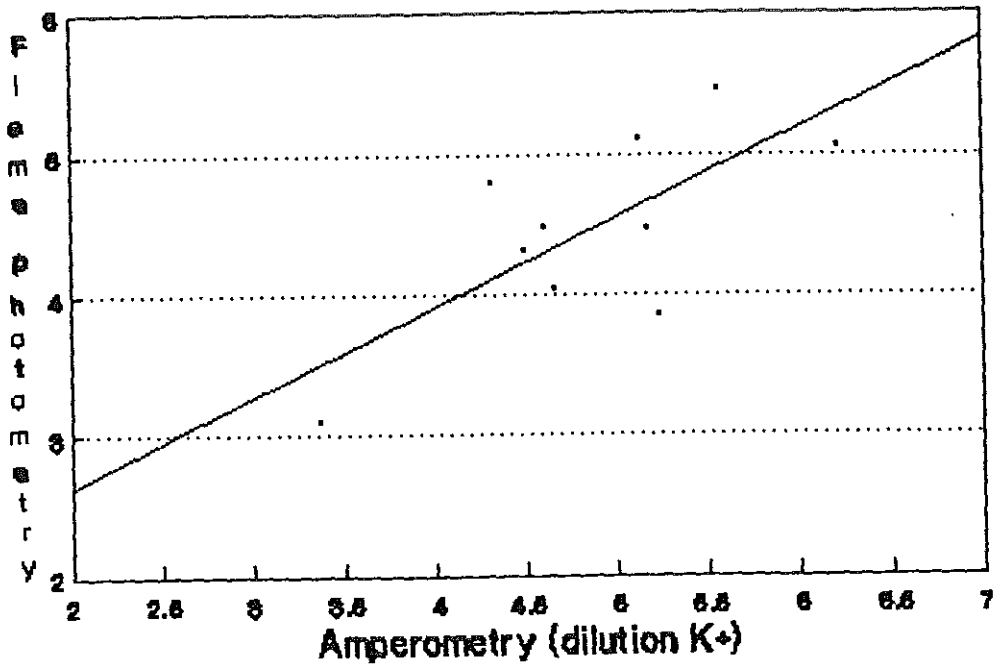


Fig. 25 Comparison of flow injection amperometric results with flame photometric data for K^+ ion measurements (indirect, after the sample).

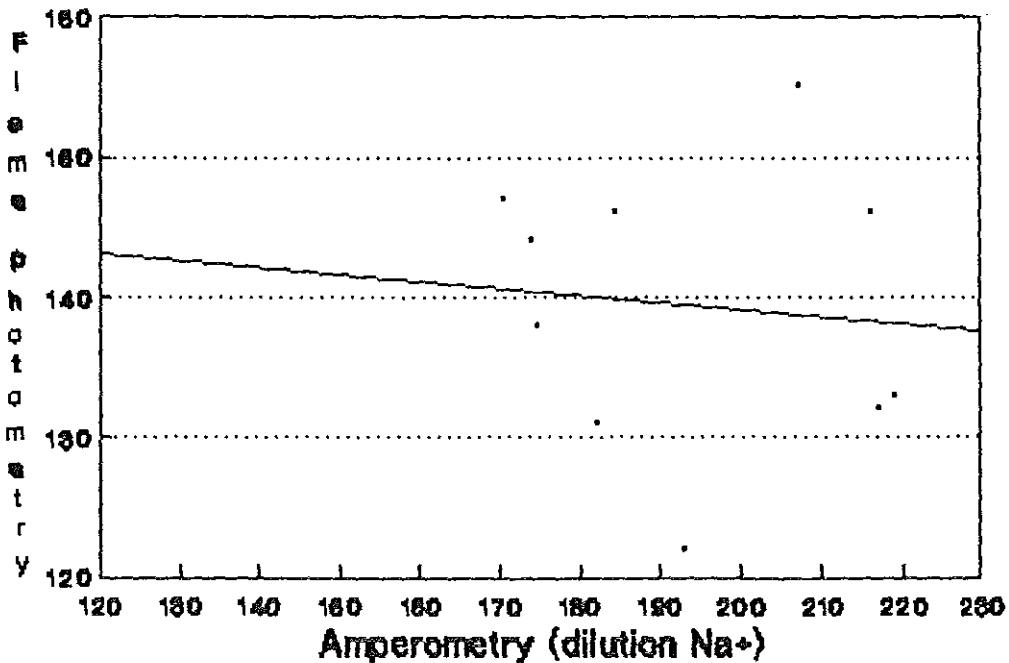


Fig. 26 Comparison of flow injection amperometric results with flame photometric data for Na^+ ion (indirect, after the sample).

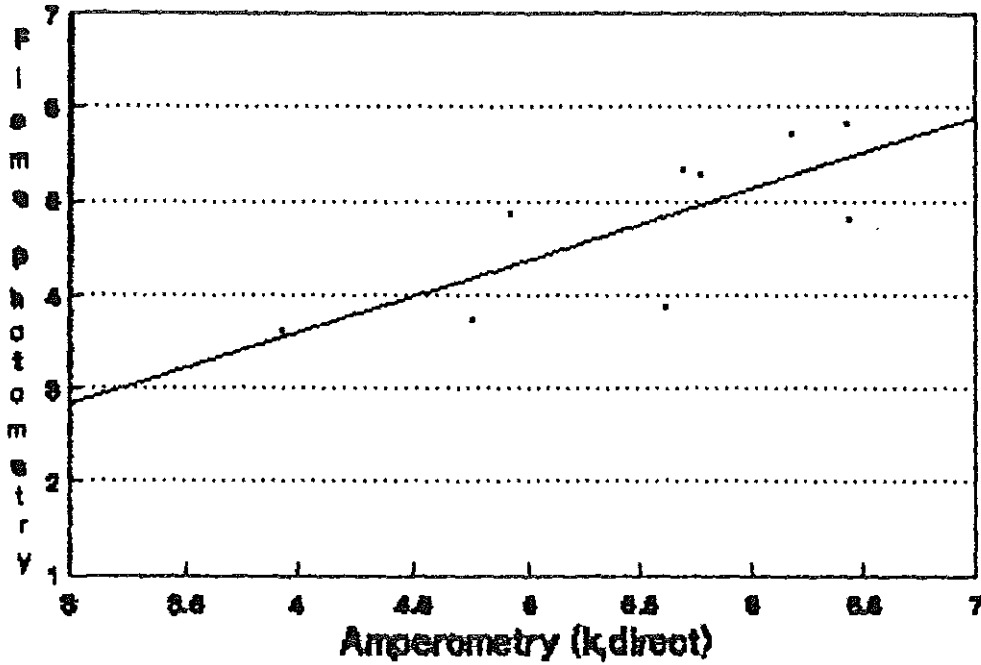


Fig. 27 Comparison of flow injection amperometric results with flame photometric data for K^+ ion measurements (direct, before the sample).

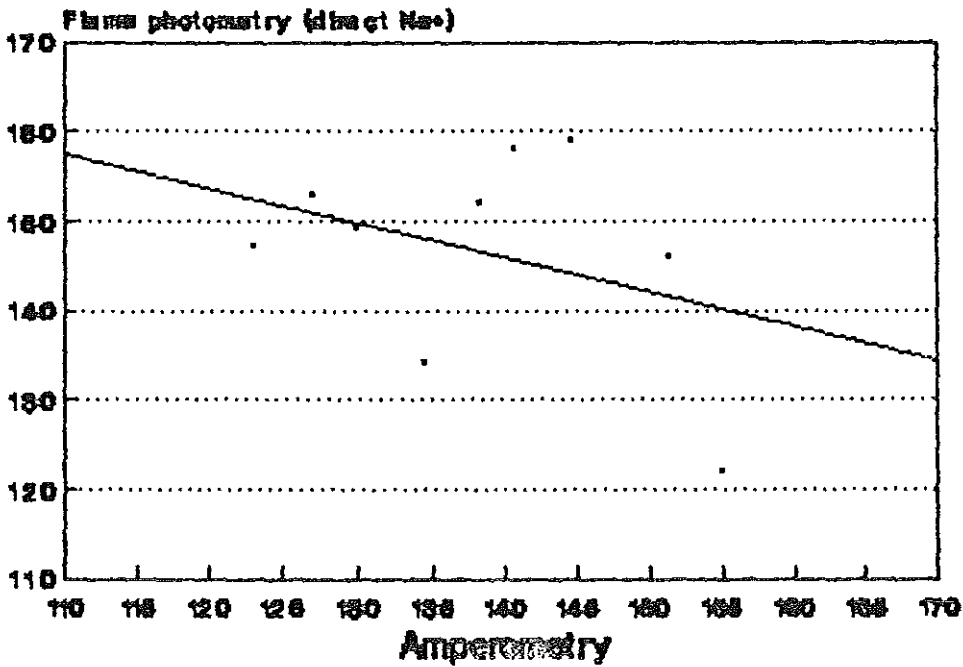


Fig. 28 Comparison of flow injection amperometric results with flame photometric data for Na^+ measurements (direct, before the sample).

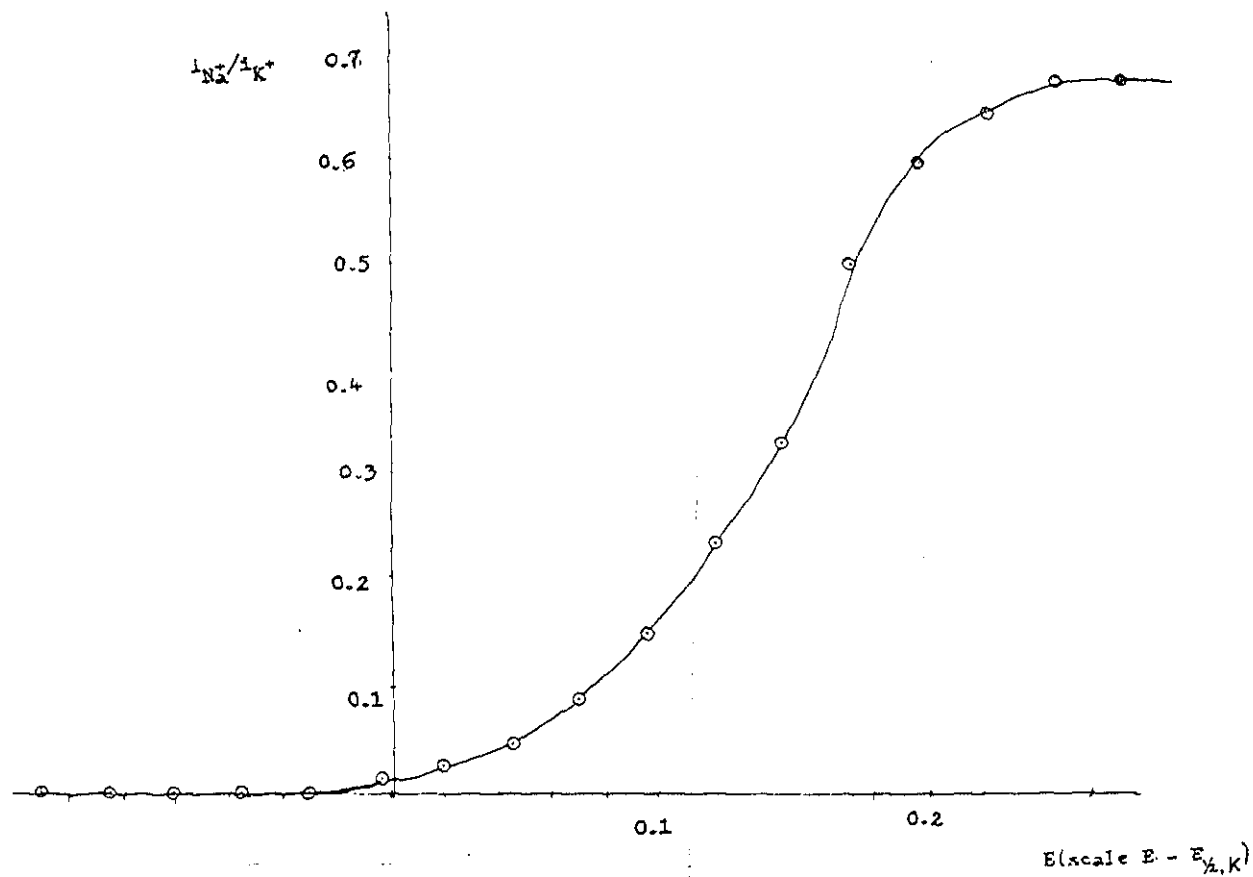


Fig. 29 The relationship between the relative partial sensitivities of Na^+ and K^+ ions (i_{Na^+}/i_{K^+}) and the change in potential difference (scale was $\Delta E - \Delta E_{1/2, K}$).

Table VI. The ratios of the partial sensitivities at the two potentials chosen for the determination of K^+ and Na^+ ions and the difference in the corresponding potentials from Fig. 18.

Form of measurement	Time of measurement	At 0.350v	At 0.500v	The difference in potential
Direct measurement	Before the sample	0.0041	0.17	0.126
	After the sample	0.004	0.21	0.14
Indirect measurement	Before the sample	0.0197	0.392	0.15
	After the sample.	0.007	0.343	0.167

The ratio in partial sensitivities of Na^+ and K^+ obtained from the calibration graphs at the potential differences ΔE_1 and ΔE_2 were calculated and the difference in the potentials corresponding to these ratios was determined from the plot. The results obtained are given in Table VI. The ratios of the partial sensitivities of the two ions at any time should give the same difference in potentials, whether it is of the form of Fig. 22 or of the form of the calibration curves.

But practically the difference in potential corresponding to the ratios of the partial sensitivities of the ions and the difference between the two potentials chosen for the determination of K^+ and Na^+ , which was 0.150 v was not the same in all of the cases except in the case of direct measurement before the sample. The results are summarized in Table VI. It is possible to see from this table that there should be an error in one of the two ways. The results from the flow injection investigation for the standard K^+ and Na^+ ions were in accordance with the theoretically expected ones. Therefore, the error should result from the determination of the real sample. Based on this proposal when the proper functioning of the sample loop was checked it was found out that the sample loop was not working properly. This must have arisen after the flow injection investigation was made on the standard solutions. Therefore, we assume that this inconsistent results, which are obtained in flow injection amperometry may be due to the defect arisen in the sample loop. It was very difficult within the capacity of the department to repair the

sample loop, and repeat the experiments. As a result we stick to a hint that would be obtained from these results, the voltammetric investigations and previously reported results as to the application of the method in clinical analysis of blood electrolytes. But we suggest that the investigation should continue with an improved sample loop to reach a reliable conclusion. The choice of the potentials for the calibration has its own contribution in the variation of the partial sensitivities. The choice of the potentials for the calibration graphs should be in such a way that one of them should be in the limiting or close to the limiting current range. This should be so because any change introduced in the potential does not affect the current.

4.4. Potentiometric Measurements

The selectivity coefficient measurement for the liquid state K^+ - selective electrode based on DB24C8 neutral carrier is shown in Fig. 30. The potential of the electrode at a constant level of the primary K^+ ion and varying concentration of an interfering Na^+ ion was measured. The results were plotted against the negative logarithm of the molar concentration of Na^+ ion. The selectivity coefficient, $K_{i,j}^{pot}$ was evaluated from the ratio of C_{K^+}/C_{Na^+} at the point of intersection of the extrapolation of the horizontal and linear portion of the graph shown in Fig. 30. It was found to be 0.17 which is high, showing that the preference of K^+ ion over Na^+ ion was not so pronounced. The calibration curve for the determination of K^+

in the absence of Na^+ is shown in Fig. 31. The slope in the linear range (1.26×10^{-4} to 0.126 M) is -54 mV/dec. for K^+ and -40 mV/dec. for Na^+ in the absence of K^+ . When this electrode was used for the potentiometric determination of K^+ ion in blood serum samples the results summarized in Table VII are obtained. As can be seen from the table the results by no means are comparable with that of flame photometry. Therefore, statistical evaluation was omitted. The cause for the discrepancy in results between the two methods must be investigated further.

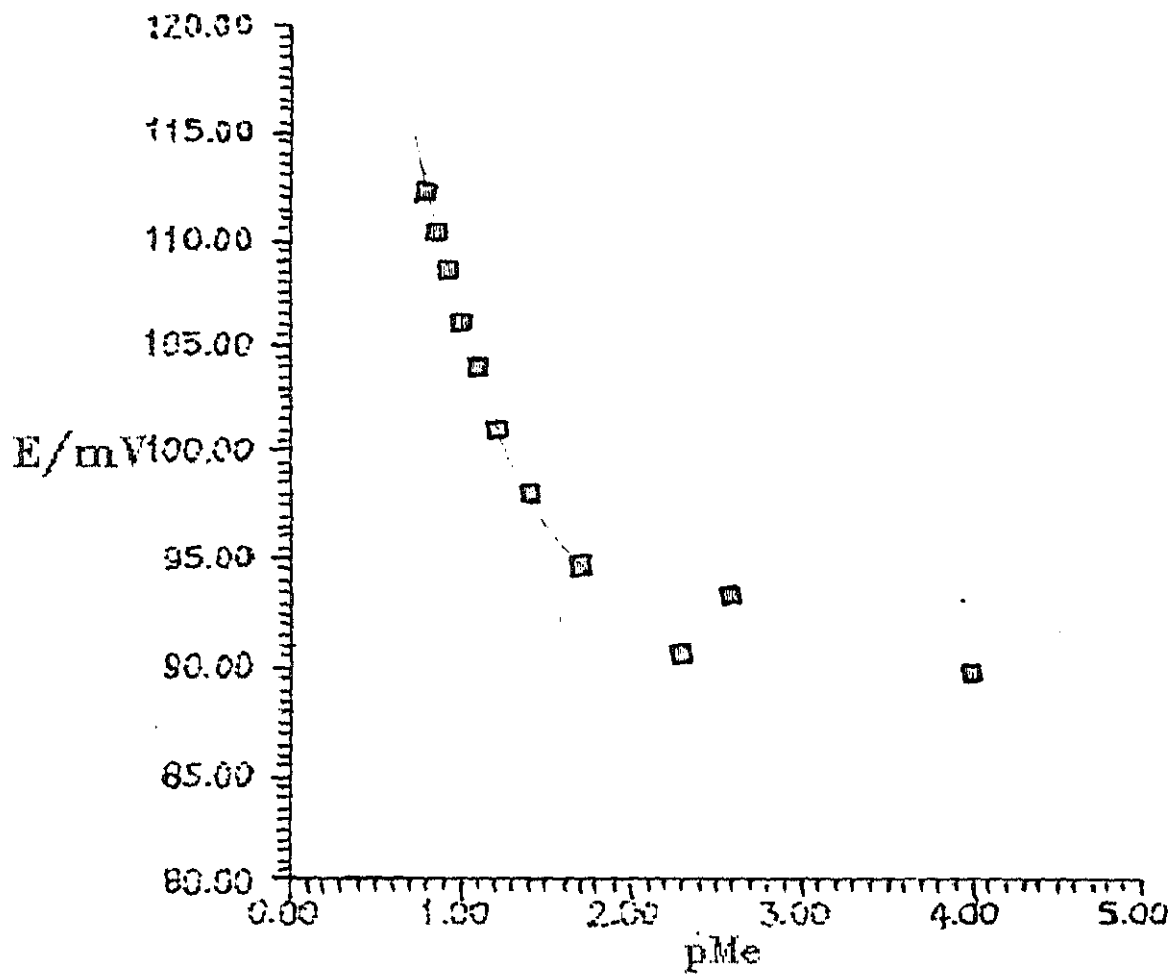


Fig. 31 Calibration curve for potentiometric measurement of K^+ ion in the absence of Na^+ .

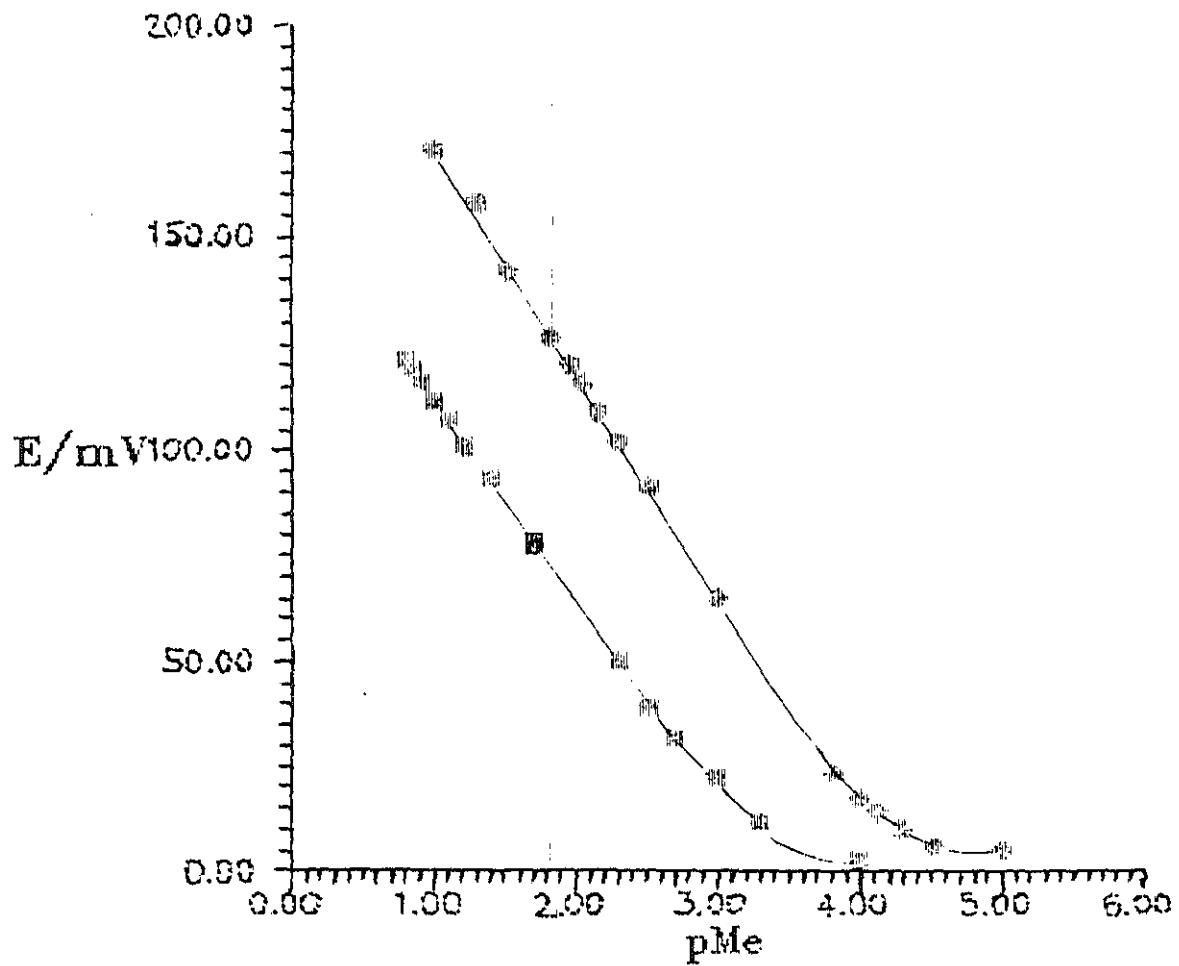


Fig. 30 Calibration curve for potentiometric measurement of K^+ ion in the presence of varying concentration of the interfering Na^+ .

Table 7. Results obtained from potentiometric measurement.

sample No.	Flame Photometry C_{K^+}/mM	Potentiometry	
		direct C_{K^+}/mM	indirect C_{K^+}/mM
10	6.17	41.0	58.66
19	5.72	64.6	83.39
41	4.85	36.7	76.37
88	4.43	72.4	91.06
60	5.81	51.5	99.43

5. CONCLUSION

Ac and dc Cyclic Voltammetric and Flow Injection Amperometric investigations were made in this work. The results obtained from the voltammetric investigations were encouraging. The influence of the employed ionophores in facilitated transfer of K^+ and Na^+ on the selectivity of the method was studied. According to these study B15C5 was found to form a stable complex with K^+ . From the difference in half-wave potentials of K^+ and Na^+ ions observed, it can be concluded that, B15C5 was an appropriate ionophore in simultaneous determination of K^+ and Na^+ ions in blood serum. DB24C8 was found to be an unappropriated in simultaneous determination of K^+ and Na^+ ions in blood serum, as the half-wave potentials of the two ions was very close to one another. Stability constants of the metal-ionophore complex was determined by using Cyclic Voltammetry and Flow Injection Amperometry. The results obtained for K^+ - ionophore complex in general were in good agreement with those obtained from the literature. Concentrations of K^+ and Na^+ ions in blood serum were determined by Flow Injection Amperometric and Flame Photometric methods. The results obtained from Flow Injection Amperometry did not correlate well with those of Flame Photometry. This phenomenon was not observed in previous experimental reports [81] and are inconsistent with what is observed in voltammetric investigations. Therefore, the discrepancies should arise from the defect in the sample loop. Eventhough these results obtained from Flow Injection

Amperometric analysis do not correlate well with those of Flame Photometry, they give a good hint as to the application of the method in clinical analyses, specially in stat measurements of K^+ and Na^+ ions in blood serum. In addition the voltammetric investigations and previous reports [81] very well indicate that Flow Injection Amperometric method can be applied well in clinical analyses of blood electrolytes.

6. Appendix

Calibration Graphs and The Results obtained from Flow Injection Amperometry.

Table 1. Results obtained with Flow injection amperometric method in an indirect measurement by using B15C5 ionophore. All concentrations in mM.

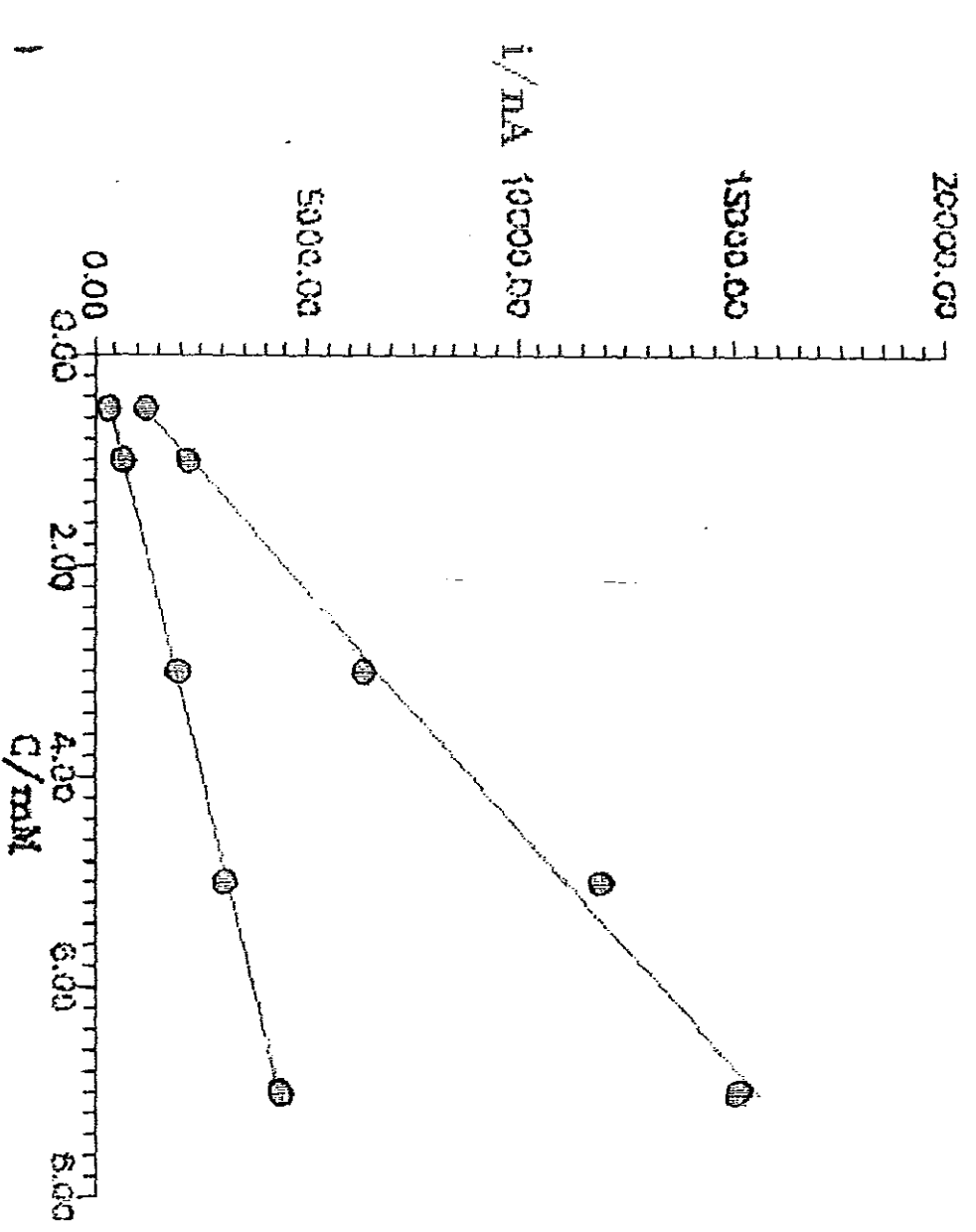
S.N	Before the sample				After the sample				flame.ph.	
	with int.		without int.		with int.		without int.		C _{K+}	C _{Na+}
	C _{K+}	C _{Na+}	C _{K+}	C _{Na+}	C _{K+}	C _{Na+}	C _{K+}	C _{Na+}	C _{K+}	C _{Na+}
67	0.1	138.76	0.76	137.07	3.36	182.18	3.95	99.92	3.09	131
89	1.35	133.87	1.95	135.57	5.16	174.58	5.74	175.32	4.45	138
53	1.61	133.56	2.21	135.27	5.55	173.91	6.13	174.65	5.46	144
6	1.04	130.33	1.63	132.05	4.6	170.24	5.18	170.98	4.48	147
1	1.61	166.45	2.20	168.16	6.21	216.89	6.79	217.63	5.05	132
2	0.70	140.84	1.30	142.45	4.31	184.29	4.89	185.02	4.79	146
3	1.21	147.64	1.8	149.35	5.22	192.69	5.80	193.42	3.85	122
4	0.48	164.99	1.08	165.65	4.48	216	5.06	216.75	4.32	146
5	0.57	167.08	1.16	168.91	4.65	218.84	5.23	219.57	4.03	133
71	0.1	158.44	1.59	160.16	5.12	207	5.7	207.74	5.11	155
20					2.79	134.89	3.37	52.66		
21					0.32	3.17				

Table 2. Results obtained from Flow injection amperometric method in the direct measurement by using B15C5 ionophore. All concentrations in mM.

S.No	Before the sample				After the sample				Flame photometry	
	With intercept		without intercept		With intercept		Without intercept		C _K .	C _{Na} .
	C _K .	C _{Na} .	C _K .	C _{Na} .	C _K .	C _{Na} .	C _K .	C _{Na} .		
19	6.21	126.54	6.18	140.57	5.31	112.57	5.46	76.73	5.72	158
41	4.93	120.65	4.91	126.93	4.19	107.12	4.34	109.93	4.85	153
74	5.79	130.44	5.76	144.46	4.94	115.41	5.09	118.22	5.28	159
45	5.72	124.09	5.69	138.12	4.88	110.32	5.02	113.13	5.31	152
68	3.94	115.74	3.92	129.77	3.33	108.62	3.47	105.43	3.6	149
60	6.44	110.25	6.42	122.88	5.54	92.57	5.65	101.47	5.81	147
66	4.77	120.26	4.74	134.30	4.05	106.72	4.2	109.53	3.72	134
3	5.63	140.87	5.61	154.90	4.81	123.6	5	126.41	3.85	122
2	6.46	137.25	6.43	151.28	5.54	121.23	5.68	124.04	4.79	146
20	5.39	127.38	5.37	141.41	4.6	112.74	4.74	115.55		
A	5.13	124.22	5.10	138.25	4.37	110.07	4.51	112.88		
B	5.21	152.44	5.18	166.47	4.45	171.18	4.59	135.34		

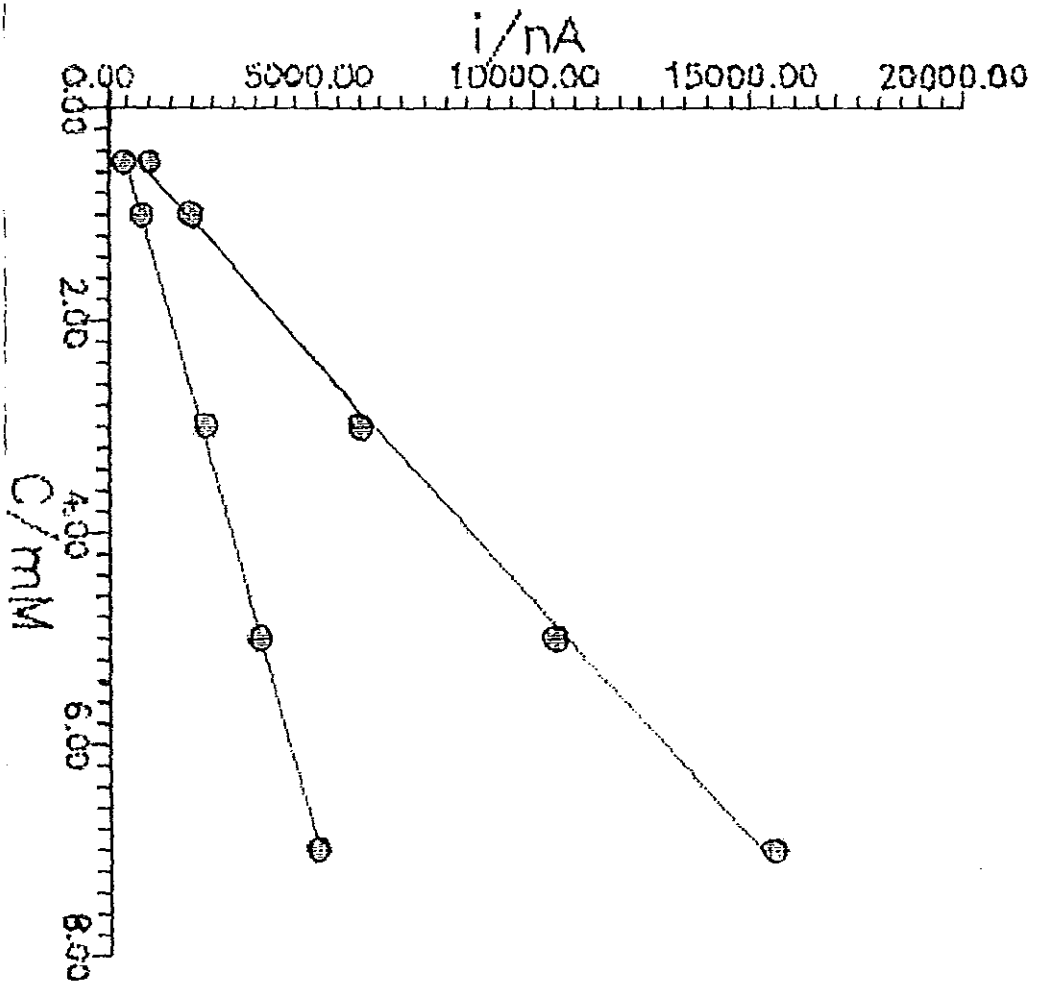
Table 3. Results obtained from Flow Injection Amperometry using DB24C8 ionophore. All concentrations in mM.

S.N	Before the sample				After the sample				Flame ph.	
	with int		without int.		with int		without int		C _{K+}	C _{Na+}
	C _{K+}	C _{Na+}	C _{K+}	C _{Na+}	C _{K+}	C _{Na+}	C _{K+}	C _{Na+}	C _{K+}	C _{Na+}
67	8.18	73.9	8.34	72.1 1	4.54	116. 63	7.01	85.3 8	3.09	131
89	11.5 4	69.3 2	11.7	50.1 4	9.0	103. 26	11.2 7	91.1 8	4.45	138
53	15.0 5	57.9 4	15.2 2	38.7 7	13.8 1	78.7 8	16.1	66.6 9	5.46	144
6	15.2	59.5 8	15.3 7	40.4	13.9 0	81.9 0	16.1 9	69.8 1	4.48	147
1	9.02	85.8 1	9.18	84.0 3	5.09	137. 18	7.38	125. 09	5.05	132
4	3.15	106. 88	3.31	87.7	2.24	115. 18	0.04 7	159. 75	4.32	146
5	4.76	105. 36	4.92	86.1 8	1.06	178. 17	1.23	166. 08	4.03	133
71	9.62	80.7 5	9.78	61.5 8	6.08	126. 89	8.37	114. 80	5.11	155
A	8.38	70.0 7	8.54	50.8 9	5.16	106. 69	7.45	94.6 6		
B	8.18	84.5 5	8.34	65.3 8	4.15	135. 24	6.44	123. 15		



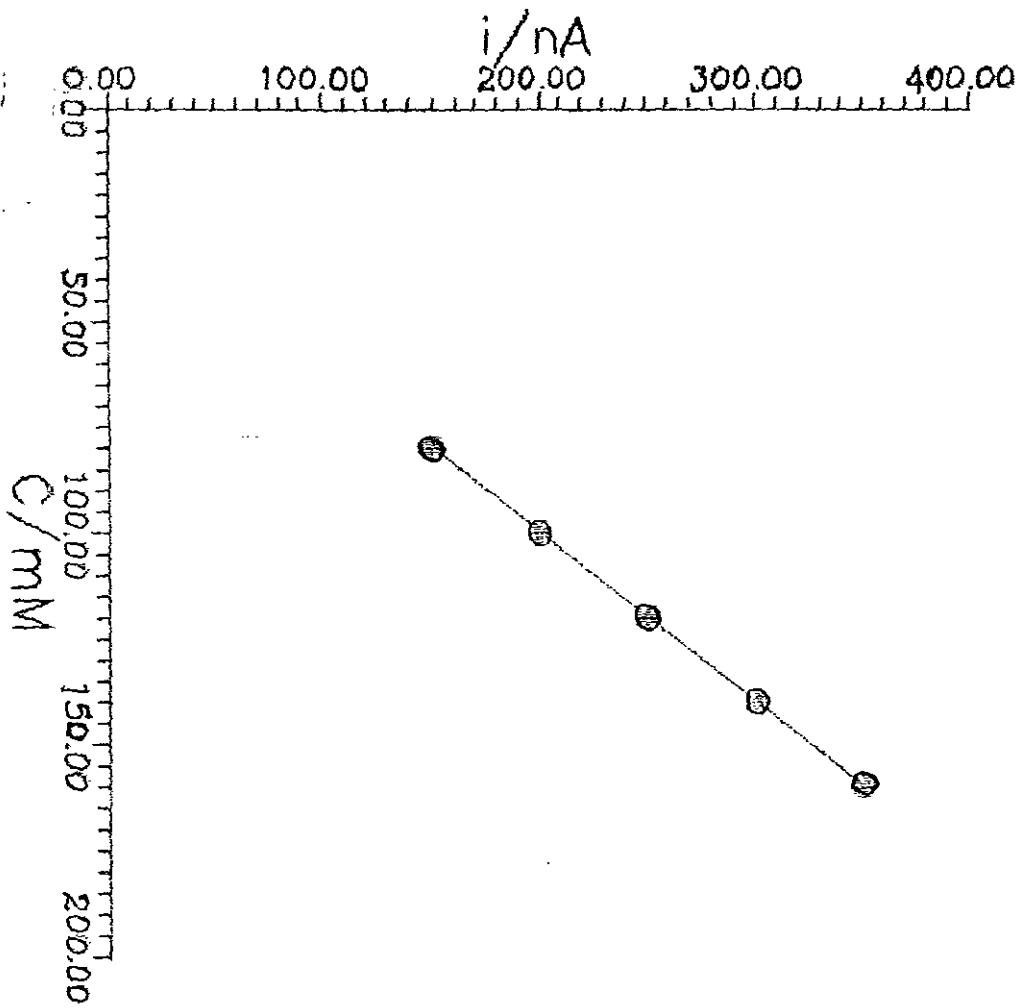
Direct in presence of H15C5 before the sample (K⁺ at 350 and 500 mV)

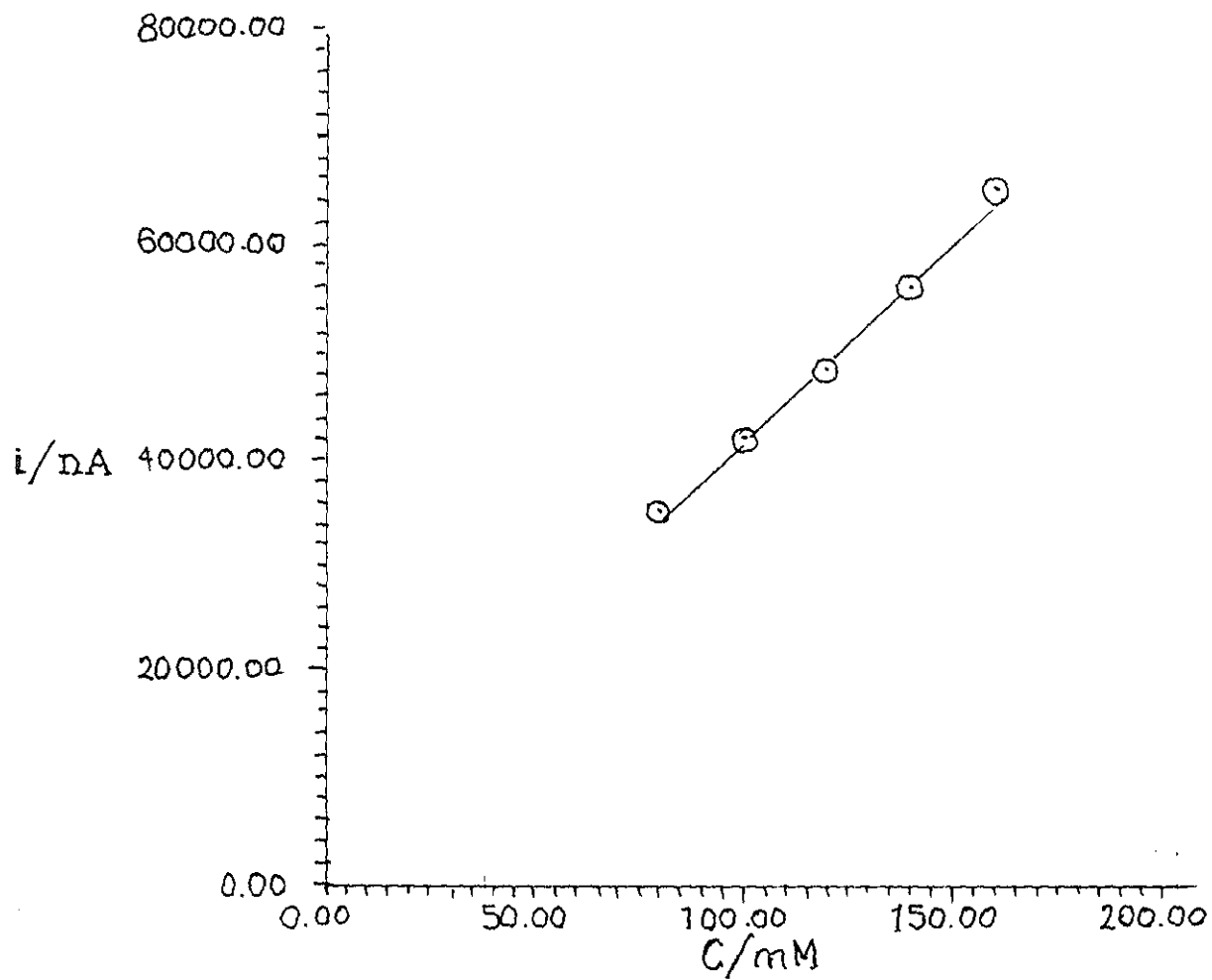
6.250



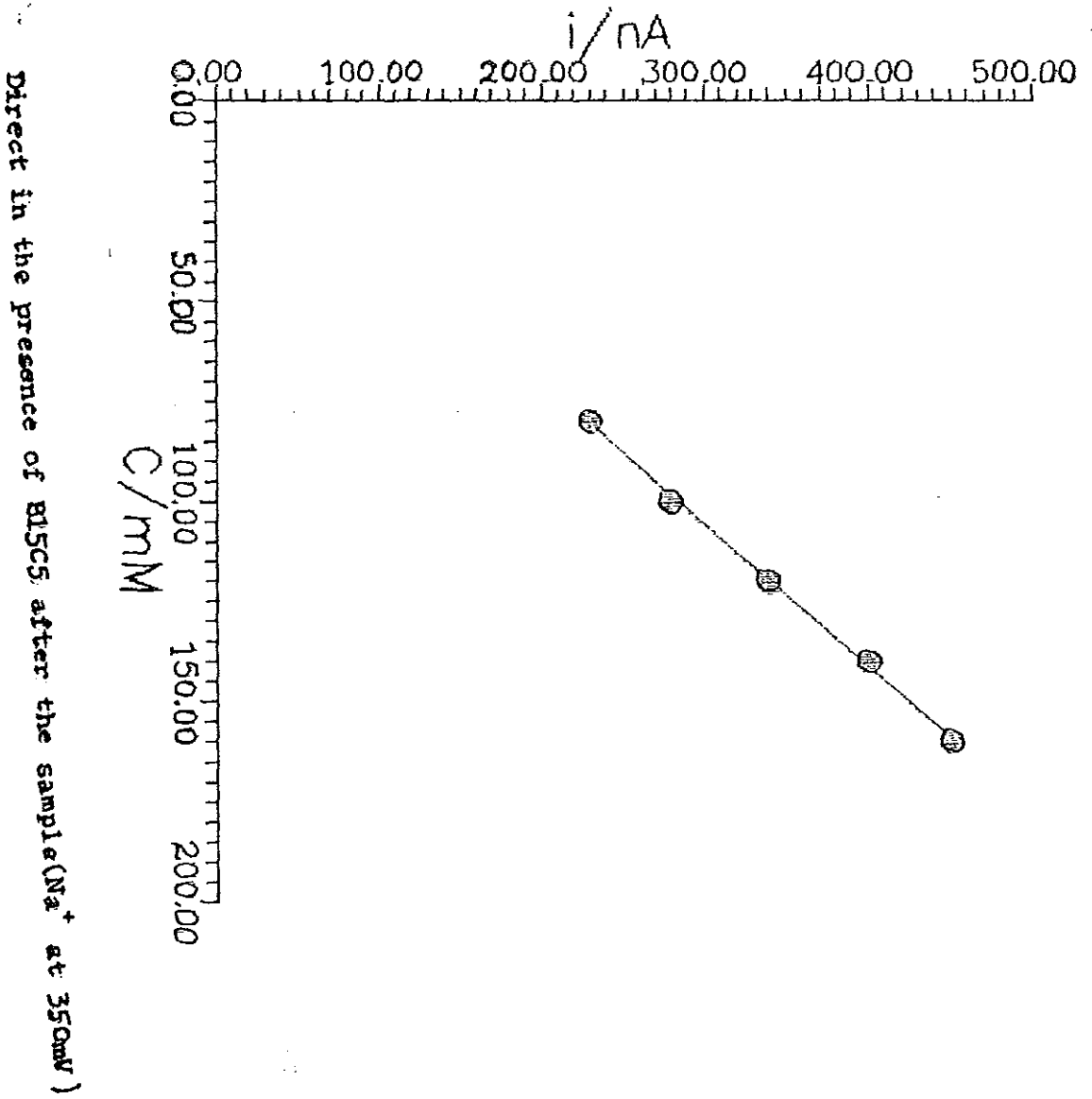
Direct in the presence of KI5C5 after the sample (K^+ at 350 and 500mV)

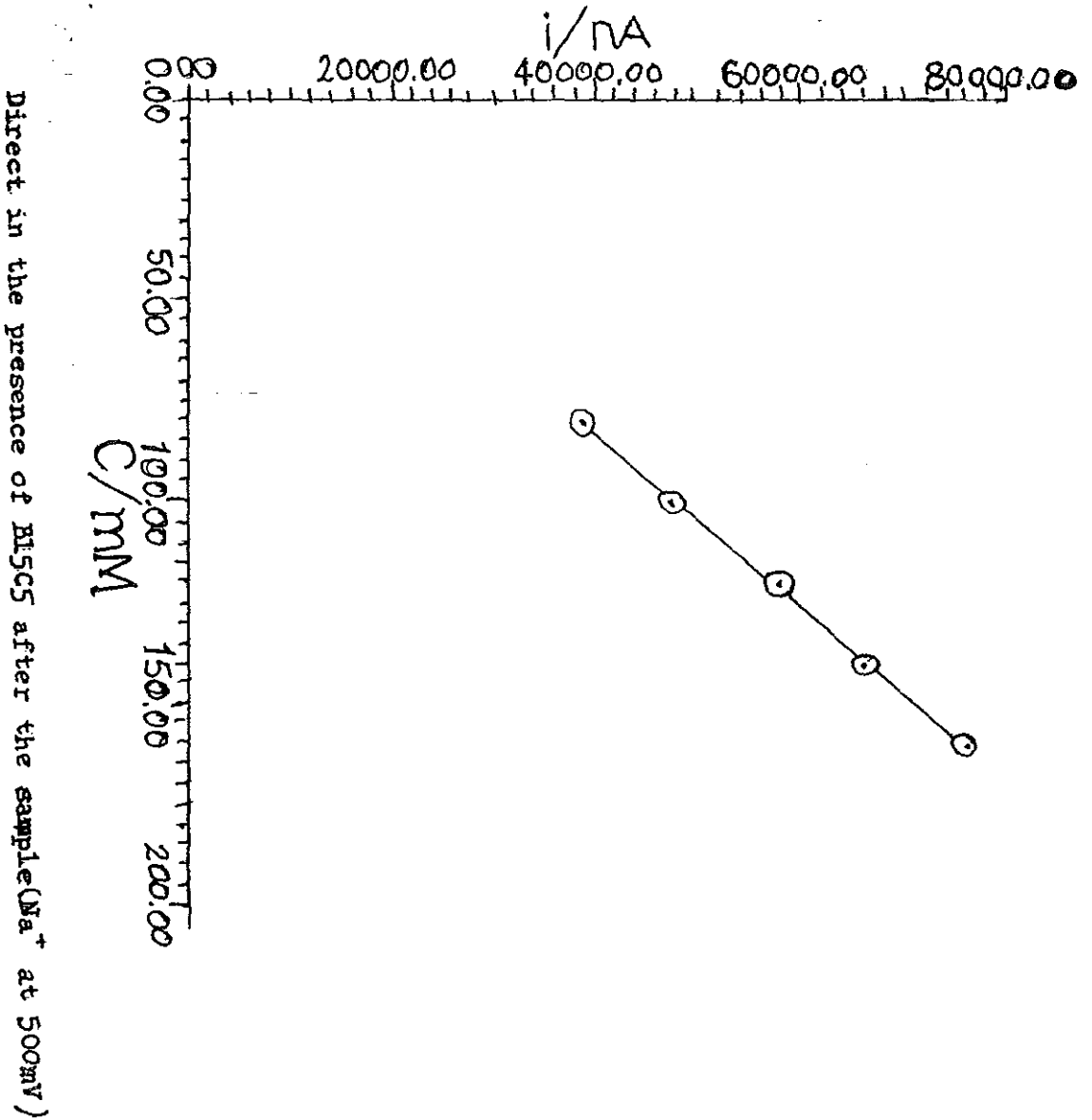
Direct in the presence of BISCs before the sample (Na^+ at 350 mV)

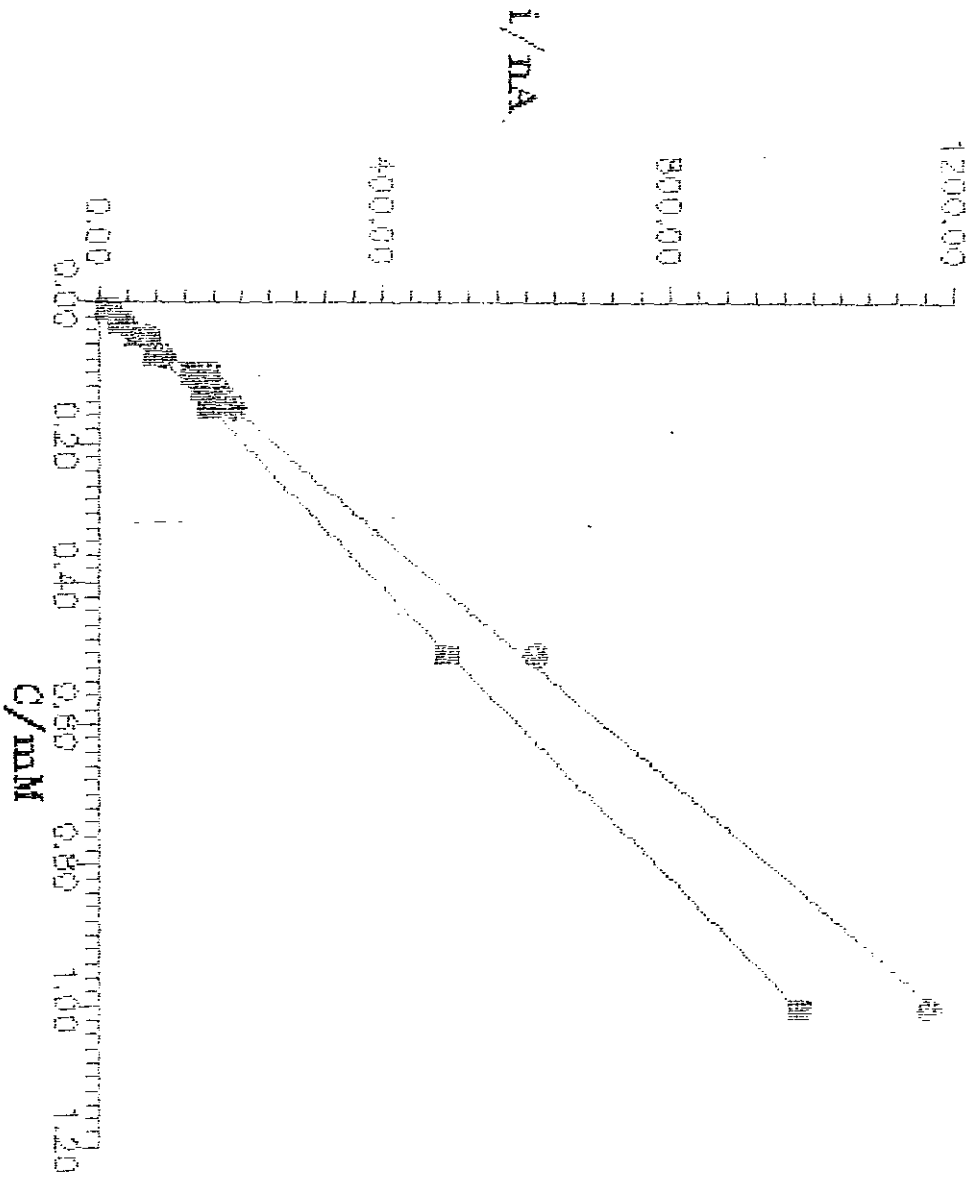




Direct in the presence of B15C5 before the sample(Na^+ at 500mV)

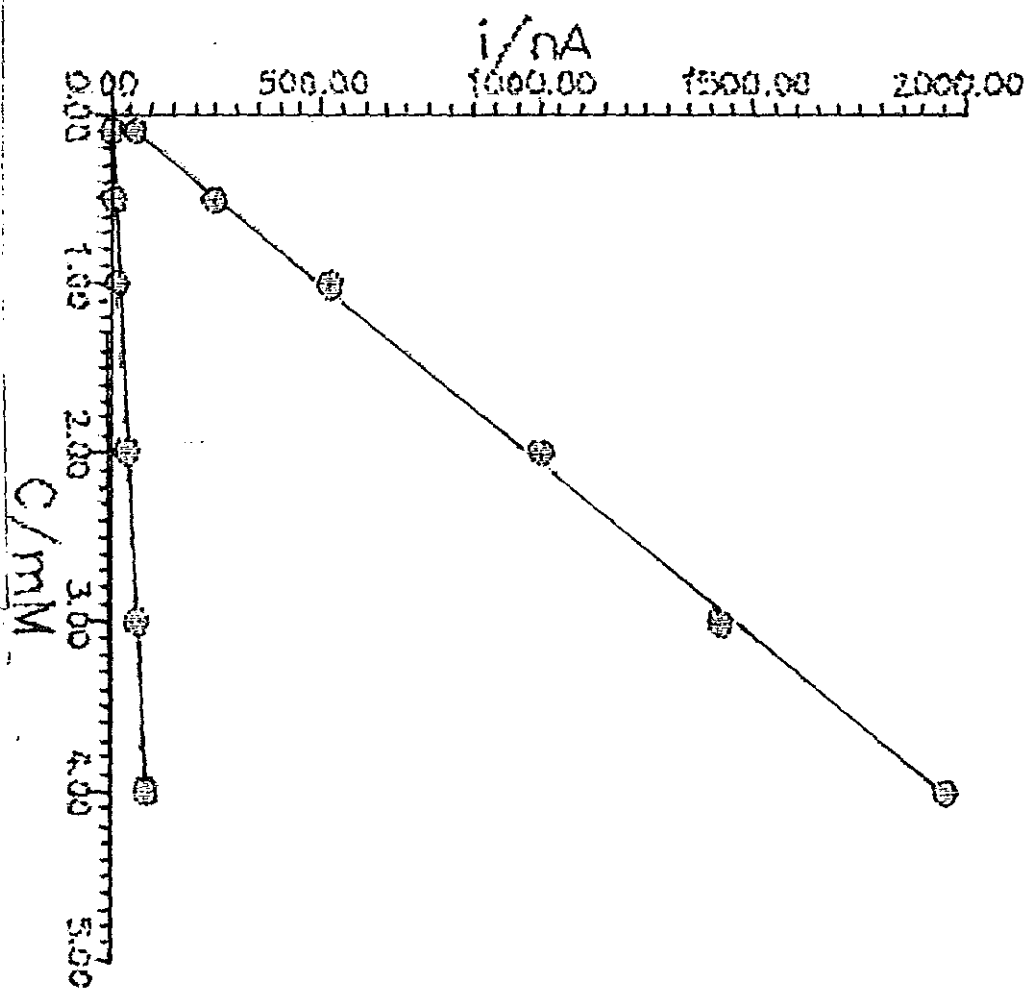




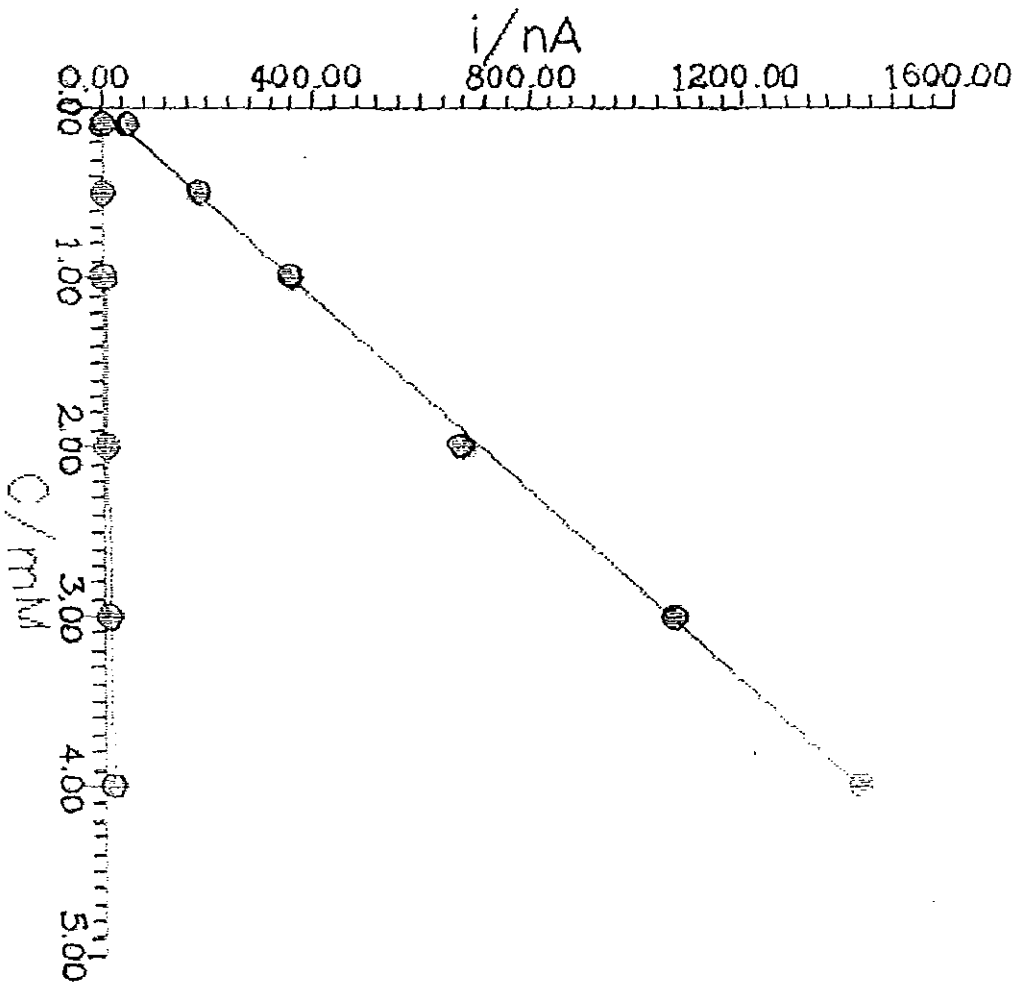


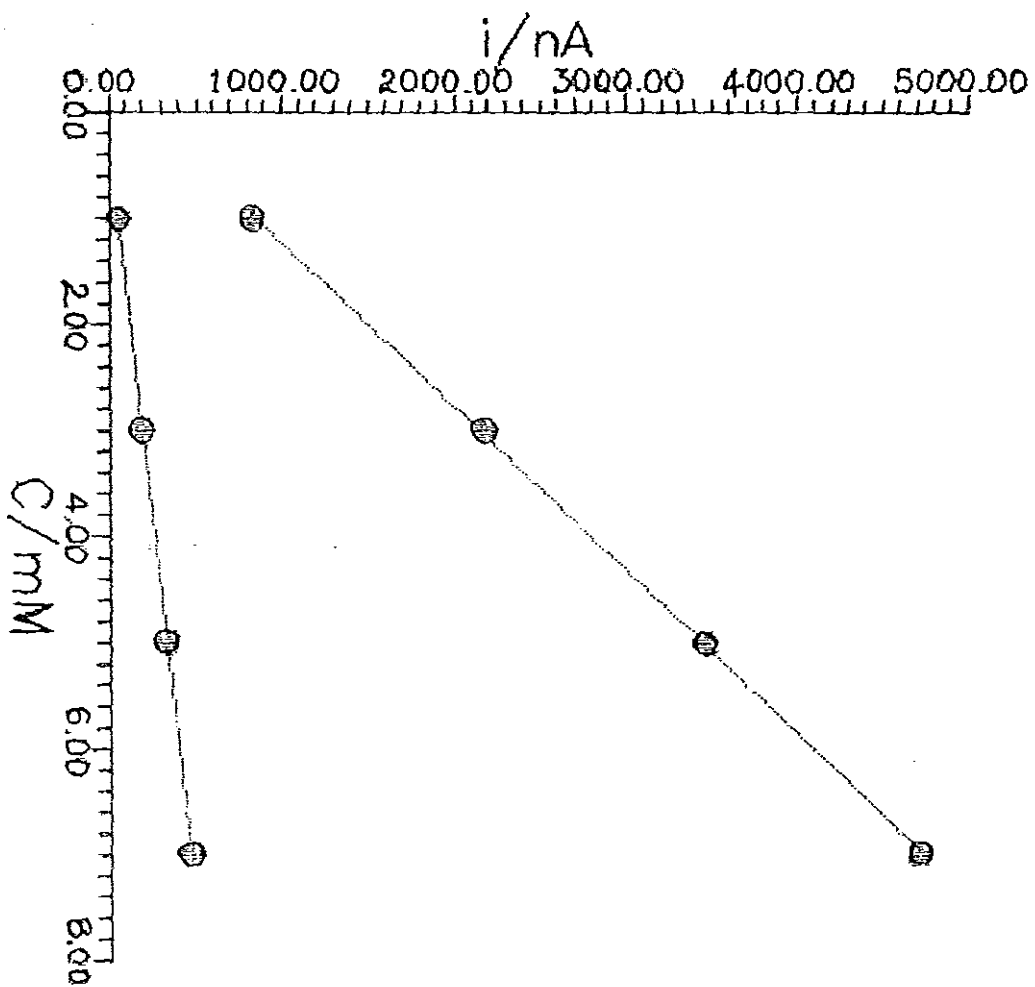
Indirect in the presence of BISCs before the sample (K^+ at 350 and 500 mV)

Indirect in the presence of HSCS before the sample (Mg^{2+} at 350 and 500mV)

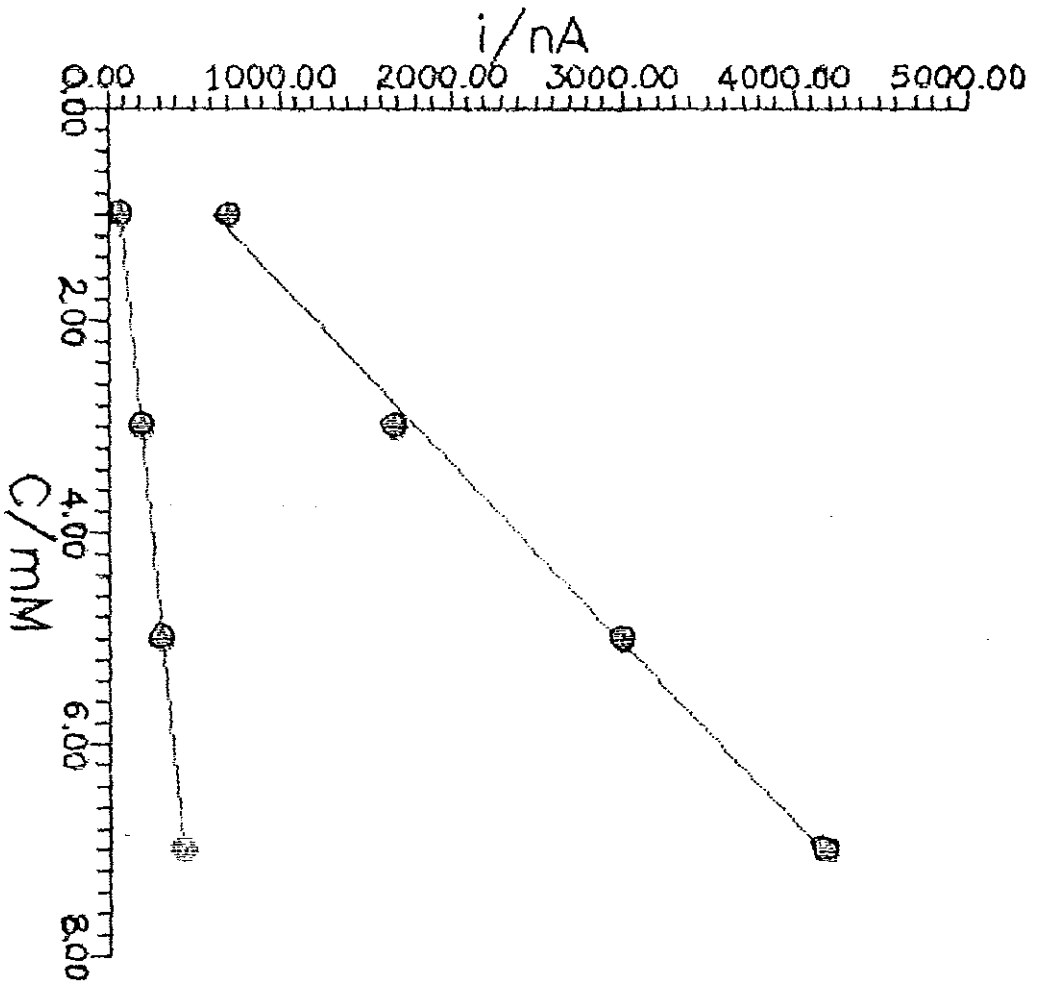


Indirect in the presence of HSCS after the sample (Na^+ at 350 and 500 mV)

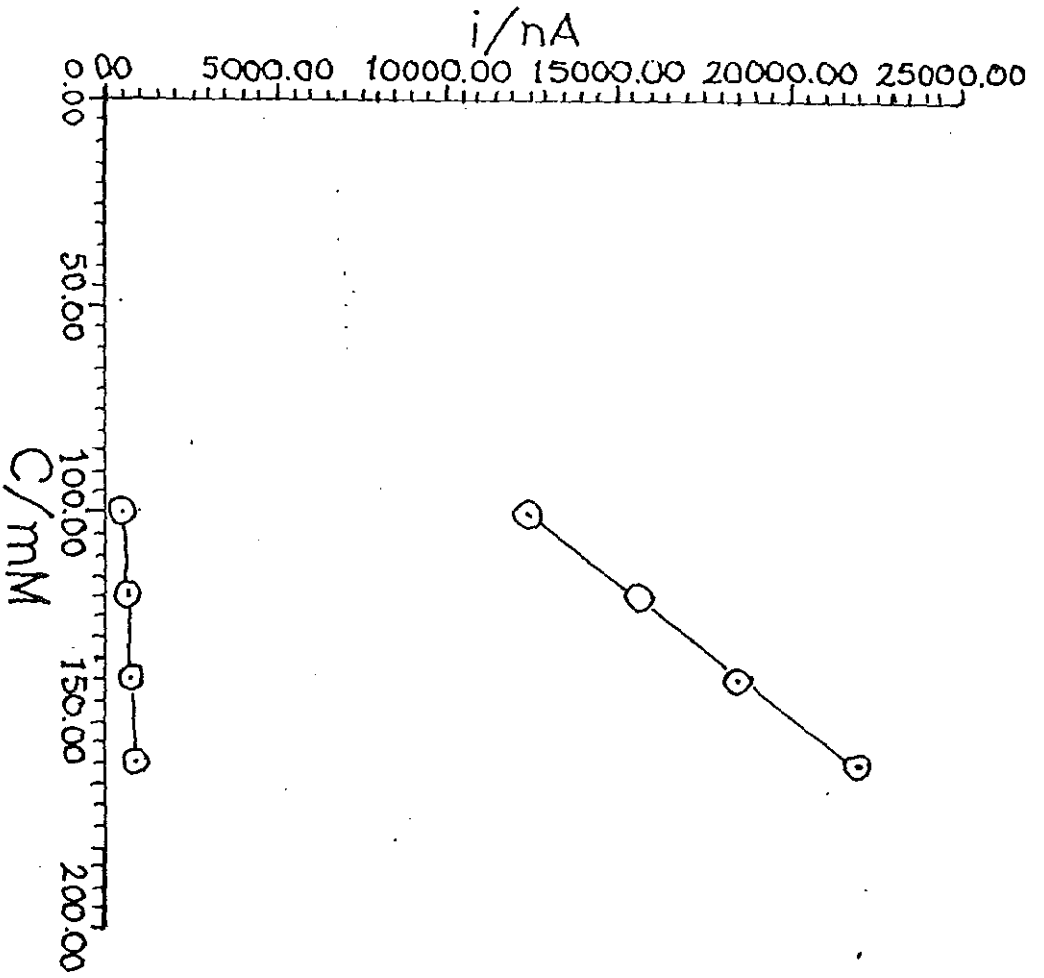




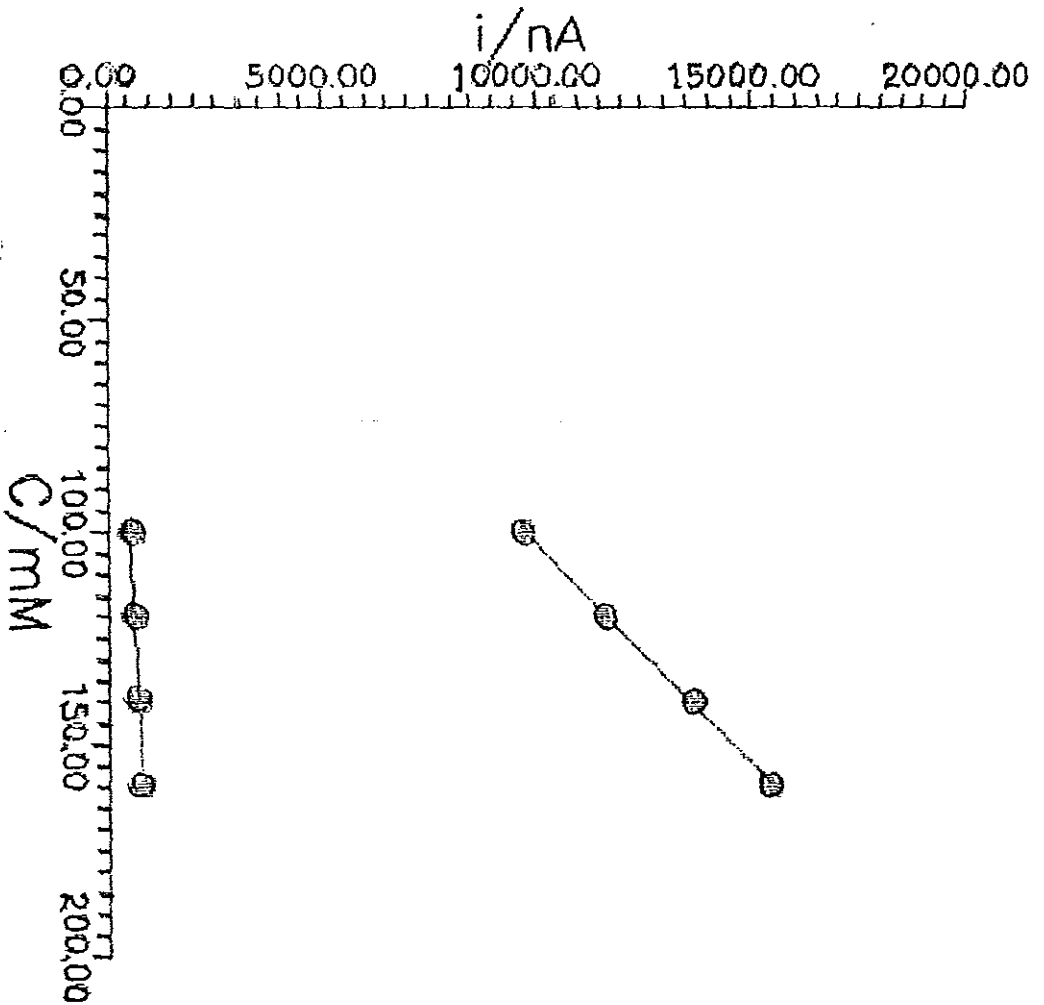
Direct in the presence of $DB24CG$ before the sample (K^+ at 728 and 825 mV)



Direct in the presence of DB2408 after the sample (K^+ at 728 and 825 mV/s)



Effect in the presence of DB24C8 before the sample (K⁺ at 728 and 825 mV)



Direct in the presence of DB24C8 after the sample (μM^+ at 728 and 825 mV/s)

7. REFERENCES

1. H.G.J. Worth, *Analyst*, 113(1988)373.
2. H.F. Osswald, R. Aspel, W. Diamai and Simon, *Clin. Chem.*, 25(1979)39.
3. G.H. Williams, and R.G. Dluky, Control of Aldosterone Secretion. In : *International Text Book on Hypertension* (2nd ed.) edited by J. Genest, Mc Graw hill, New York, 1983 pp 320-338.
4. S. Kimura, S. Hayashi, Y. Yamaguchi, R. Fyshimi, N. Amino, and K. Miyai, *Clin. Chem.*, 38(1992)44.
5. P.M.Hald, *J.Biol.Chem.*, 167(1947)499.
6. S.M. Friedman, S.L. Wang, J.H.Walton, *J. Appl. Physio.*, 18(1963)950.
7. R.L. Coleman, C.C. Yong and L. Sidoni, *Clin. Chem.*, 26(1980)1921.
8. J.D. Czaban and A.D. Cormier, *Clin. Chem.*, 26(1980)1923.
9. F.S. Apple, D.D. Koch, S. Graves, and J.H. Ladenson, *Clin. Chem.*, 28(1982)1931.
10. J.D. Czaban, A.D. Cormier and K.D. Legg, *Clin. Chem.*, 28(1982)1986.
11. G.B. Levy, *Clin. Chem.*, 27(1981)1435.
12. D.N. Baron, *Clin. Chem.*, 27(1981)642.
13. R.L. Coleman and C.C. Young, *Clin. Chem.*, 27(1981)1938.

14. S. Kamata, and K. Onoyama, *Anal. Chem.*, 63(1991)1295.
15. S. Tuladhar, G. Williams, and C. D'silva, *Anal. Chem.*, 63(1991)2282.
16. W. Nernst and E.H. Rjesenfeld, *Ann. Phys.*, 8(1902)600 (see Ref. [82]).
17. J.W. Ross, *Science*, 156(1967)1378.
18. C. Gavach, T. Mlodnicka and J. Guastalla, *C.R. Acad. sci.*, 266(1968)1196, *Chem. Abstr.*, 69(1968)7815c.
19. L. Sinru and H. Freiser, *J. Electroanal. Chem.*, 191(1985)437.
20. P. Lauger, *Science, N.Y.*, 178(1972)24.
21. D. Homolka, L.Q. Jimg, A. Hofmanova, M.W. Khalil, J. Koryta, V. Marecek, S. Samec, S.K. Sen, P. Vanysek, J. Weber, and V. Brezina, *Anal. Chem.*, 52(1980)1606.
22. P. Vanysek, W. Ruth and J. Koryta, *J. Electroanal. Chem.*, 148(1983)117.
23. Z. Yoshida and H. Freiser, *J. Electroanal. Chem.*, 54(1974)361.
24. J. Koryta, *Electrochim. Acta*, 24(1979)293.
25. A. Hofmanova, Le Q. Hung and M.W. Khalil, *J. Electroanal. Chem.*, 135(1982)257.
26. Z. Samec, D. Homolka and V. Marecek, *J. Electroanal. Chem.*, 135(1982)265.
27. D. Homolka, K. Holub, and V. Marecek, *J. Electroanal. Chem.*, 138(1982)29.
28. E. Makrlik, L.Q. Hung and A. Hofmanova, *Electrochim. Acta*, 28(1983)847.

29. E. Makrlik and L.Q. Hung, *J. electroanal. Chem.*, 158(1983)285.
30. W. Erkang and P. Zhicheng, *J. Electroanal. Chem.*, 189(1985)1.
31. W. Erkang and P. Zhicheng, *J. Electroanal. Chem.*, 189(1985)21.
32. Z. Yoshida and H. Freiser, *J. Electroanal. Chem.*, 179(1984)31.
33. T. Kakulani, Y. Nishiwaki, T. osakai, and M. Senda, *Bull. Chem. Soc. Jpn.*, 59(1986)781.
34. J. Koryta, *Electrochim. Acta*, 32(1987)419.
35. L. Sinru and H. Freiser, *Anal. Chem.*, 59(1987)2834.
36. L. Zeryihun, M.Sc. Thesis, Addis Ababa University, 1993
37. J. Koryta, *Electrochim. Acta*, 31(1986)515.
38. C.J. Pedersen, *J. Am. Chem. Soc.*, 89(1967)2495.
39. I.M. Kolthoff, *Anal. Chem.*, 51(1979)1R.
40. J. Koryta, *Electrochim. Acta*, 29(1984)445.
41. C. Gavach and F. Henry, *J. Electroanal. Chem.*, 162(1984)307.
42. O.R. Melroy, R.P. Buck, F.S. Stover and H.C. Hughes, *J. Electroanal. Chem.*, 121(1981)93.
43. B. Hundhammer, T. solomon, and H. Alemu, *J. Electroanal. Chem.*, 149(1983)179.
44. Z. Samec, V. Marecek, J. Koryta, and M.W. Khalil, *J. Electroanal. Chem.*, 83(1977)393.
45. J. Koryta, P. Vanysek, and M. Brezina, *J. Electroanal. Chem.*, 67(1976)263.

46. J. Koryta, P. Vanysek and M. Brezina, *J. Electroanal. Chem.*, 75(1977)211.
47. T. Osaki, T. Kakutani and M. Senda, *Bunseki Kagaku*, 33(1984)E371 (see Ref. [50]).
48. M. Senda, T. Kakiuchi, and T. Osakai, *Electrochim., Acta*, 36(1991)253.
49. J. Koryta, *Electrochim. Acta*, 33(1988)189.
50. S. Wilke, H. Franzke and H. Muller, *Anal. Chim. Acta*, 268(1992)285.
51. B. Hundhammer and S. Wilke, *J. Electroanal. Chem.*, 26(1989)133.
52. M. Senda and Y. Yamamoto, 2nd Electroanalytical Symposium, Matrafured, Akademiai Kiado, Budapest, 1992.
53. B. Hundhammer, T. Solomon, T. Zeryhun, M. Abegaz, and A. Bekele, *J. Electroanal. Chem.*, in press.
54. J.F. Vanstaden, *Talanta*, 38(1991)1033.
55. H.A. Mottola, *Anal. Chem.*, 53(1981)1313A.
56. D. Betteridge, *Anal. Chem.*, 50(1978)832A.
57. K.K. Stewart, *Anal. Chem.*, 55(1983)931.
58. Reference 54 and references cited there in.
59. F.M. Karpfen and J.E.B. Randles, *Trans. Faraday Soc.*, 49(1953)823.
60. P. Vanysek, *Electrochemistry on Liquid/Liquid Interface*, In: *Lecture Notes in Chemistry*, Springer-Verag, Berlin, Heidelberg, N. York, Tokyo, 1985.
61. D.A. Owensby, A.J. Parker, and J.W. Diggle, *J. Am. Chem. Soc.*, 96(1974)2682.

62. L. Sinru Z. Zaofan, and H. Freiser, *J. Electroanal. Chem.*, 210(1986)137.
63. L. Sinru and H. Freiser, *J. Electroanal. Chem.*, 191(1985) 437.
64. P. Vanysek, W. Ruth, and J. Koryta, *J. Electroanal. Chem.*, 148(1983)117.
65. J. Koryta, G.W. Ruth, and P. Vanysek, *Faraday Discuss. Chem. Soc.*, 77(1984)209.
66. V. Horvath and G. Horvai, *Anal. Chim. Acta*, 273(1993)145.
67. A.M. Bond and H. O'hahoran, *Anal. Chem.*, 50(1978)216.
68. R.S. Nicholson and I. Shain, *Anal. Chem.*, 36(1964)706.
69. A.M. Bond, "Modern Polarographic Methods in Analytical Chemistry", Marcel Dekker, INC. New York and Basel, 1980.
70. H. Gunasingham and B. Fleet, *Anal. Chem.*, 55(1983)1409.
71. M.T. Mai, M.Sc. Thesis, Technische Hochschule, Leuna Merseburg, 19
72. C.J. Pedersen, *J. Am. Chem. Soc.*, 92(1970)386.
73. P.R. Mallinson and M.R. Truter, *J. Chem. Soc. Perkin Trans 11*(1972)1818.
74. C.J. Pedersen, and H.K. Frenddorff, *Angew. Chem. Int. Ed. Engl.*, 11(1972)16.
75. G. Michaux and J. Reisse, *J. Am. Chem. Soc.*, 104(1982)6895.
76. G.W. Gokel, D.M. Goli, C. Minganti, and L. Echevoyen, *J. Am. Chem. Soc.*, 105(1983)6786.
77. G.W. Gokel, *Chem. Soc. Rev.*, 21(1992)39.
78. J.A. Dean(ed), "Lange's Hand Book of Chemistry(11th ed.)" Mc Graw-Hill Book Company, New York, 1973, p. 6-30.

79. A.K. Covington(ed.), "Ion Selective Electrode Methodology", Vol. II, CRS Press. Inc., Florida, 1979, p.42.
80. A. Sabela, V. Marecek, Z. Samec and R. Fuoco, *Electrochim. Acta*, 37(1992)231.
81. M. Abegaz, M.Sc. Thesis, Addis Ababa University, 1990.
82. P. Vanysek and R.P. Buck, *J. Electroanal. Chem.*, 163(1984)1.